

BRL R 1825

BRL

AD

12

REPORT NO. 1825

ADA 017078

AMBIENT ELECTRON DENSITY PROFILES -
PROJECT SECEDE II

William A. Dean

August 1975

Approved for public release; distribution unlimited.

DDC
RECEIVED
NOV 11 1975
RESERVE
B

USA BALLISTIC RESEARCH LABORATORIES
ABERDEEN PROVING GROUND, MARYLAND

Destroy this report when it is no longer needed.
Do not return it to the originator.

Secondary distribution of this report by originating
or sponsoring activity is prohibited.

Additional copies of this report may be obtained
from the National Technical Information Service,
U.S. Department of Commerce, Springfield, Virginia
22151.

ACCESSION for	
NTIS	White Section <input checked="" type="checkbox"/>
DDC	Buff Section <input type="checkbox"/>
UNAN. COUNCIL	<input type="checkbox"/>
JUSTIFICATION	
BY	
DISTRIBUTION/AVAILABILITY CODES	
Dist.	Avail. and/or SPECIAL
A	

The findings in this report are not to be construed as
an official Department of the Army position, unless
so designated by other authorized documents.

UNCLASSIFIED

SECURITY CLASSIFICATION OF THIS PAGE (When Data Entered)

REPORT DOCUMENTATION PAGE		READ INSTRUCTIONS BEFORE COMPLETING FORM
1. REPORT NUMBER REPORT NO. 1825	2. GOVT ACCESSION NO. (14)	3. RECIPIENT'S CATALOG NUMBER BRL-1825
4. TITLE (and Subtitle) (6) AMBIENT ELECTRON DENSITY PROFILES - PROJECT SECEDE II	5. TYPE OF REPORT & PERIOD COVERED (9) Final rept.	
7. AUTHOR(s) (10) WILLIAM A. DEAN	6. PERFORMING ORG. REPORT NUMBER	
9. PERFORMING ORGANIZATION NAME AND ADDRESS US Army Ballistic Research Laboratories Aberdeen Proving Ground, MD 21005	8. CONTRACT OR GRANT NUMBER(s)	
11. CONTROLLING OFFICE NAME AND ADDRESS US Army Materiel Command 5001 Eisenhower Avenue Alexandria, VA 22333	10. PROGRAM ELEMENT, PROJECT, TASK AREA & WORK UNIT NUMBERS (12) 84P.	
14. MONITORING AGENCY NAME & ADDRESS (if different from Controlling Office)	12. REPORT DATE 11 AUGUST 1975	
	13. NUMBER OF PAGES 89	
	15. SECURITY CLASS. (of this report) UNCLASSIFIED	
	15a. DECLASSIFICATION/DOWNGRADING SCHEDULE	
16. DISTRIBUTION STATEMENT (of this Report) Approved for public release; distribution unlimited.		
17. DISTRIBUTION STATEMENT (of the abstract entered in Block 20, if different from Report)		
18. SUPPLEMENTARY NOTES		
19. KEY WORDS (Continue on reverse side if necessary and identify by block number) RF Transmission Experiment Multifrequency Beacon Ionospheric Electron Density Sporadic-E Activity Vertical Electron Content High-Altitude Barium Release SECEDE Project Multiple Receiver Sites (Continued on Rocket-Borne RF Beacon Dispersive Phase reverse side)		
20. ABSTRACT (Continue on reverse side if necessary and identify by block number) (kst) Project SECEDE II was a series of high-altitude barium releases made at Eglin Air Force Base, Florida, during the period from 16 January to 2 February 1971. An RF transmission experiment using a rocket-borne beacon and four fairly widely separated ground-based receiving stations was one of several methods employed for making ion cloud diagnostic measurements. That function constituted the primary role of the RF transmission experiment. However, since the beacon rockets were programmed to fly behind the ion cloud, relative to the (Continued on reverse side)		

UNCLASSIFIED

SECURITY CLASSIFICATION OF THIS PAGE(When Data Entered)

19. KEY WORDS (CONT.)

Dispersive Phase Rate	Rocket Antennas
Composite Electron Density Profiles	Horizontal Ionospheric
Experiment Geometry	Stratification
Ground Station Equipment	Time Varying Ionosphere

20. ABSTRACT (CONT.)

ground receiving stations, for only a short period of time when the beacon rocket was near apogee, a large amount of data for the ambient ionosphere was collected. A unique opportunity thus presented itself for making electron density measurements of the ambient ionosphere from data gathered over four widely separated propagation paths simultaneously. These measurements are the subject of this report

The RF transmission experiment, the experiment geometry, and the analysis methodology are briefly discussed. Individual electron density profiles for each of four receiving sites for six rocket beacon flights, along with a composite profile for each rocket flight, are presented. The dispersive phase data from which the profiles were derived are included.

Generally, the four individual profiles generated from each rocket flight show excellent internal consistency within the limits of experimental errors which are discussed.

UNCLASSIFIED

SECURITY CLASSIFICATION OF THIS PAGE(When Data Entered)

TABLE OF CONTENTS

	Page
LIST OF ILLUSTRATIONS	5
LIST OF TABLES.	7
I. INTRODUCTION.	9
II. THE RF TRANSMISSION EXPERIMENT.	10
A. Background.	10
B. Geometry for SECEDE II.	12
C. Equipment for SECEDE II	13
III. METHOD OF ANALYSIS.	15
IV. DISCUSSION OF ERRORS.	16
V. DISCUSSION OF RESULTS	19
A. Event PLUM, Early RF Beacon	19
B. Event REDWOOD, Early RF Beacon.	21
C. Event OLIVE, Early RF Beacon.	22
D. Event OLIVE, Late RF Beacon	22
E. Event SPRUCE, Late RF Beacon.	23
F. Event QUINCE, Early RF Beacon	24
VI. SUMMARY	25
REFERENCES.	83
DISTRIBUTION LIST	85

LIST OF ILLUSTRATIONS

Figure	Page
1. Map of the SECEDE II test area.	28
2. Typical beacon rocket trajectory	29
3. Angles derived from typical beacon rocket trajectory.	30
4. Site 1 dispersive phase for Event PLUM early beacon.	31
5. Site 1 electron density profile for Event PLUM early beacon.	32
6. Site 2 dispersive phase for Event PLUM early beacon.	33
7. Site 2 electron density profile for Event PLUM early beacon.	34
8. Site 3 dispersive phase for Event PLUM early beacon.	35
9. Site 3 electron density profile for Event PLUM early beacon.	36
10. Site 4 dispersive phase for Event PLUM early beacon.	37
11. Site 4 electron density profile for Event PLUM early beacon.	38
12. Four-site composite electron density profile for Event PLUM early beacon	39
13. Site 1 dispersive phase for Event REDWOOD early beacon	40
14. Site 1 electron density profile for Event REDWOOD early beacon	41
15. Site 2 dispersive phase for Event REDWOOD early beacon	42
16. Site 2 electron density profile for Event REDWOOD early beacon	43
17. Site 3 dispersive phase for Event REDWOOD early beacon	44
18. Site 3 electron density profile for Event REDWOOD early beacon	45
19. Site 4 dispersive phase for Event REDWOOD early beacon	46
20. Site 4 electron density profile for Event REDWOOD early beacon	47
21. Four-site composite electron density profile for Event REDWOOD early beacon	48
22. Site 1 dispersive phase for Event OLIVE early beacon	49
23. Site 1 electron density profile for Event OLIVE early beacon	50
24. Site 2 dispersive phase for Event OLIVE early beacon	51
25. Site 2 electron density profile for Event OLIVE early beacon	52
26. Site 3 dispersive phase for Event OLIVE early beacon	53
27. Site 3 electron density profile for Event OLIVE early beacon	54

LIST OF ILLUSTRATIONS (CONT.)

Figure	Page
28. Three-site composite electron density profile for Event OLIVE early beacon	55
29. Site 1 dispersive phase for Event OLIVE late beacon	56
30. Site 1 electron density profile for Event OLIVE late beacon	57
31. Site 2 dispersive phase for Event OLIVE late beacon	58
32. Site 2 electron density profile for Event OLIVE late beacon	59
33. Site 3 dispersive phase for Event OLIVE late beacon	60
34. Site 3 electron density profile for Event OLIVE late beacon	61
35. Site 4 dispersive phase for Event OLIVE late beacon	62
36. Site 4 electron density profile for Event OLIVE late beacon	63
37. Four-site composite electron density profile for Event OLIVE late beacon	64
38. Site 1 dispersive phase for Event SPRUCE late beacon	65
39. Site 1 electron density profile for Event SPRUCE late beacon	66
40. Site 2 dispersive phase for Event SPRUCE late beacon	67
41. Site 2 electron density profile for Event SPRUCE late beacon	68
42. Site 3 dispersive phase for Event SPRUCE late beacon	69
43. Site 3 electron density profile for Event SPRUCE late beacon	70
44. Site 4 dispersive phase for Event SPRUCE late beacon	71
45. Site 4 electron density profile for Event SPRUCE late beacon	72
46. Four-site composite electron density profile for Event SPRUCE late beacon	73
47. Site 1 dispersive phase for Event QUINCE early beacon	74
48. Site 1 electron density profile for Event QUINCE early beacon	75
49. Site 2 dispersive phase for Event QUINCE early beacon	76
50. Site 2 electron density profile for Event QUINCE early beacon	77
51. Site 3 dispersive phase for Event QUINCE early beacon	78
52. Site 3 electron density profile for Event QUINCE early beacon	79
53. Site 4 dispersive phase for Event QUINCE early beacon	80
54. Site 4 electron density profile for Event QUINCE early beacon	81
55. Four-site composite electron density profile for Event QUINCE early beacon	82

LIST OF TABLES

Table	Page
1. Site Locations for RF Transmission Experiment	12
2. Characteristics of the Transmission Experiment Equipment. . .	14
3. Electron Content/Dispersive Phase Relationship.	15
4. Results of Error Propagation Analysis	18
5. Vertical Electron Content from Four Widely Separated Receiving Sites	26

I. INTRODUCTION

SECEDE II was one of a series of high-altitude barium release programs sponsored by the Defense Advanced Research Projects Agency (DARPA) with participation by the Defense Nuclear Agency (DNA) and the Atomic Energy Commission (AEC). During SECEDE II six barium release rockets were flown from Eglin Air Force Base, Florida. The releases took place between 16 January and 2 February 1971.

The experimental program for SECEDE II included an RF transmission experiment in which a rocket-borne, multifrequency beacon transmitted radio signals to a ground-based receiving station. Appropriate multiplication and mixing of the received signals produced dispersive phase which provides information regarding ionization along the propagation paths. During SECEDE II four widely separated ground stations were employed, and the beacon rocket was flown on a trajectory which would pass behind the barium ion cloud as observed from at least one of the receiving stations.

The beacon rockets were programmed to fly behind the barium ion cloud for approximately one minute while the rocket was near apogee. Received signals from the beacon rocket were processed for dispersive phase for the entire duration of the rocket flights, yielding large amounts of data for the ambient ionosphere while the rocket was not behind the ion cloud. Although no particular requirement was made for ambient ionospheric data from the transmission experiment, this situation did present an unusual opportunity to derive electron density profiles from dispersive phase data gathered over four widely separated propagation paths simultaneously. The opportunity is also presented, for the first time with the transmission experiment, to test the effects on the derivation of densities of some of the simplifying assumptions that are made in the process of those derivations. In particular, the assumption of horizontal stratification of the ionosphere is severely tested by the geometry of the experiment - receiving stations far removed from the rocket launch area and signal propagation over widely separated paths. The assumption that the ionosphere is unchanging with time is tested, to a lesser degree, since most of the rockets are fired during the sunset transitional period; however, the time differential between rocket ascent and rocket descent is short in duration - only 4-6 minutes.

Altogether nine beacon rockets were launched during the SECEDE II test program. Dispersive phase data from three of the flights were not adequate for reduction to electron density profiles because of either rocket failure, rocket tumble, or inadequate signal-to-noise ratio. For each of the six remaining flights, we used all of the available dispersive phase data that was unperturbed by signal transmission through the ion clouds to produce electron density profiles. Eight separate profiles were derived for most of the rocket flights, consisting of one profile from data collected during rocket ascent and one profile from data collected during rocket descent for each of the four receiving sites.

Rocket ascent and rocket descent profiles are presented for each receiving site for each rocket flight from which a comparison may be made between rocket ascent and rocket descent profiles. A composite profile made up from all of the individual profiles for each beacon rocket flight is also shown. The composite profile allows a comparison of the individual profiles derived from data collected over the widely separated propagation ray paths.

II. THE RF TRANSMISSION EQUIPMENT

A. Background

For many years the Ballistic Research Laboratories (BRL) have been engaged in instrumenting sounding rockets with payloads consisting of multifrequency propagation beacons for the purpose of measuring the electron density and related parameters of the ionosphere. Initially a two-frequency propagation beacon using a technique similar to that devised by Seddon,¹ but with much different frequencies, was employed. During ensuing years continual modifications of the experiment were made to improve its reliability and to increase its versatility. Generally, the modifications consisted of improved beacon circuit design, an increase in the number of beacon frequencies, improved antenna design, and improved ground receiving station signal processing equipment.

Prominent among the projects in which BRL participated with the multifrequency propagation experiment are:

- the Strongarm series of sounding rocket firings to altitudes of 1500 km at Wallops Island, Virginia, in 1959 and 1960;
- the FISH BOWL series of high-altitude nuclear weapons tests in 1962;
- an Air Force Cambridge Research Laboratories (AFCRL) chemical release experiment in 1967;
- the SECEDE III project involving the release of barium plasma in Alaska in 1969; and

¹J. C. Seddon, "Propagation Measurements in the Ionosphere with the Aid of Rockets," J. Geophys. Res., Vol. 58, Sep 53, pp 323-335.

- a PCA event at Fort Churchill, Canada, in 1964.

Additionally, several test flights were conducted during periods of system modification. Evaluation of the system and results of participation in various projects are well documented in References 2-12.

- ²S. T. Marks et al., "Summary Report on Strongarm Rocket Measurements of Electron Density to an Altitude of 1500 Kilometers," BRL Report 1187 (AD 404189), January 1963.
- ³W. W. Berning, "Operation DOMINIC, FISH BOWL SERIES, Project Officer's Report 2018, Project 6.3, 'D-Region Physical Chemistry,'" Defense Nuclear Agency, Washington, DC, November 1964 (SECRET-RD).
- ⁴W. A. Dean and H. T. Lootens, "Ionosphere Measurements with a Four-Frequency Phase-Coherent Beacon," BRL Report 1396 (AD 835034), March 1968.
- ⁵W. A. Dean and H. T. Lootens, "Certification Flight of MIGHTY SKY Project 603-C Rocket Payload," BRL Report 1418 (AD 843101), October 1968.
- ⁶H. T. Lootens, "Rocket Measurements of Electron Density, Electron Temperature and Earth's Magnetic Field above Fort Churchill," BRL Report 1415, August 1968. (AD #676109)
- ⁷R. E. Prenatt, W. A. Dean, and W. W. Berning, "Electron Content of Barium Plasmas in the High Atmosphere," BRL Report 1459 (AD 700960), December 1969.
- ⁸W. A. Dean, "Auroral Zone Electron Density Profiles - Project SECEDE III Rockets," BRL Memorandum Report 2078 (AD 878631), November 1970.
- ⁹R. E. Prenatt and G. A. Bowers, "The RF Transmission Experiment in SECEDE II and a Model for the Electron Concentration in the Ion Cloud from High Altitude Barium Release PLUM," BRL Report 1645, May 1973. (AD #911669L)
- ¹⁰W. A. Dean and I. L. Chidsey, Jr., "Final Report on BRL Participation in Operation PCA 69," BRL Report 1669, September 1973. (AD #914672L)
- ¹¹W. A. Dean, "Electron Density Profiles for the 1969 PCA Event," paper published in the Proceedings of COSPAR Symposium on Solar Particle Event of November 1969, AFCRL Report 72-0474, Special Report 144, 11 August 1972.
- ¹²I. L. Chidsey, Jr., "Multifrequency Polar Cap Absorption Measurements," paper published in the Proceedings of COSPAR Symposium on Solar Particle Event of November 1969, AFCRL Report 72-0474, Special Report 144, 11 August 1972.

For SECEDE II BRL was given the responsibility for design and construction of the primary rocket payload instrumentation for the beacon rockets. The instrumentation consisted of the multifrequency propagation beacon and its associated rocket antenna system. Further responsibility assigned to BRL was the implementation and operation of one of the four ground receiving stations. As a spin-off of its participation in the SECEDE II program, BRL acquired copies of the RF transmission data from all four receiver sites. These data were used as a basis for this report.

B. Geometry for SECEDE II

The geometry for SECEDE II as it pertains to the RF transmission experiment is depicted in Figure 1. There were ten separate rocket launch pads used during the program, all located in close proximity to one another at Site A-15A at Eglin Air Force Base, Florida. All of the beacon rockets were fired in a general southerly direction as shown. The ground receiving stations were located generally east of Panama City, Florida, some 160 km from the launch facilities. Coordinates of the pertinent site locations are shown in Table 1.

Table 1
Site Locations for RF Transmission Experiment

<u>Site</u>	<u>Coordinates</u>	<u>Elevation Ft. MSL</u>
Launch Area*	N 30° 23' 14" W 86° 48' 13"	10
Receiver Site 1	N 30° 26' 13" W 85° 13' 31"	135
Receiver Site 2	N 30° 14' 04" W 85° 12' 15"	65
Receiver Site 3	N 30° 05' 56" W 85° 14' 07"	35
Receiver Site 4	N 29° 53' 21" W 84° 58' 42"	10

*The launch area coordinates listed reflect the average position of several launch pads used during the program.

The next two illustrations depict some of the parameters for a typical beacon rocket trajectory for the SECEDE II program. In Figure 2 the rocket altitude above sea level and the horizontal range from the Site 2 ground receiver are shown. Elevation, azimuth and look angles, as a function of time, relative to the Site 2 receiver are shown in Figure 3. The elevation and azimuth angles refer to the direction of the line of sight to the beacon rocket as viewed from the receiver station. The look angle is that angle between the longitudinal axis of the beacon rocket and the line of sight to the ground receiving station. The only particular importance attached to the look angle is that for adequate signal reception the angle should not be less than about 15 degrees because the beacon rocket transmitting antennas have a deep null directly off the tail of the rocket.

C. Equipment for SECEDE II

The rocket-borne beacons operated in a CW mode and transmitted five harmonically related phase-coherent signals. The rocket antennas, a new BRL design, were longitudinal slot antennas such that the rocket spin frequency did not appear in signals received at the ground stations, as had been the case for previous designs.

At each of the four receiving sites, new receiving and data generating equipment, designed and produced by Electrac, Inc.;¹³ was used. Only four of the transmitted frequencies could be received at three of the receiving sites, while all five frequencies could be received at Site 3, the BRL site. Also at Site 3 a modified version of the standard BRL receiving system was co-located with the Electrac receiving system. (The standard BRL receiving systems incorporated three frequencies of 36.44, 145.76, and 583.04 MHz. For SECEDE II the 583.04-MHz frequency receiver was replaced by an 874.59-MHz receiver for compatibility with the transmitted signals.)

The 36.44-MHz frequency was included primarily for the use of BRL, which had responsibility for furnishing background ambient electron densities for SECEDE II. Although the 36.44-MHz frequency was considered useless for transmitting through the ion clouds because of probable signal blackout and other phase perturbations of a serious nature, its increased sensitivity for determining ambient densities warranted its use.

Some characteristics of the RF transmission experiment equipment are listed in Table 2.

For the work reported here only dispersive phase data extracted from the 145.76-MHz and 874.59-MHz signals from the Electrac system were used.

¹³R.W. Honey, "RF Beacon Ground Stations Dispersive-Phase/Differential Doppler Measurement System," RADC TR-72-151, Final Technical Report, Electrac, Inc., Anaheim, CA, March 1972.

Table 2

Characteristics of the Transmission Experiment Equipment

Transmitter

Frequencies: 36.44 MHz, 145.76 MHz, 291.53 MHz, 437.29 MHz,
874.59 MHz

Operating Mode: CW

Power Outputs: 1 watt at 36.44 and 145.76 MHz
2 watts at 291.53, 437.29, and 874.59 MHz

Rocket-borne Antennas

Type: 36.44 MHz - Body-fed dipole using entire rocket structure, 145.76 MHz and higher. Cross connected, dual cylindrical slots fed in phase. Slots parallel to longitudinal axis of rocket.

Beamwidth: 36.44 MHz - Main lobe centered 50° from aft end of longitudinal axis of rocket. Six db half-beamwidth is 25°. Deep null off tail of rocket.
145.76 MHz and higher - Main lobe perpendicular to longitudinal axis of rocket. Six db half-beamwidth is 60°. Deep null off tail of rocket.

Gain (Main lobe): 36.44 MHz - +3 db
145.76 MHz and higher - 0 db

Ground Antennas*

Type: (Electrac) Crossed dipoles for 36.44 MHz
One crossed log periodic at the remaining frequencies

(BRL) Crossed yagis for 36.44 MHz
Crossed yagis at 145.76 MHz
Helix at 874.59 MHz

Polarization:

(Electrac) Right circular per IEEE standards

(BRL) Left and right circular at 36.44 and 145.76 MHz
Right circular at 874.59 MHz

Receiver and Data Circuits*

Electrac: System designed and constructed by Electrac for SECEDE II.

BRL: System designed and constructed by BRL.

*The BRL system and the 36.44 MHz channel of the Electrac system were present at Site 3 only.

III. METHOD OF ANALYSIS

The method of producing electron concentration profiles from dispersive phase data has been described in detail in earlier reports and will be reviewed only briefly here.

A rocket carries a radio beacon which transmits two or more harmonically related, phase-coherent signals to a ground-based receiving station. Appropriate multiplication and mixing of the received signals produce a beat frequency called dispersive Doppler. Integration of the dispersive Doppler (i.e., counting the cycles) produces dispersive phase. In cases where the geomagnetic field and electron collisions can be ignored, and where the signals can be assumed to follow identical ray paths between the rocket and the ground, the dispersive phase is proportional to the electron content in a column of unit cross section along the ray path, so that

$$\int N_e dr = K\phi_{dd},$$

where N_e is the electron concentration, dr is an element of ray path length, ϕ_{dd} is the dispersive phase, and K is a constant for given frequency pairs. The value of K depends on the frequencies used and on the manner in which the signals are multiplied and mixed. The various values of K for the SECEDE II systems are listed in Table 3.

Table 3
Electron Content/Dispersive Phase Relationship

Dispersive Phase Channel	Dispersive Phase Is Produced From**	K^{***}
36,145 (BRL)*	$2\phi_{145} - 8\phi_{36}$	$.361 \times 10^{14}$
145,874 (BRL)*	$1/3\phi_{874} - 2\phi_{145}$	5.58×10^{14}
36,145 (ELECTRAC)*	$1/4\phi_{145} - \phi_{36}$	2.89×10^{14}
145,874 (ELECTRAC)	$1/6\phi_{874} - \phi_{145}$	11.1×10^{14}
291,874 (ELECTRAC)	$1/3\phi_{874} - \phi_{291}$	24.4×10^{14}
437,874 (ELECTRAC)	$1/2\phi_{874} - \phi_{437}$	43.4×10^{14}

*Site 3 only.

** $\phi_f \equiv$ phase path at frequency f .

***Assuming propagation path is the same at both frequencies.

For this particular study we decided to use the most sensitive dispersive phase channel which was available at all receiving sites to avoid giving any one site an advantage or disadvantage, as the case may be. We, therefore, selected the 145,874 (ELECTRAC) channel.

If the ionosphere is assumed to be horizontally stratified, the electron content in a vertical column can be computed from

$$\int N_e dh = \cos \theta \int N_e dr,$$

where θ is the angle between the vertical and the propagation ray path. Since the angle θ , and therefore $\cos \theta$, varies along the ray path, an average value of $\cos \theta$ is normally used. The point along the ray path at which the value of $\cos \theta$ is computed is such that about half of the measured electron content is between the point and the rocket and half is between the point and the ground receiver.

If the ionosphere can be assumed to be unchanging with time, then the average electron concentration, in successive altitude intervals throughout the rocket flight, may be computed from

$$\overline{N_e} = \frac{\Delta \int N_e dh}{\Delta h},$$

where $\overline{N_e}$ is the average electron concentration and Δh is the altitude interval.

IV. DISCUSSION OF ERRORS

It may be worthwhile, before presenting the results of the present work, to discuss some sources of error and to make some estimate of the accuracy with which electron densities can be determined using the RF propagation system.

As has been noted earlier, average electron densities in a given altitude increment are determined by differencing of the vertical electron content and averaging over the desired altitude interval. Of course, the vertical electron contents are derived from dispersive phase data that are collected along a propagation path which deviates significantly from the vertical, especially for the SECEDE II program. Some error in the vertical electron contents, hence in the derived electron densities, could result during the transformation from ray path electron content to vertical electron content. The magnitude of any such errors would depend largely on instabilities or lack of homogeneity in the ionosphere at the time of the measurements. An

additional receiving site near the beacon rocket launcher would have been useful in assessing the effect of this possible error source; however, evaluating such errors was beyond the scope of the SECEDE II program. During the BARBIZON¹⁴ program in the Hawaiian Islands, similar propagation experiment geometry was employed but a receiving station at the launcher complex was also used. On the basis of that one experiment, which consisted of two beacon rocket flights, any errors due to significantly non-vertical propagation paths were found to be minimal for the condition of the ionosphere at the time of that experiment.

Another characteristic of the RF transmission experiment which causes some concern, especially when the system is used to measure ionospheric parameters under naturally or artificially disturbed conditions, is that the basic measurement of dispersive phase yields a measure of electron content over the total length of the propagation path. [A polar cap absorption event (PCA) serves as an example of a naturally disturbed ionosphere, while nuclear detonations and barium releases are examples of artificial disturbances.] Therefore a change in electron density anywhere along the propagation path, no matter how far removed from the beacon rocket, is reflected in the measured data as a change in total ray path electron content at the rocket altitude. These circumstances may introduce serious errors in any derived electron densities during highly disturbed conditions in the ionosphere. Of course, this is the reason why no attempt has been made to define ambient ionospheric conditions during times the beacon was propagating through the barium ion clouds for SECEDE II. During the entire SECEDE II program, however, significant Sporadic-E activity was in evidence. An analysis of that situation indicates that the total electron content from the lower edge of the ionosphere up through the E-region amounts only to about 2.5 percent of the total ray path content when the rocket is near peak altitude. Additionally, the total electron content through the E-region is equivalent, on the average, to about 40 percent of the change in electron content between the 1-km altitude layers above the E-region used for the present derivation of densities. A complete depletion of electrons below the top of the E-region during a time the beacon rocket was traversing 1 km at higher altitudes could, conceivably, introduce an error of up to 40 percent in the derived density. Being more realistic, though, a 10 percent change in content through the E-region would result in errors of only up to 4 percent in the derived densities at higher altitudes. An error of that magnitude is considered to be quite acceptable.

¹⁴W. A. Dean, R. E. Prenatt, and G. A. Bowers, "The RF Transmission Experiment For Operation BARBIZON," BRL Report in publication.

A third possible source of error is a function of the precision with which the basic data is measured and a function of the lower of the two frequencies employed in the production of dispersive phase. The dispersive phase measurements were made with a precision of about 0.005 cycles or about 2 degrees of phase. Design requirements of the dispersive phase system imposed an error in recovered phase shift to be less than about $3\frac{1}{2}$ degrees due to noise and receiver and recorder instabilities. No attempt has been made to evaluate the actual fidelity of the system, although there is every reason to believe that its performance clearly met the design requirements. [An analysis was performed using the basic measurement precision of $\pm 2^\circ$ with typical dispersive phase data and a typical beacon rocket trajectory to determine how jitter in measurement of the 145/874 MHz dispersive phase propagates through the system of equations for deriving electron densities.] The results of the error propagation analysis are shown in Table 4 for selected altitudes.

Table 4
Results of Error Propagation Analysis

Altitude	Electron Concentration	Error in Electron Concentration for $\pm 2^\circ$	Percentage Error
100	1.363×10^{10}	$\pm 6.474 \times 10^9$	47.5
150	1.579×10^{10}	$\pm 5.444 \times 10^9$	34.5
200	1.197×10^{11}	$\pm 4.726 \times 10^9$	3.9
250	4.099×10^{11}	$\pm 3.870 \times 10^9$	0.9

We emphasize that the errors listed here are the maximum statistical errors which would be encountered for a 2-degree error in one direction at one end of the measurement interval and a 2-degree error in the opposite direction at the other end of the measurement interval. We suggest that such a situation rarely exists in practice, and later results reported here tend to confirm that conclusion. In any event, one might logically argue against reporting electron densities derived for altitudes below about 160 km. We do report those densities, however, because we feel that a good qualitative description of abnormalities and layering in the E-region is exhibited and that the accuracy of the densities reported for the lower altitudes is better than indicated in Table 4.

V. DISCUSSION OF RESULTS

The results presented here for each of the six beacon rocket flights analyzed will include dispersive phase and dispersive phase rate data collected at each of the receiving sites, electron density profiles derived from each set of dispersive phase data from both beacon rocket ascent and beacon rocket descent where data were available, and a composite electron density profile encompassing all of the individual profiles from each rocket flight. There is no intent here to present the best possible profile for the time of each beacon rocket flight. The intent has been to exhibit the difference, or lack of significant differences, among profiles derived from dispersive phase data collected over significantly different propagation paths. Selecting the best possible profile for each rocket flight might have involved a computation of the mean electron density at each altitude along with some statistically determined deviation from the mean. Instead, we have compared all of the available profiles for each rocket flight and, at each altitude, selected the largest and smallest electron density and plotted these as a function of altitude to show the total spread for all of the profiles.

For nearly all of the profiles presented, considerable differences will be noted among the various profiles for each beacon rocket flight for altitudes below about 160-180 km. Some evidence of layers of ionization is also present. Such layering is undoubtedly the result of significant Sporadic-E activity that was in evidence in ionsonde data throughout the period of the tests. Some of the variations in density, for densities below 10^{10} electrons per cubic meter, may result from lack of sensitivity in the measurement system using 145 MHz as the lower frequency for the dispersive phase system.

It will be noted during the discussion of results from the individual rocket flights that some events are designated as "late" and some as "early". These designations have no particular significance in the present report but merely indicate that the beacon rockets were deployed to pass behind the ion cloud within two to three minutes of formation of the cloud in the case of the "early" designation. If the designation is "late," the beacon rocket was launched to pass behind the ion cloud after the formation of striations within the cloud.

A. Event PLUM, Early RF Beacon

The beacon for this event was launched at 23:45:31 UT (17:45:31 CST) on 20 January 1971. All four receiving stations had continuous signal from about 4 seconds after rocket lift until a few seconds before rocket impact, and dispersive phase data of excellent quality were recovered at all four sites. The dispersive phase and dispersive phase rate data for receiving sites 1, 2, 3, and 4 are shown in Figures 4, 6, 8, and 10, respectively. As indicated, continuous dispersive data were processed at each of the four receiving sites,

but the beacon rocket did pass behind the barium ion cloud relative to each of the sites. The discontinuities in the various curves reflect the period of time when the received signals were perturbed as a result of being transmitted through some portion of the ion cloud. Because of the difference in aspect, the time of occurrence and the duration of the discontinuities differ from receiving site to receiving site. All of the discontinuities, however, occur near the time of beacon rocket apogee, leaving dispersive data unaffected by transmission through the ion cloud for a large percentage of the beacon rocket flight. Each set of dispersive phase rate data shows similar variations before 100 seconds and after 400 seconds. As will be seen, these variations are reflected as variations in electron density in the E-region.

Figures 5, 7, 9, and 11 show the electron concentration profiles derived from the dispersive phase data gathered at receiving sites 1, 2, 3, and 4, respectively. Each illustration shows two profiles, one derived from dispersive phase data collected during beacon rocket ascent and one derived from dispersive phase data collected during rocket descent. The beacon rocket attained a peak altitude of about 270 km, but because of barium cloud effects the profiles have been terminated at about 240 km or below. In general, the agreement between rocket ascent profiles and rocket descent profiles is excellent, even below 160 km where the difference between the two profiles is considerably less than the possible errors noted in the previous section. Layering is very evident at the lower altitudes and is typical of derived densities in the presence of Sporadic-E activity. We emphasize that the actual altitude of the layers is open to question, since the derived densities reflect changes in density anywhere along the propagation ray path below the rocket altitude. However, good consistency among the profiles derived from each of the four individual receiving sites lends considerable credence to the reported densities.

The next illustration, Figure 12, is a composite of the preceding eight profiles. You will recall that this composite is made up of, as the upper limit, the maximum electron density found in any of the individual profiles for each altitude and, as the lower limit, the minimum electron density at each altitude from each of the individual profiles. A useful bit of information that was not programmed in our computer computation of densities would be the average density from all available profiles for each beacon rocket flight. However, such an average would have shown definitive density layers at about 96 km and again at about 120 km and a relatively smooth profile above 120 km. The narrowing of the separation between upper and lower limits around 140 km is simply a result of the fact that fewer profiles went into making up the composite because of differences in the time of ion cloud interference relative to the various receiving sites.

B. Event REDWOOD, Early RF Beacon

The beacon rocket associated with the REDWOOD event was launched as an early time rocket at 23:49:51 UT (17:49:51 CST) on 26 January 1971. Continuous, excellent quality, dispersive phase data were recovered at all four receiving sites. The beacon rocket did pass behind some portion of the barium ion cloud relative to all four receiving sites at a time just shortly before the rocket attained peak altitude. The beacon rocket remained behind the ion cloud for approximately 100 seconds relative to receiver Site 1 and gradually lesser amounts of time for the more southerly receiver sites.

All of the dispersive phase data, even for times when transmission was through the ion cloud, are presented for Sites 1-4 in Figures 13, 15, 17, and 19, respectively. The dispersive phase rate data exhibits deviations in slope from what would be anticipated in an undisturbed ionosphere beginning shortly after 280 seconds and ending at about 380 seconds. Similar deviations may be noted for the other receiver sites with the disturbance starting later in time and being shorter in duration.

These slight deviations in dispersive phase rate have a marked effect on derived electron densities to such an extent as to make the derived densities totally unreliable. As a result, no densities are shown for the rocket descent part of the flight during which the beacon was transmitting through the barium ion cloud.

The electron density profiles for each of the four receiver sites are shown in Figures 14, 16, 18, and 20. Below about 140 km the behavior of the ionosphere was so erratic as to cause actual decreases in the measured ray path electron content which, in turn, caused unrealistic negative values of electron density. Consequently, no densities are reported below 140 km.

With the exception of the Site 2 profiles there is, again, excellent agreement among the rocket ascent and rocket descent profiles. There is a possible explanation for the disagreement evidenced in the Site 2 profiles. All of the dispersive phase data for the present work were taken from strip chart recorders. The strip chart for the Site 2 record had no beacon rocket flight timing marks. The rocket lift time could easily be identified from the nature of the signal, and thereafter constant chart speed was assumed. If the assumed chart speed were slightly in error or if the chart speed were not precisely constant, a growing error in time might accrue. Such an error in time could introduce a divergence in profiles similar to that noted in the profiles derived from the Site 2 receiver data.

A composite of the eight individual profiles is shown in Figure 21. Only rocket ascent data make up the composite above 250-260 km because of the aforementioned transmission through the barium ion cloud. At the lower altitudes the spread between maximum and minimum densities at each altitude reflects, to a large extent, the divergence between the ascent and descent profiles from the Site 2 receiver station.

C. Event OLIVE, Early RF Beacon

The beacon rocket associated with the OLIVE event was launched as an early-time (before striations) rocket at 23:52:17 UT (17:52:17 CST) on 29 January 1971. Continuous dispersive phase data of excellent quality were recovered at all four RF receiving stations; however, no strip chart record was available for the Site 4 receiver. The beacon rocket attained a peak altitude of about 263 km. The rocket disappeared behind the barium ion cloud relative to the Site 1 receiver at approximately 262 km on the rocket upleg and emerged from behind the cloud at an altitude of about 245 km on the rocket downleg. The rocket disappeared behind the barium cloud at earlier times and emerged at later times relative to the more southerly stations. All of the dispersive phase data available for times when the transmission path was free of the barium ion cloud are shown in Figures 22, 24, and 26 for receiver Sites 1, 2, and 3, respectively.

The electron density profiles for the three receiver sites are shown in Figures 23, 25, and 27. Again there was no timing on the strip chart recorder from the Site 2 receiver. The divergence between the ascent and descent profile indicates the probability of significant and progressive error in the assumed timing associated with the data from that receiver. Although the ascent profile for the Site 2 receiver is in good agreement with the profiles from the other receiver sites, the descent profile is in such poor agreement that it should be considered unreliable. As with most of the other profiles presented here, the ever-present effects of Sporadic-F activity are reflected in the electron densities below 160-170 km.

A composite of the profiles from the three receiver sites is shown in Figure 28. The descent profile from the Site 2 receiver was not used in the makeup of the composite because of its unreliability. With that exclusion, the composite profile indicates excellent agreement among the other individual profiles.

D. Event OLIVE, Late RF Beacon

A second beacon rocket associated with the OLIVE event was launched as a late-time rocket at 00:24:00 UT on 30 January 1971 (18:24:00 CST, 29 January 1971), nearly 32 minutes after the early-time rocket for the same event. Again, continuous dispersive phase data of excellent quality were recovered at all four RF receiving stations. There was a secondary barium plasma release during the

OLIVE event. This late-time beacon rocket passed behind the secondary ion cloud as well as behind the primary ion cloud. As a result, the transmitted signals were perturbed by transmission through one or the other of the ion clouds for a sufficient amount of time during beacon rocket descent to preclude the determination of meaningful electron densities. Therefore, data for rocket ascent only are presented here.

The dispersive phase data for Sites 1, 2, 3, and 4 are shown in Figures 29, 31, 33, and 35, respectively. The rocket ascent profiles derived from those dispersive phase data are found in Figures 30, 32, 34, and 36.

A composite of the four individual profiles is shown in Figure 37. Although not clearly evident in the data presented here, there is excellent agreement among the profiles derived from the dispersive phase data for Sites 1, 2, and 3. The Site 4 electron densities are generally higher at all altitudes. There is no apparent abnormality which would account for the higher densities derived from the Site 4 data except to conclude that the densities, as presented, do represent the condition of the ionosphere along that particular propagation ray path. In any event the spread between the various profiles is not alarming. As with the other events, Sporadic-E activity is clearly evident at altitudes below 150 km.

E. Event SPRUCE, Late RF Beacon

The beacon rocket associated with event SPRUCE was launched as a late-time rocket at 00:01:24 UT on 2 February 1971 (18:01:24 CST, 1 February 1971). Continuous dispersive phase data of excellent quality were recovered at all four receiver sites. The beacon rocket did fly behind the barium ion cloud relative to all four receiver sites for periods ranging from 20 to 30 seconds shortly after beacon rocket apogee. Since the beacon rocket is changing altitude very slowly near apogee, ambient data were lost for only about 5-6 km of the rocket downleg portion of the trajectory.

The dispersive phase data from receiver Sites 1, 2, 3, and 4 are shown in Figures 38, 40, 42, and 44, respectively. The gaps in the data starting near, or shortly after, 280 seconds reflect the times when propagation was through the ion cloud relative to the various receiving sites.

Figures 39, 41, 43, and 45 represent the electron densities derived from the dispersive phase data acquired at the respective receiver sites. There is a similar separation between ascent and descent profiles for Sites 1, 2, and 3 in the altitude range from 140 km to 170 km, with a lesser separation for a smaller altitude interval for Site 4. However, there is excellent agreement among all four ascent profiles and among all four descent profiles throughout the entire rocket flight. It is worthy of re-emphasis, at this point

that, because of the rocket trajectory and the geometry involved, the propagation ray paths are traversing a portion of the lower ionosphere, during rocket descent, which is far removed from that portion of the ionosphere traversed during rocket ascent. And, because of the internal consistency among the four profiles, we conclude that the actual condition of the ionosphere along the propagation paths is reliably represented by the profiles reported here.

Figure 46 is a composite of the four ascent profiles and the four descent profiles from the beacon rocket flight for event SPRUCE. As with all the composite profiles, the maximum density at each altitude from among the eight individual profiles was used to produce the upper limit profile, and the minimum density at each altitude from among the eight profiles was used to produce the lower limit profile. The spread between lower limit and upper limit in the 140-170 km altitude range is, then, a reflection of the difference between ascent and descent profiles from the individual receiver sites, with the descent profiles contributing heavily to the lower limit and the ascent profiles forming the upper limit. As with the previous events, Sporadic-E activity is clearly evident below 140 km.

F. Event QUINCE, Early Beacon

The beacon rocket associated with the QUINCE event was launched as an early-time rocket at 16:32:31 UT (10:32:31 CST) on 2 February 1971. This rocket was the only daytime beacon rocket launched during the SECEDE II program. The rocket attained a peak altitude of 259 km and flew behind the barium cloud relative to receiver Site 3 and receiver Site 4 only. Continuous dispersive phase data of good quality were recovered at all four receiver sites.

The dispersive phase data from Sites 1, 2, 3, and 4 are shown in Figures 47, 49, 51, and 53, respectively. The gaps in the data for Site 3 and Site 4 reflect the time the beacon rocket was behind the barium cloud relative to those receiver sites. A high-density E-layer ledge is evident in all of the dispersive phase rate charts centered around 72 seconds and 431 seconds. The beacon rocket was at an altitude of 113 km during rocket ascent at 72 seconds and at an altitude of 114 km during rocket descent at 431 km.

The electron density profiles derived from the dispersive phase data for the four receiver sites are shown in Figures 48, 50, 52, and 54. Remarkable agreement exists between the rocket ascent profile and rocket descent profile from each of the individual receiver sites. Furthermore, Figure 55, which shows the composite profile, exhibits remarkably good agreement among all eight of the individual profiles.

One significant difference between these profiles and all the preceding ones is the considerably higher electron densities at all altitudes. As noted earlier, this beacon rocket was a daytime (mid-morning) firing, whereas all the previous rockets were scheduled such that darkness was present at ground level but sunlight still remained at barium release altitudes. Consequently, for the evening rockets, a very large portion of the ionosphere traversed by the beacon rockets was in darkness.

VI. SUMMARY

During the SECEDE II project five of the RF beacon rockets yielded excellent dispersive phase data at four widely separated receiving stations, and a sixth beacon rocket yielded excellent data at three of the four receiving stations. The intent was to fly the beacon rockets behind barium ion clouds relative to at least one ground receiving station, and the RF beacon data was to be used as an aid in performing ion cloud diagnostics. To a large extent, that part of the mission was most successful. However, as planned, the beacon rockets were, in general, behind the ion clouds for short periods of time around the time of beacon rocket apogee. The signals emanating from the beacon rocket were monitored for dispersive phase throughout the entire rocket flight. As a consequence, a large amount of data pertaining to the undisturbed ambient ionosphere was collected and, for the first time, at several widely spaced receiving stations. This situation presented a unique opportunity to derive electron density profiles from dispersive phase data collected over several widely spaced propagation ray paths simultaneously.

The six beacon rocket flights reported here were flown over a 14-day period - all at the same geographical location. Five of the rocket flights took place around the time of evening sunset such that the lower portion of the ionosphere traversed by the rocket was in darkness and the upper portions were still in sunlight. The sixth rocket was flown in mid-morning when all of the ionosphere traversed by the rocket was in sunlight.

All of the available dispersive phase data were used to produce electron densities at all of the receiving sites for each beacon rocket flight. The excellent agreement, in general, between the rocket ascent profile and the rocket descent profile for each rocket flight tends to confirm the validity of using the assumption that the ionosphere was unchanging with time during the short period of time between rocket ascent and rocket descent, even though most of the rockets were flown during the sunset transitional period. Some indication of the ionosphere changing with time can be seen in the two composite profiles for event OLIVE - Figures 28 and 37. The late beacon rocket was launched some 32 minutes after the early beacon rocket. However, differences between rocket ascent profiles and rocket

descent profiles, for a given rocket flight, indicate that any time variations in ionization levels for the two-to three-minute time interval involved were not significant so that no attempt was made to define a time rate of change or to make a correction for that time rate of change.

There are, in some cases, significant differences between the ascent and descent profiles below about 160 km in altitude. These differences undoubtedly arise from the fact that significant Sporadic-E activity was present during all of the evening rocket flights. These differences are not surprising considering that Sporadic-E activity is present and that the propagation ray path during rocket descent is far removed (200 km or more) from the ray path during rocket ascent. We also conclude, intuitively, that the effects of the Sporadic-E activity are magnified, in terms of electron densities, by the propagation ray path being far removed from a vertical ray path - zenith angle of 45 degrees or larger while the beacon rocket is traversing the E-region.

As to the assumption of horizontal stratification, some insight into the validity of that assumption may be gained by comparing the vertical electron content derived from the ray path electron contents collected over the widely separated propagation ray paths. Such a comparison may be made from Table 5, which gives the vertical electron content for one rocket flight as derived from data collected at each of the four receiving sites. The individual electron contents, as well as the average, are listed as a function of beacon rocket altitude.

Table 5
Vertical Electron Content From
Four Widely Separated Receiving Sites

VERTICAL ELECTRON CONTENT (ELECTRONS/SQ. METER COLUMN)					
ALT(km)	Site 1	Site 2	Site 3	Site 4	AVE.
ASCENT					
100	4.02×10^{14}	5.42×10^{14}	4.19×10^{14}	5.01×10^{14}	4.660×10^{14}
150	8.74×10^{15}	9.04×10^{15}	8.77×10^{15}	8.91×10^{15}	8.805×10^{15}
200	2.82×10^{16}	2.88×10^{16}	2.84×10^{16}	2.86×10^{16}	2.850×10^{16}
250	7.96×10^{16}	8.06×10^{16}	7.99×10^{16}	7.98×10^{16}	7.998×10^{16}
DESCENT					
250	7.95×10^{16}	7.91×10^{16}	7.97×10^{16}	7.92×10^{16}	7.938×10^{16}
200	2.82×10^{16}	2.75×10^{16}	2.83×10^{16}	2.78×10^{16}	2.795×10^{16}
150	8.78×10^{15}	8.39×10^{15}	8.79×10^{15}	8.64×10^{15}	8.650×10^{15}
100	3.54×10^{14}	2.48×10^{14}	3.60×10^{14}	3.17×10^{14}	3.198×10^{14}

As may be seen from the table, the agreement among the four individual site determinations of vertical electron content is excellent. It should also be noted that the vertical electron content derived from rocket ascent data at a given altitude is in excellent agreement with that derived from rocket descent data at the same altitude. From these observations one may infer that not only is the assumption of horizontal stratification valid but also that there is no time variation of consequence between the time of rocket ascent and rocket descent. At first glance it may appear obvious that there is a definite trend toward decreasing ionization below 100 km from a comparison of the ascent and descent data at the altitude. However, a comparison of the ascent and descent data for 150 km shows an increase in content at two sites and a decrease at the other two sites. Furthermore, the average difference between the ascent and descent 150-km data is larger than the average difference between the ascent and descent 100-km data, contradicting any conclusion that ionization is decreasing with time at the lower altitudes.

The results of this analysis have been most rewarding in that the validity of two simplifying assumptions has been greatly strengthened. In addition, it is now apparent that a single receiving station for the RF transmission experiment may confidently be used, without imposing many restrictions on its location relative to the rocket launch complex, for the determination of reliable ambient ionospheric parameters.

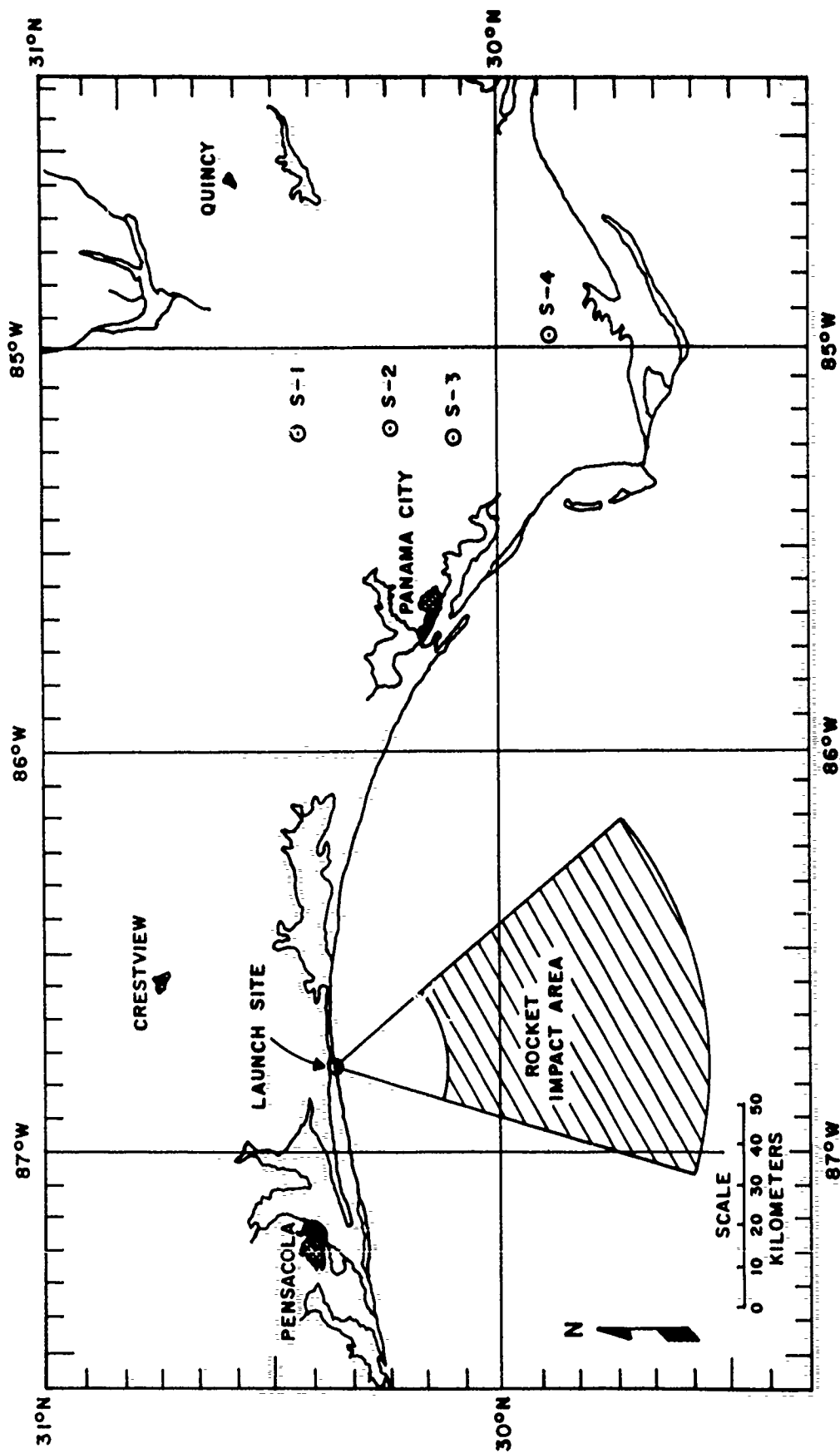


Figure 1. Map of the SECEDE II test area.

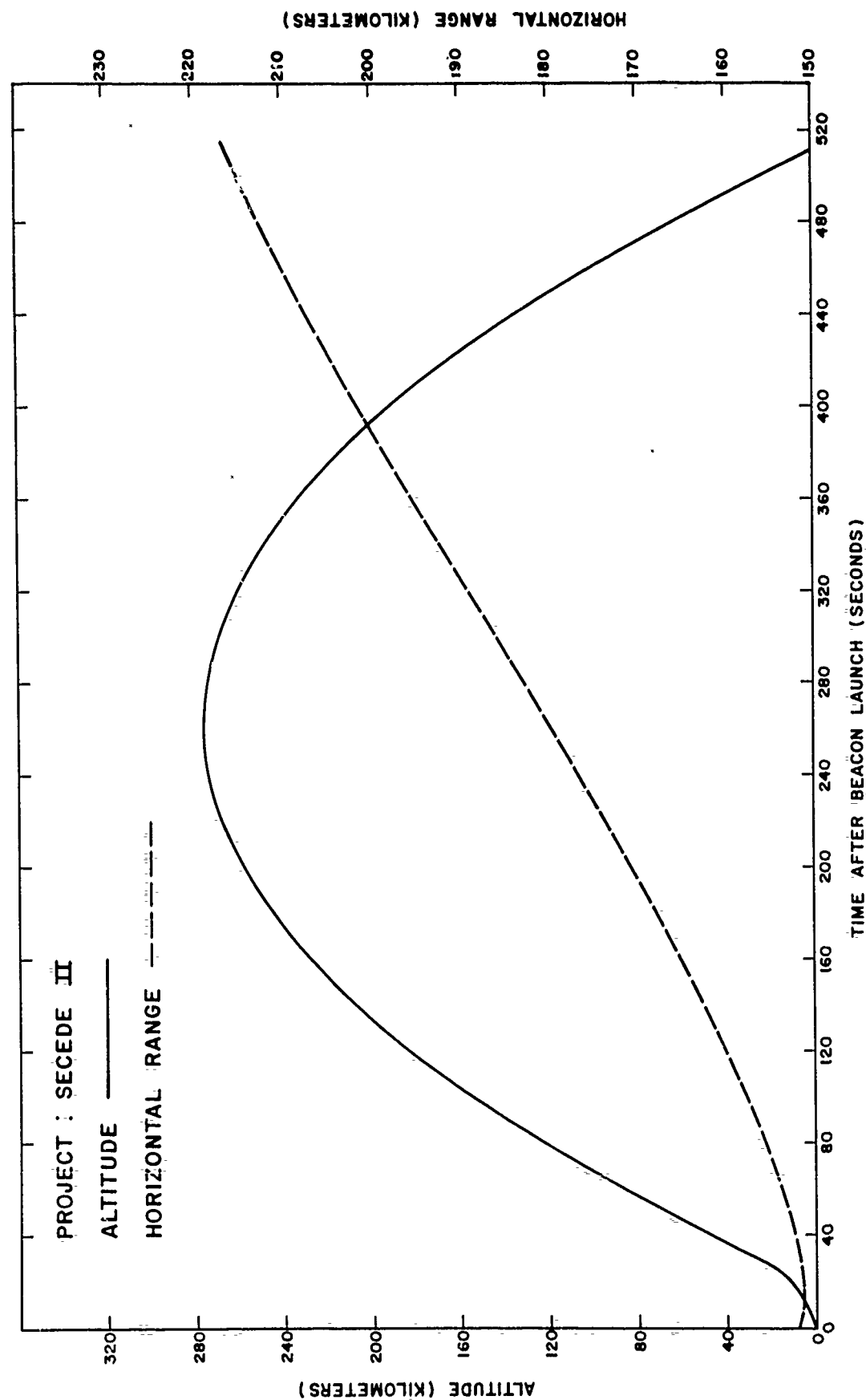


Figure 2. Typical beacon rocket trajectory

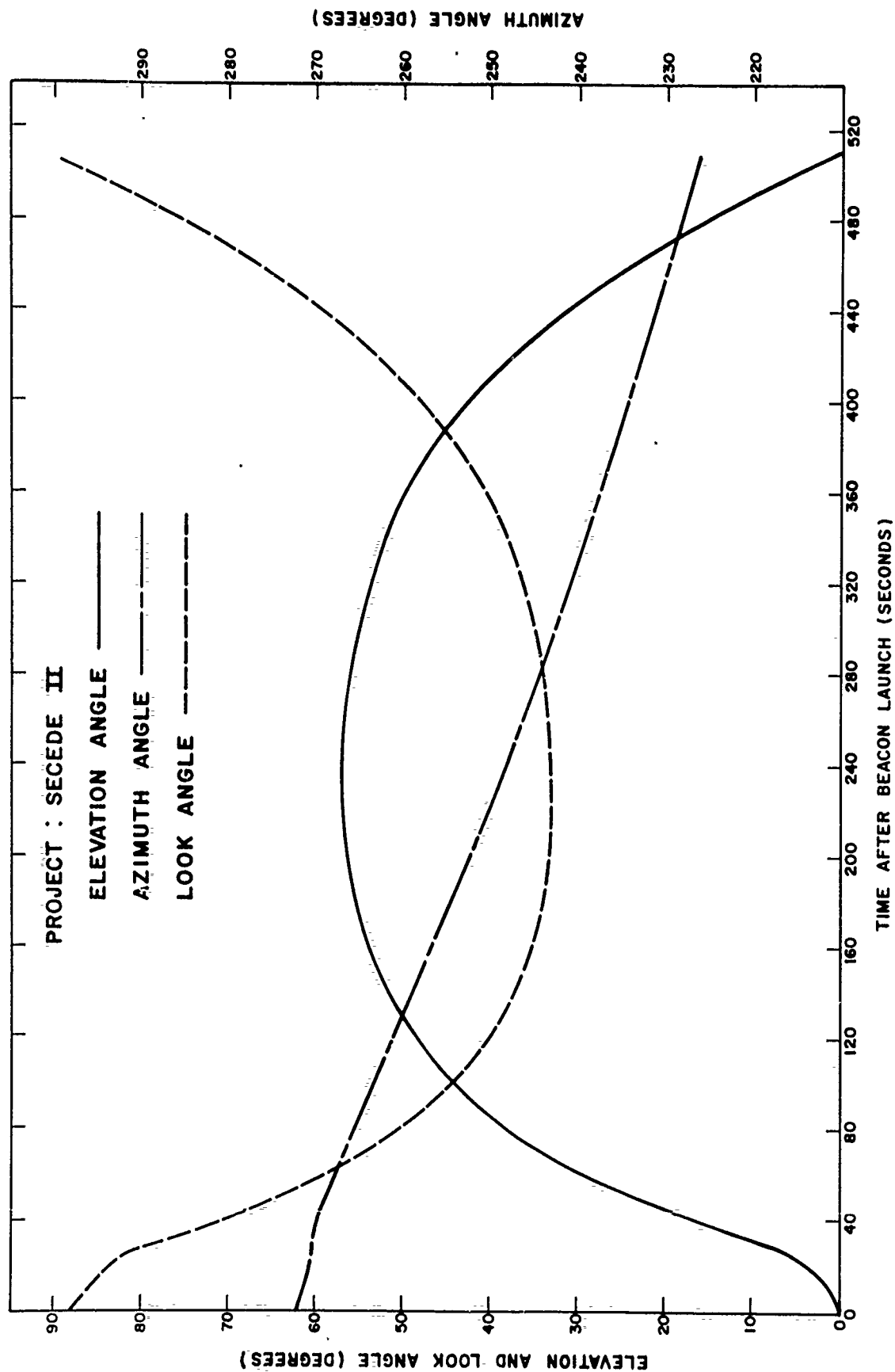


Figure 3. Angles derived from typical beacon rocket trajectory

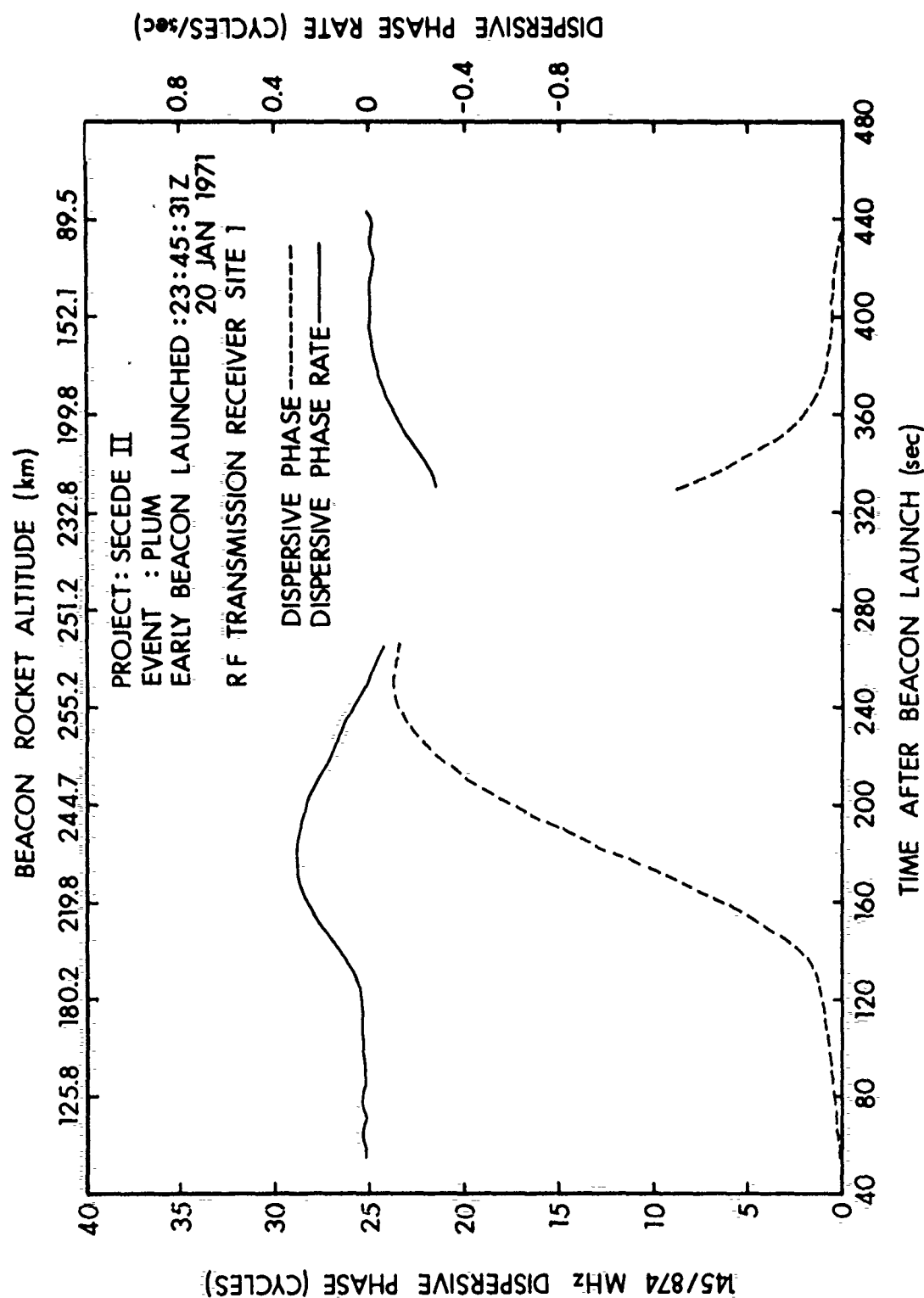


Figure 4. Site 1 dispersive phase for Event PLUM early beacon.

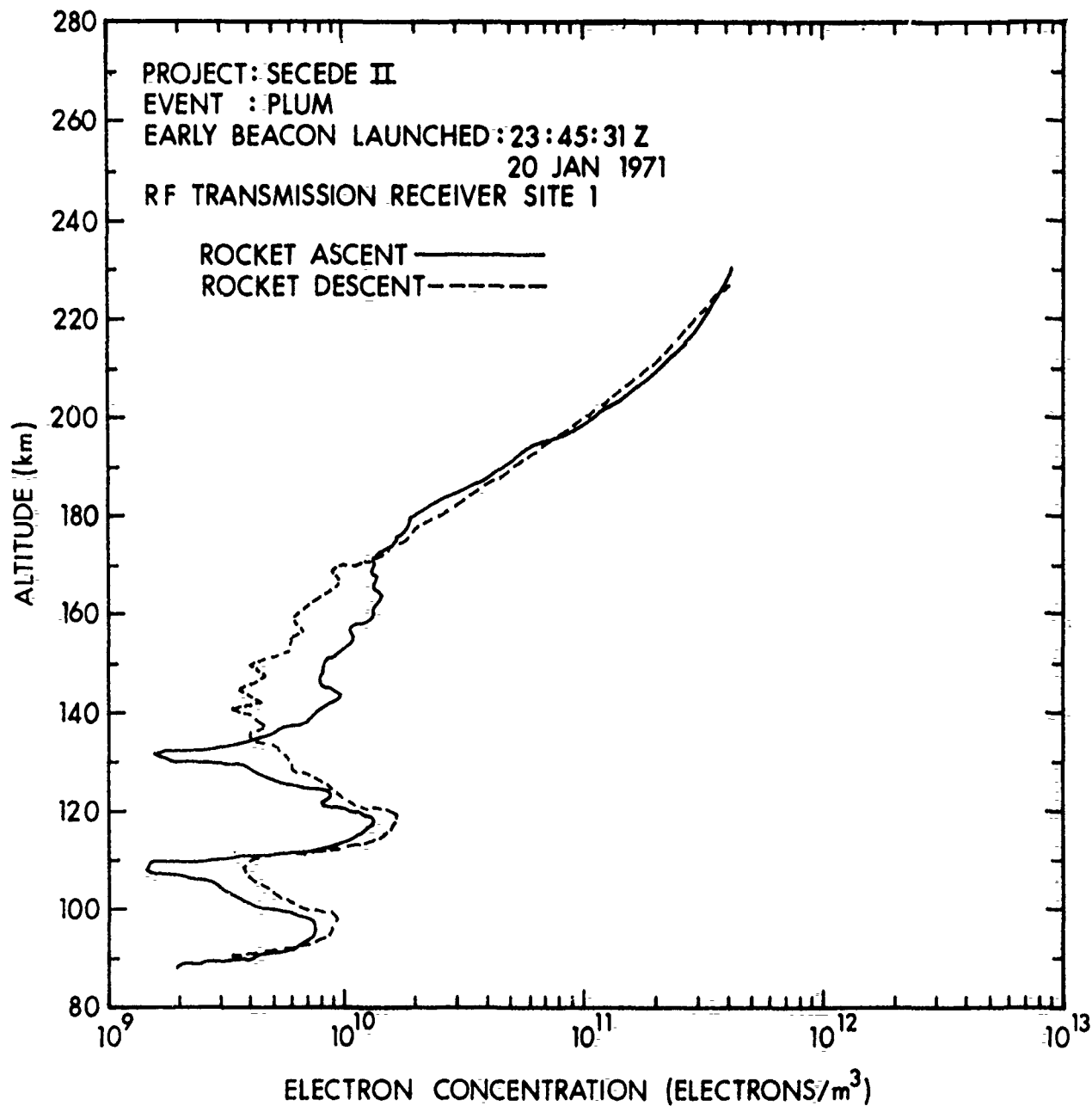


Figure 5. Site 1 electron density profile for Event PLUM early beacon.

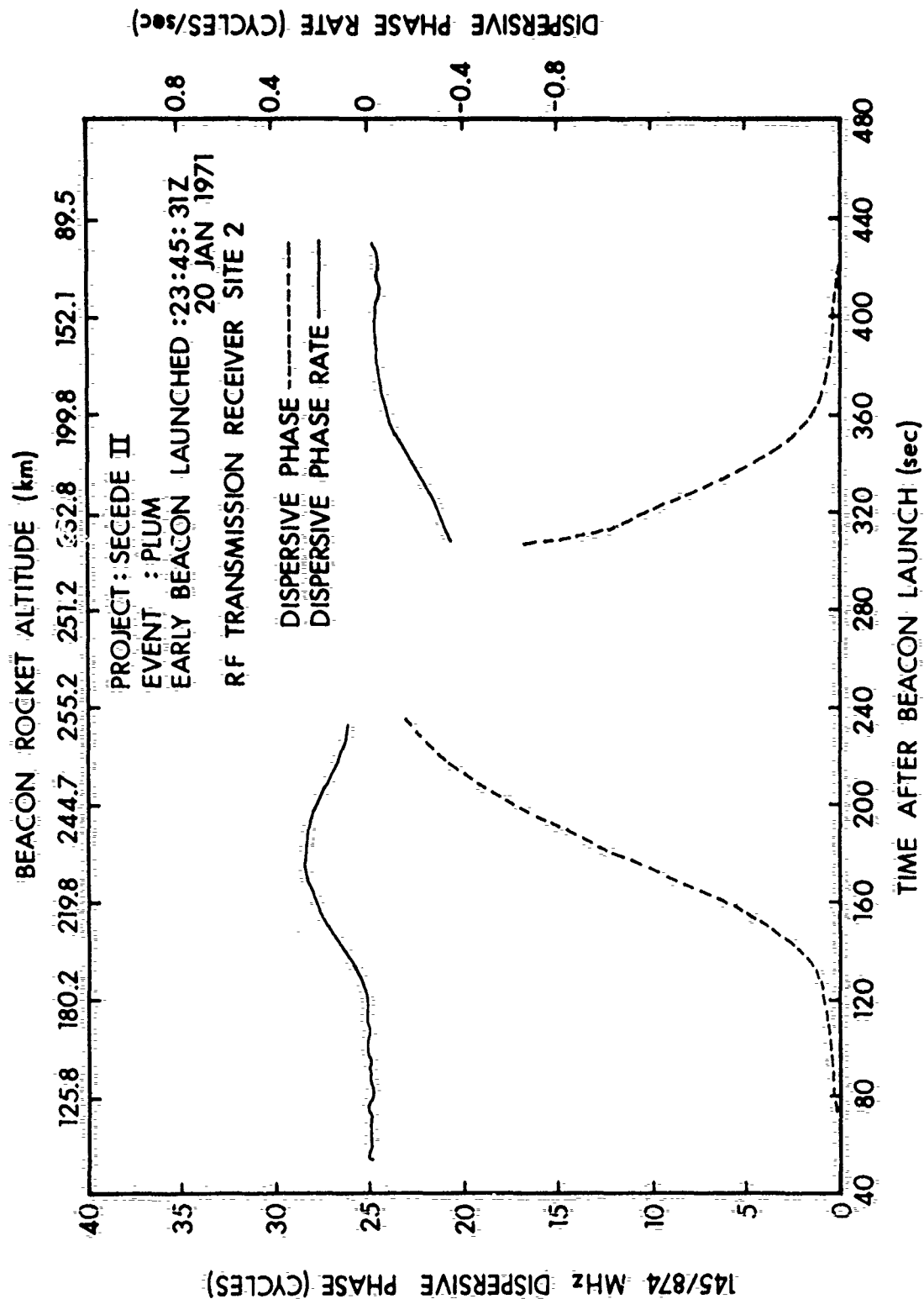


Figure 6. Site 2 dispersive phase for Event PLUM early beacon.

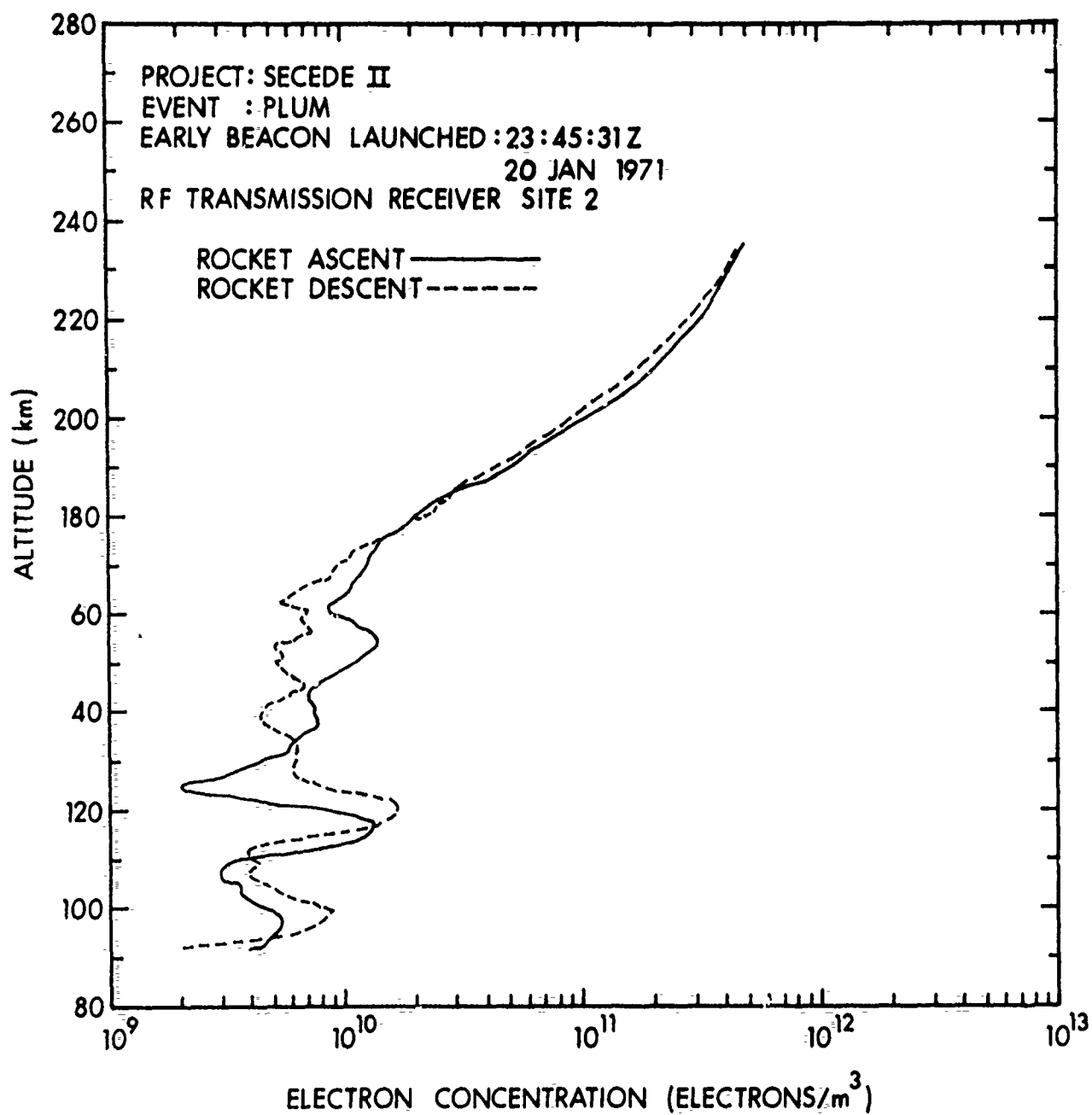


Figure 7. Site 2 electron density profile for Event PLUM early beacon.

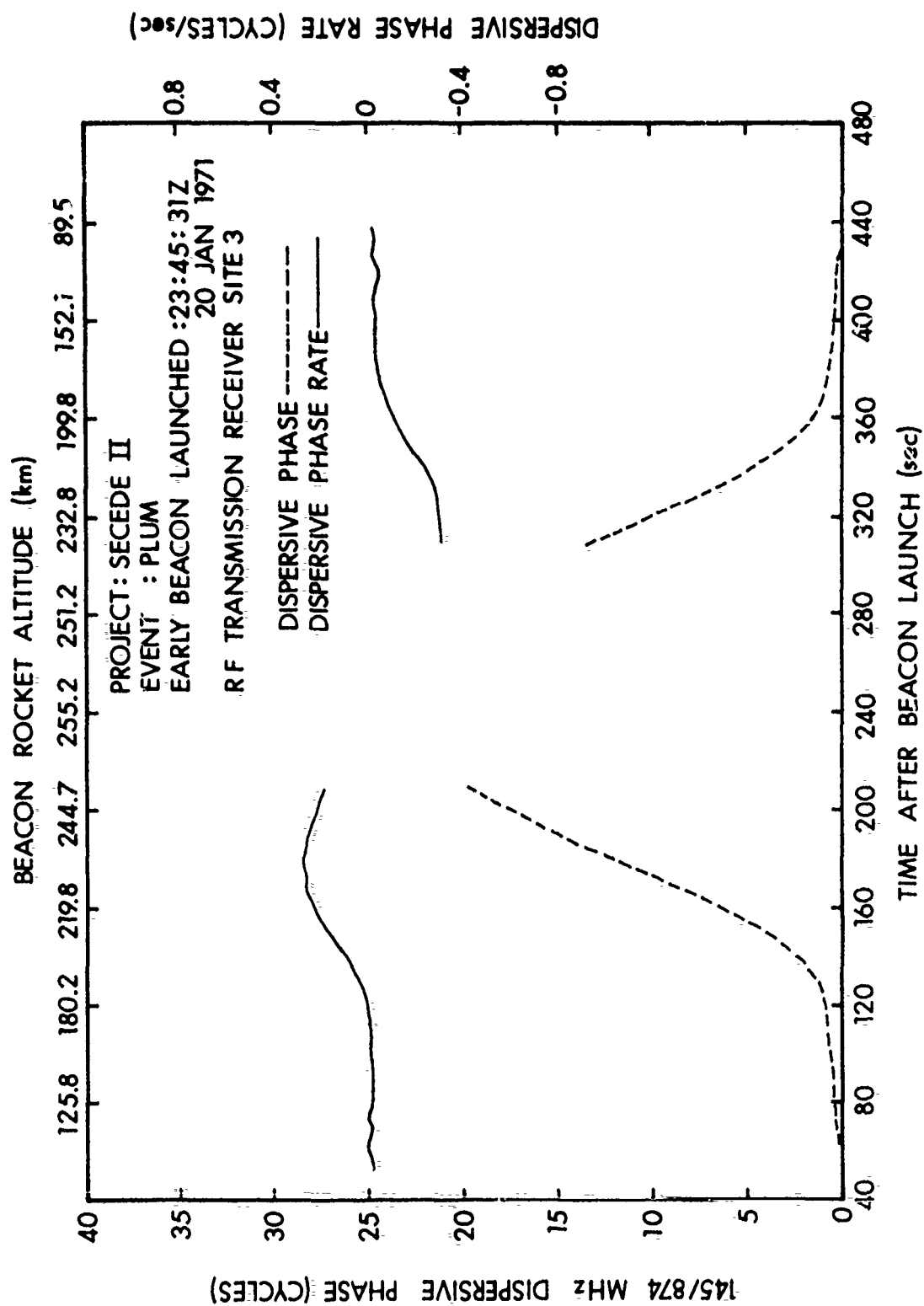


Figure 8. Site 3 dispersive phase for Event PLUM early beacon.

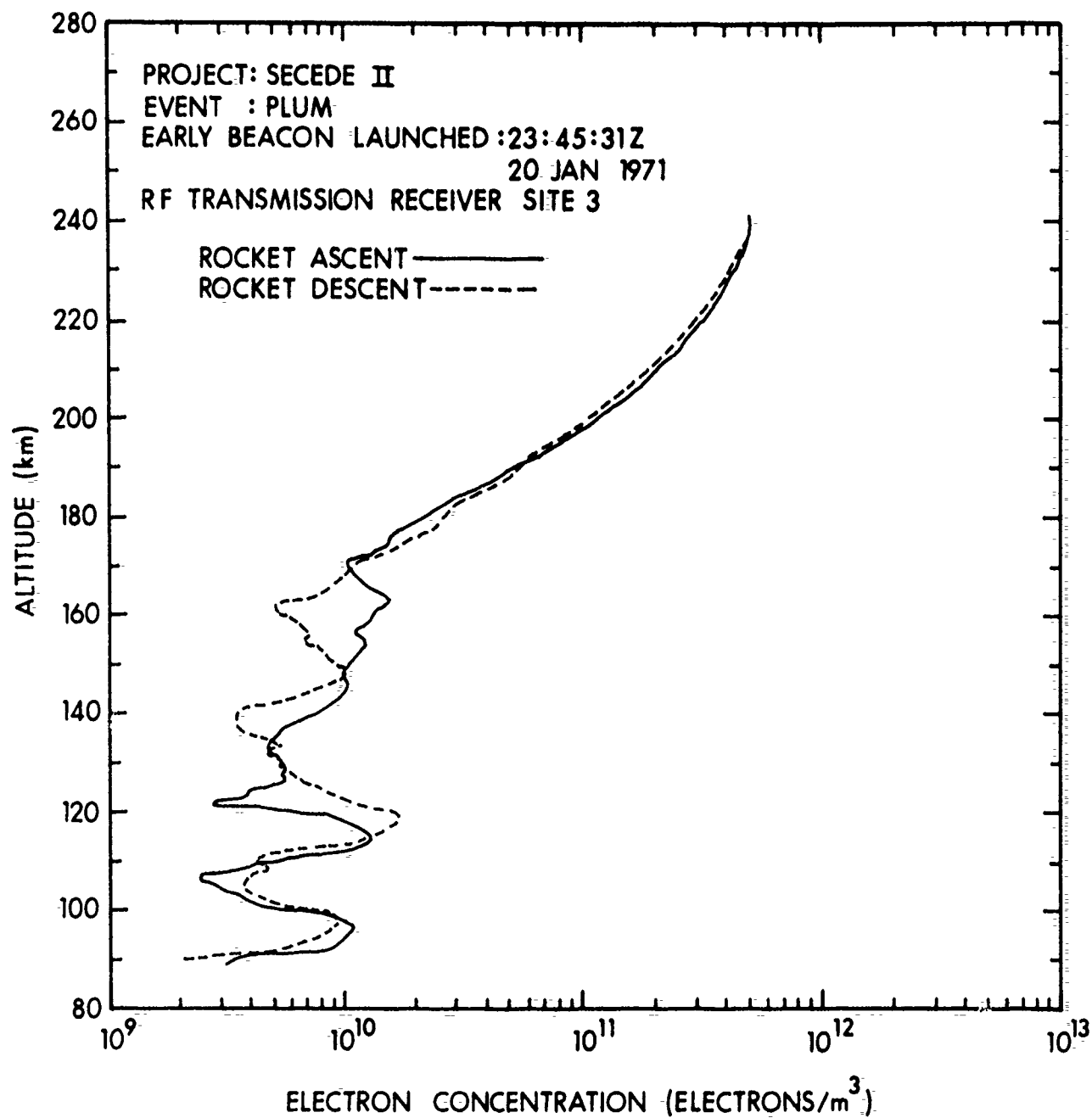


Figure 9. Site 3 electron density profile for Event PLUM early beacon.

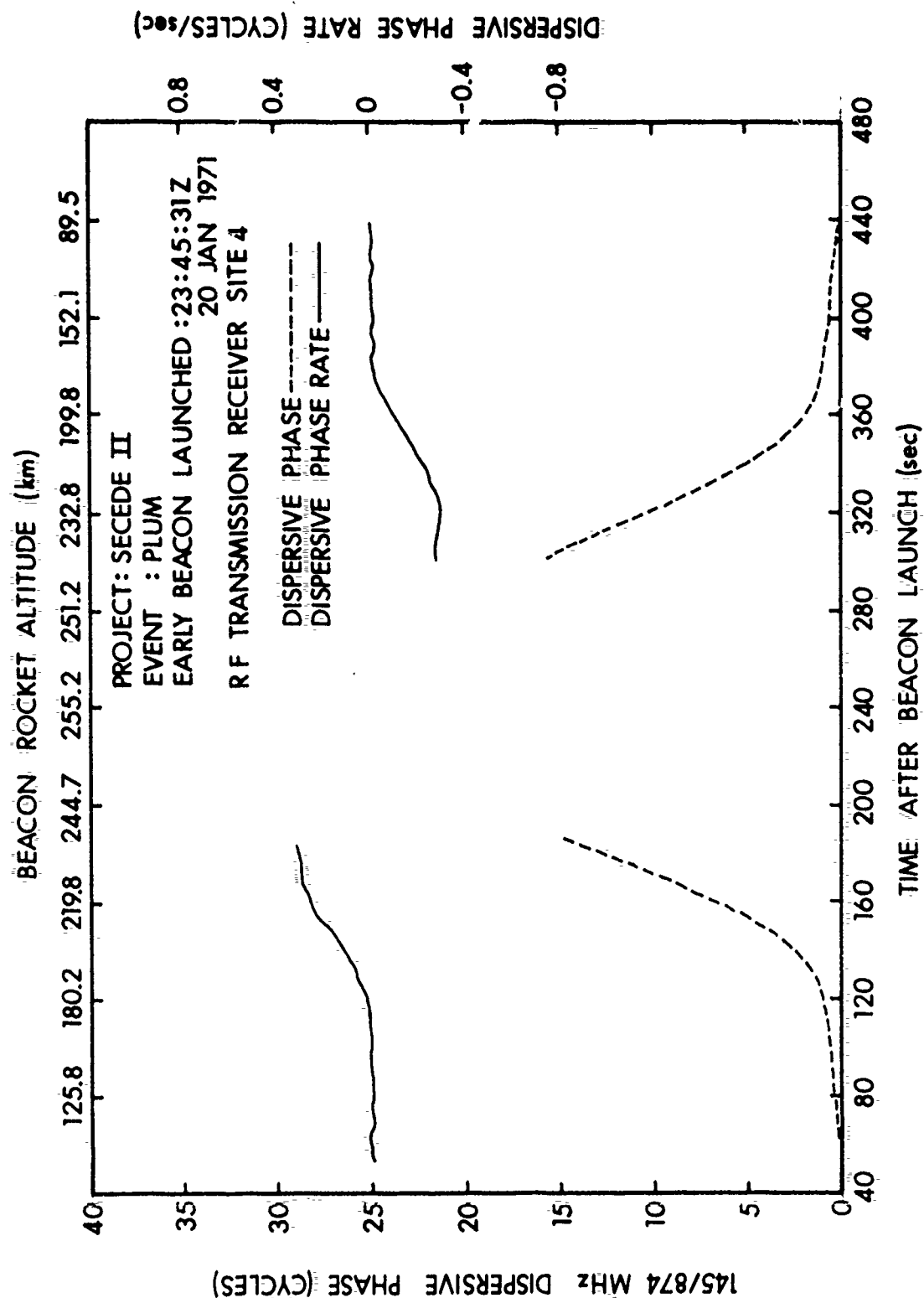


Figure 10. Site 4 dispersive phase for Event PLUM early beacon.

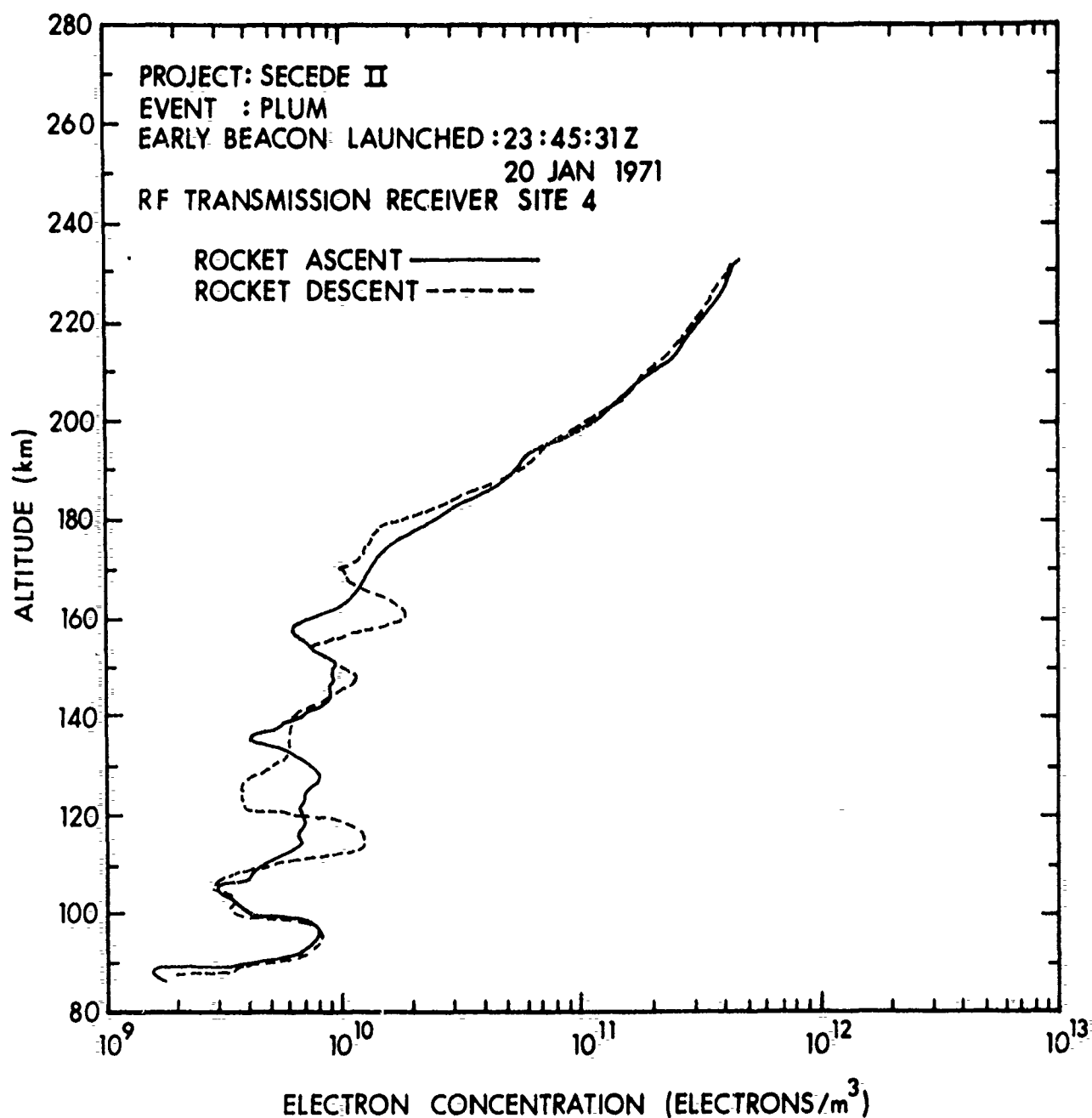


Figure 11. Site 4 electron density profile for Event PLUM early beacon.

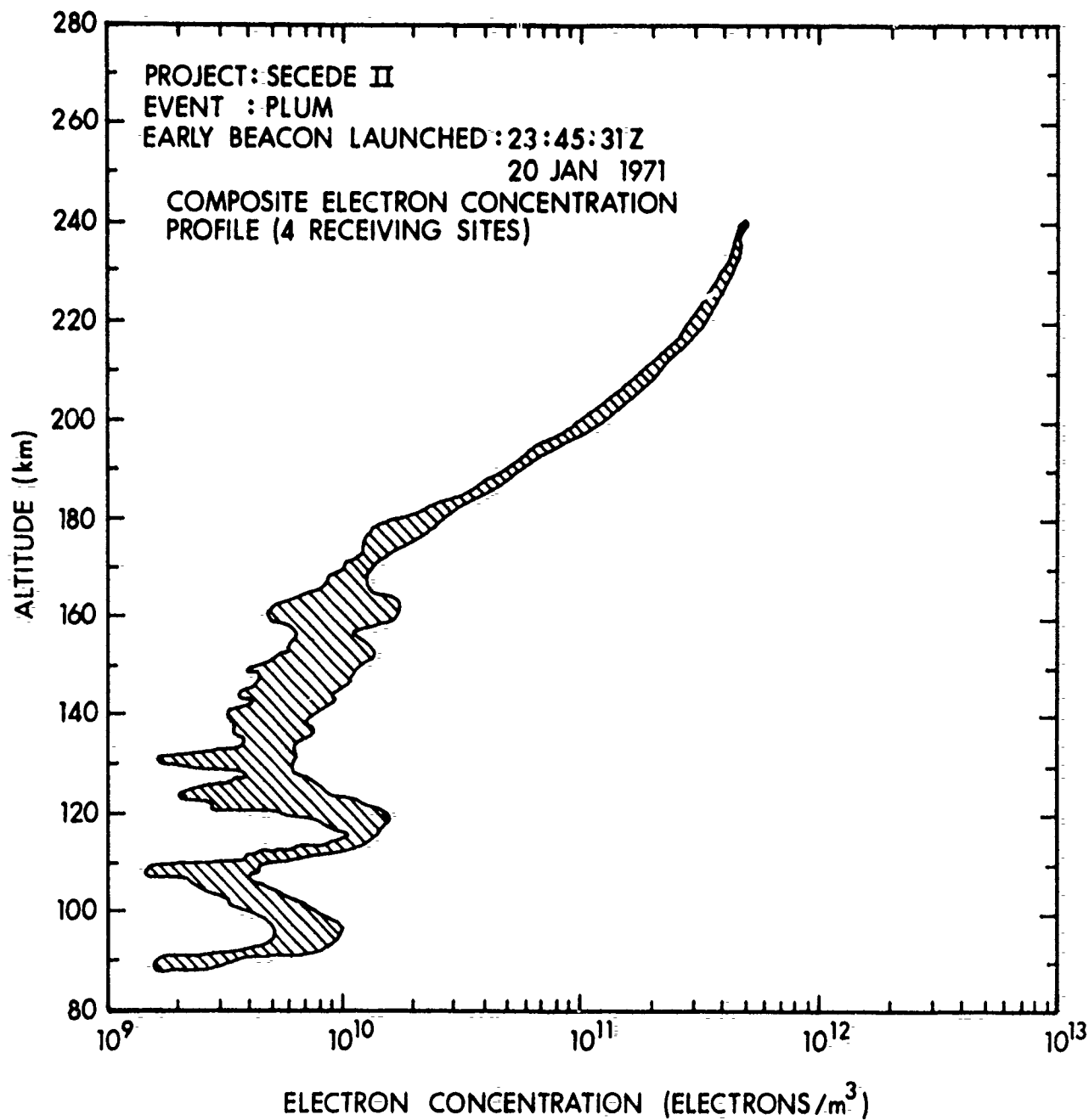


Figure 12. Four-site composite electron density profile for Event PLUM early beacon.

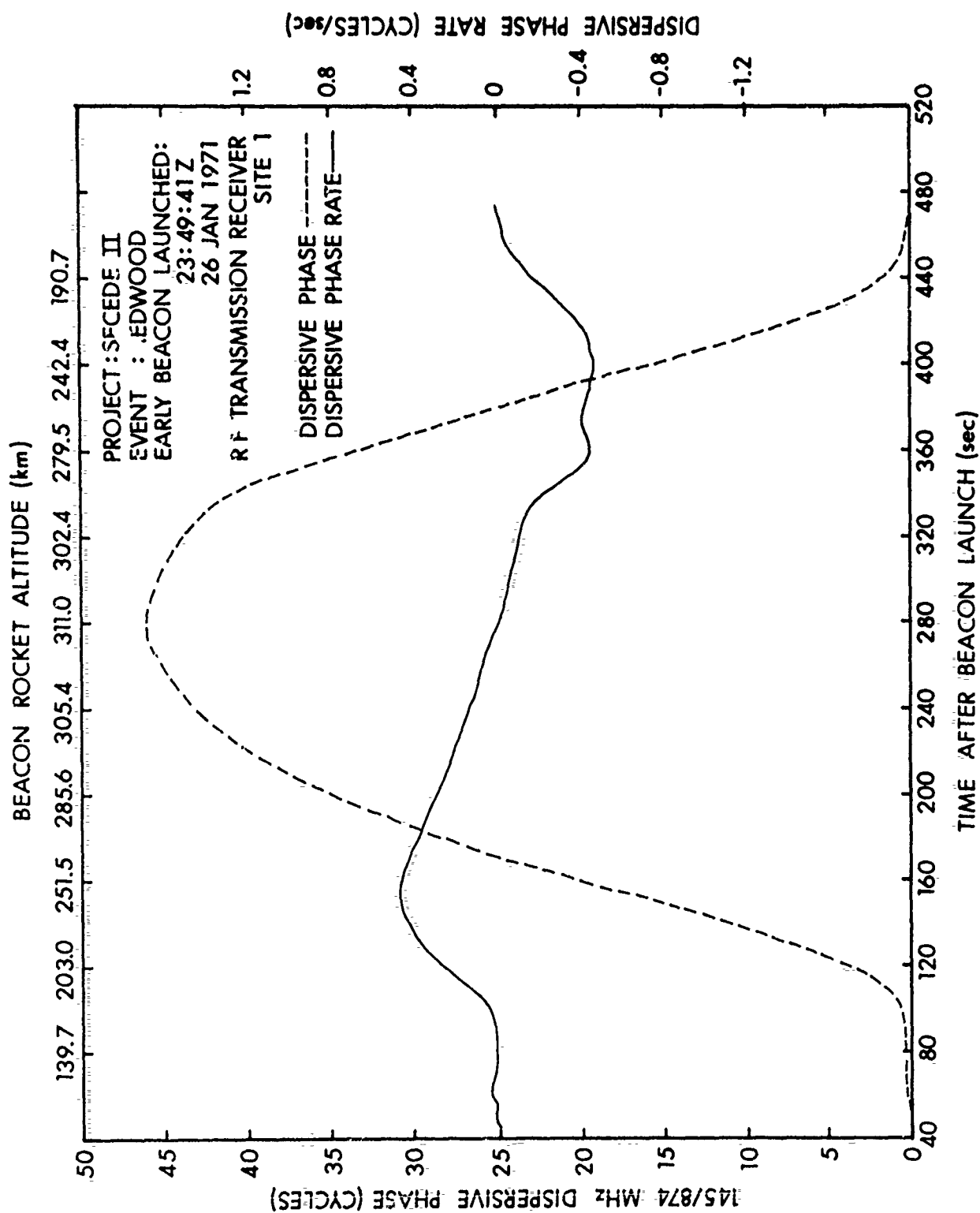


Figure 13. Site 1 dispersive phase for Event REDWOOD early beacon.

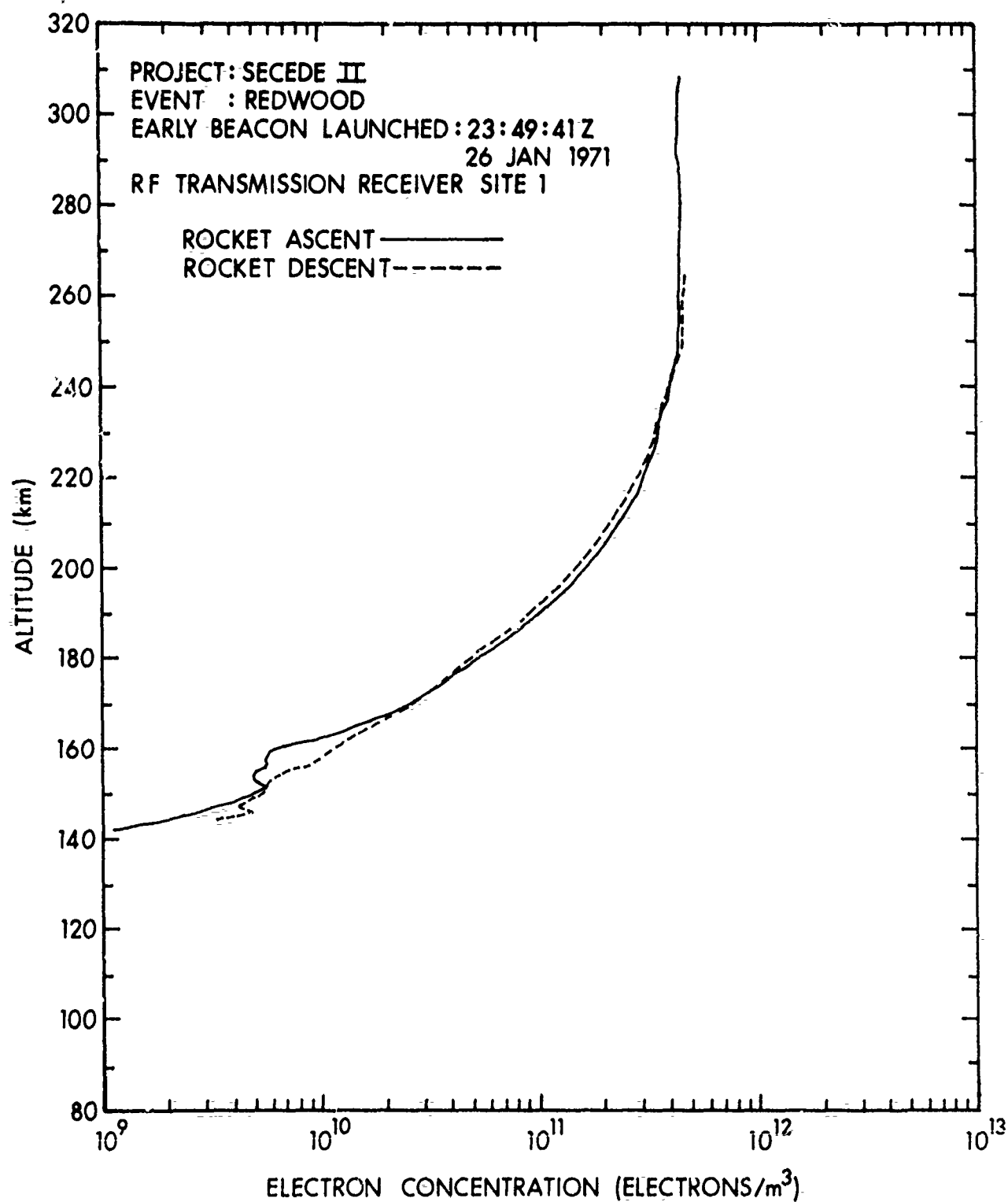


Figure 14. Site 1 electron-density profile for Event REDWOOD early beacon.

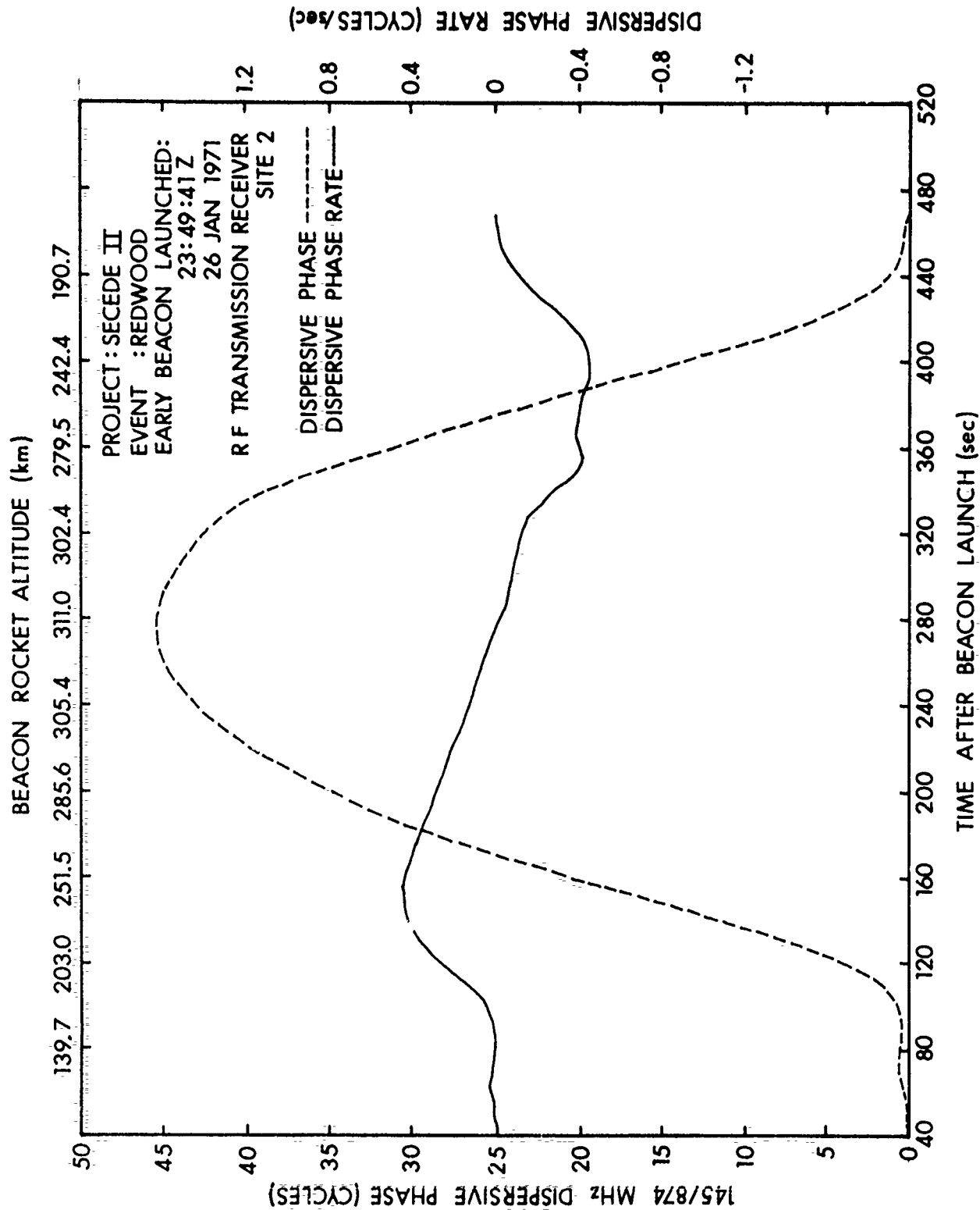


Figure 15. Site 2 dispersive phase for Event REDWOOD early beacon.

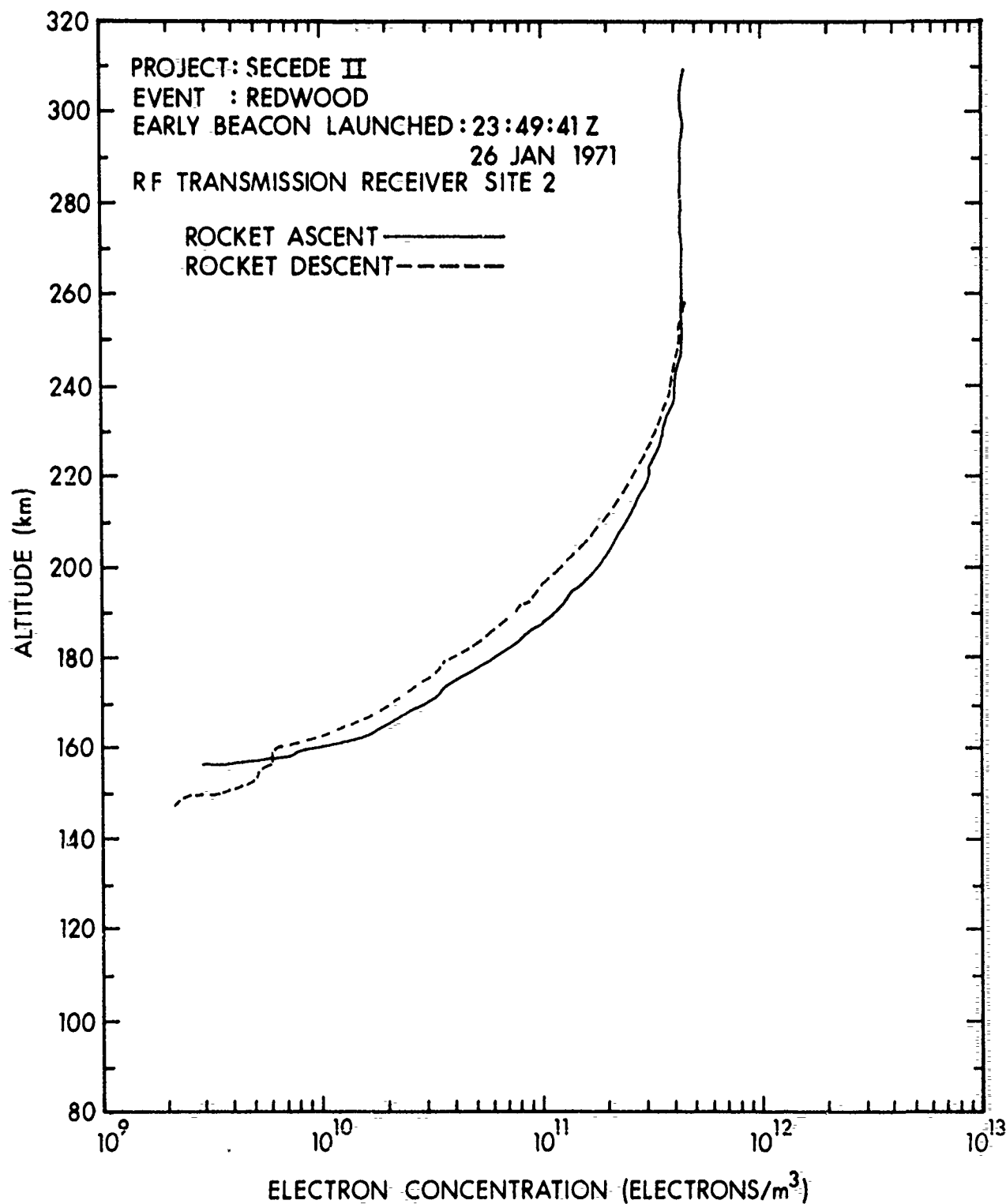


Figure 16. Site 2 electron density profile for Event REDWOOD early beacon.

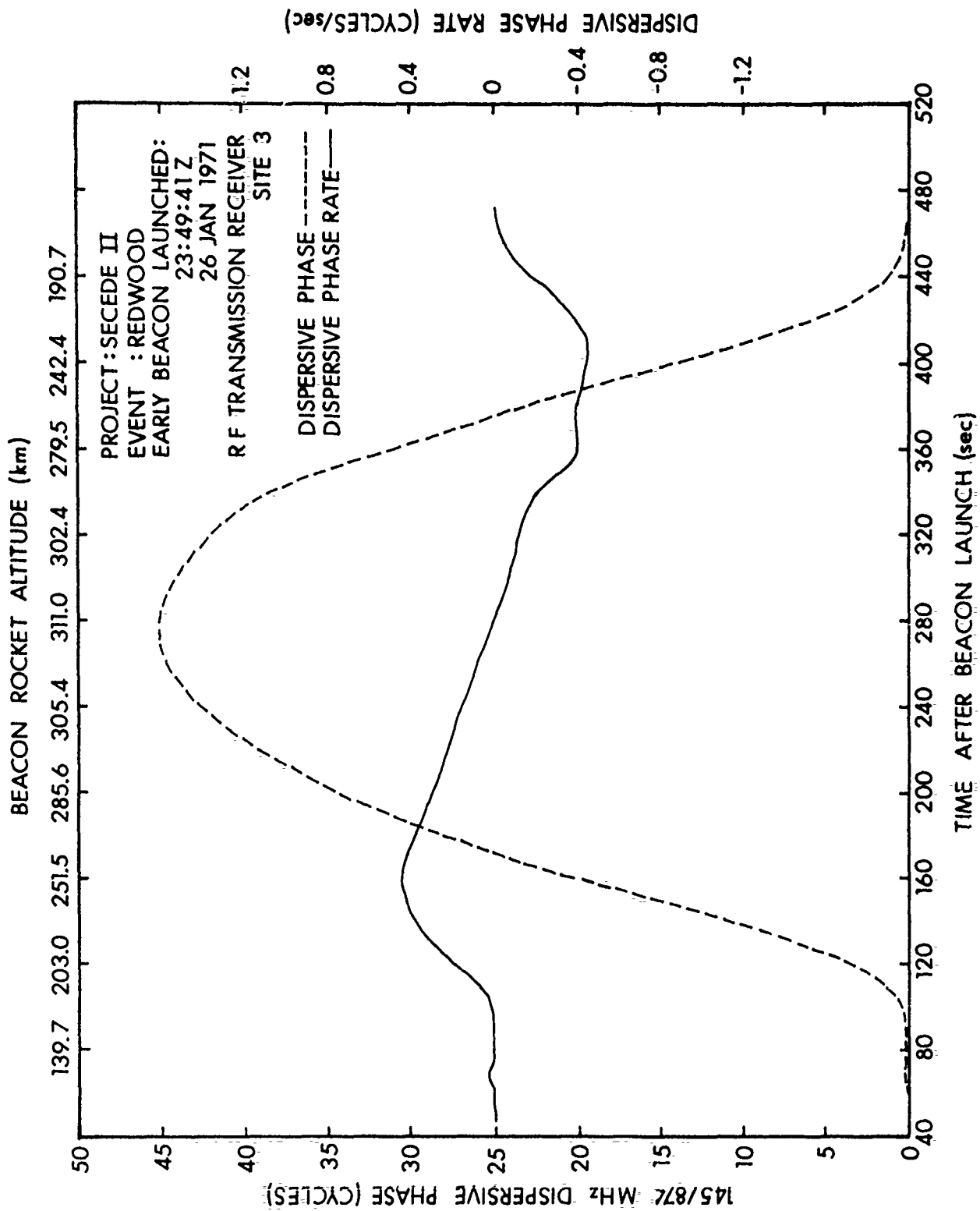


Figure 17. Site 3 dispersive phase for Event REDWOOD early beacon.

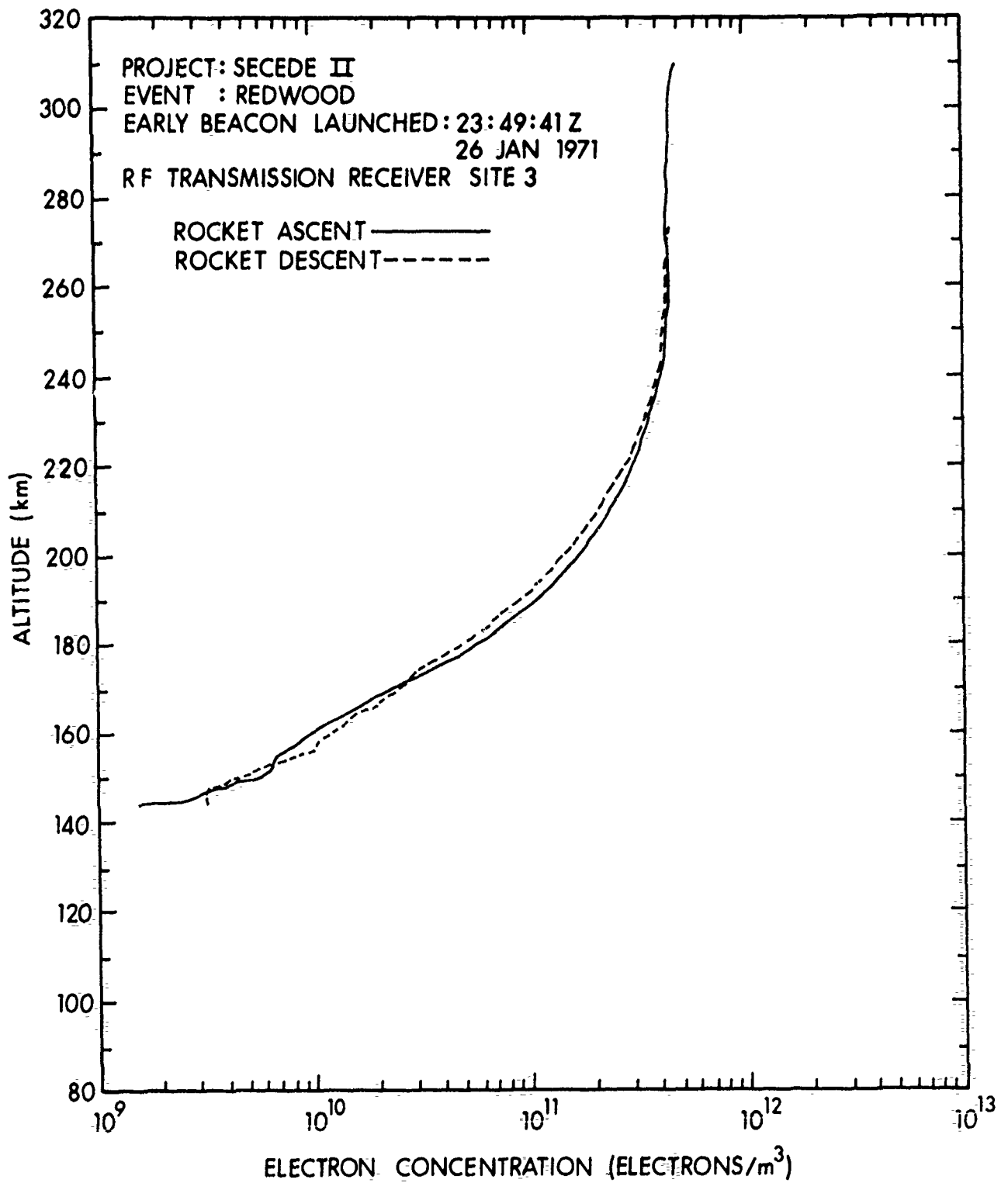


Figure 18. Site 3 electron density profile for Event REDWOOD early beacon.

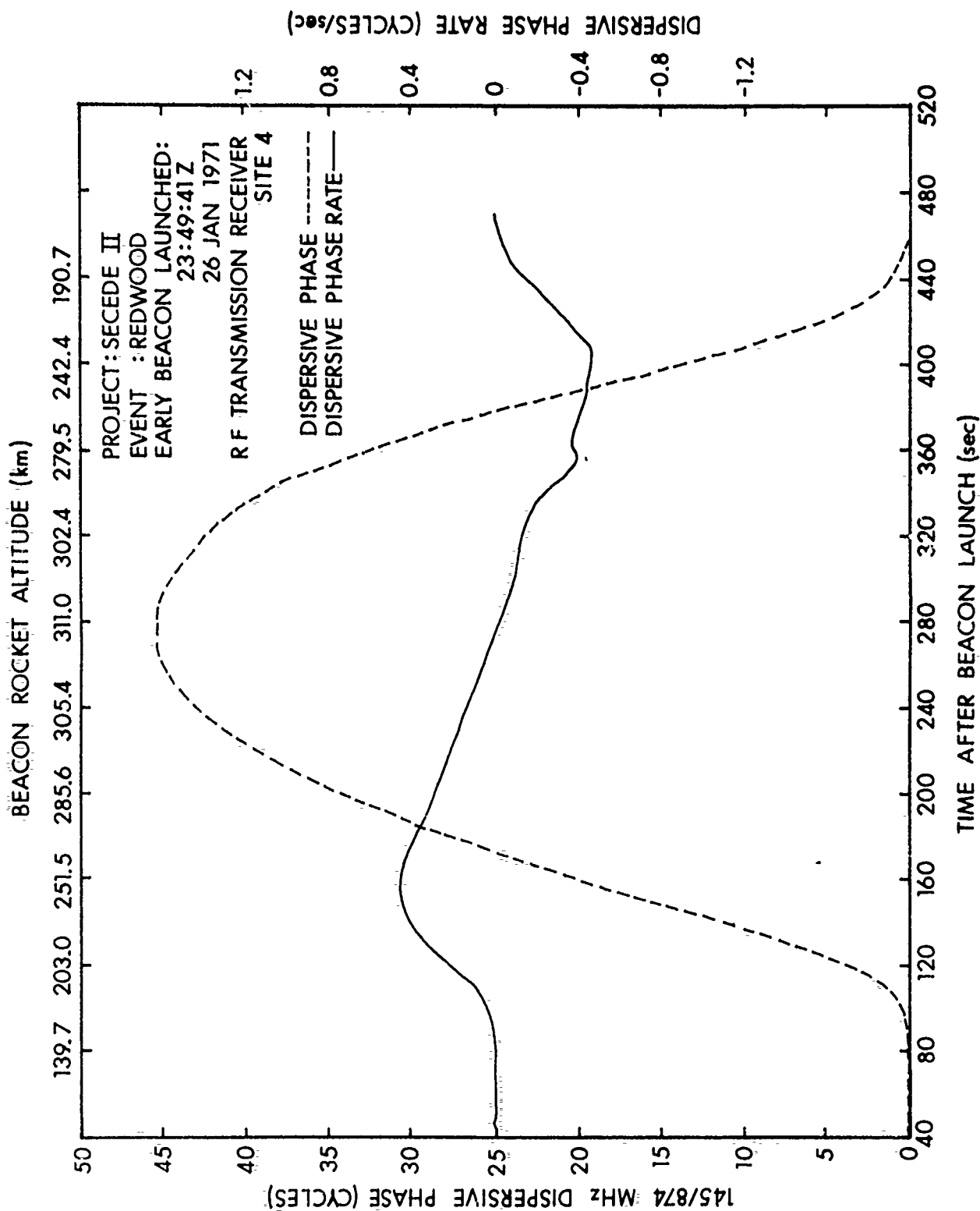


Figure 19. Site 4 dispersive phase for Event REDWOOD early beacon.

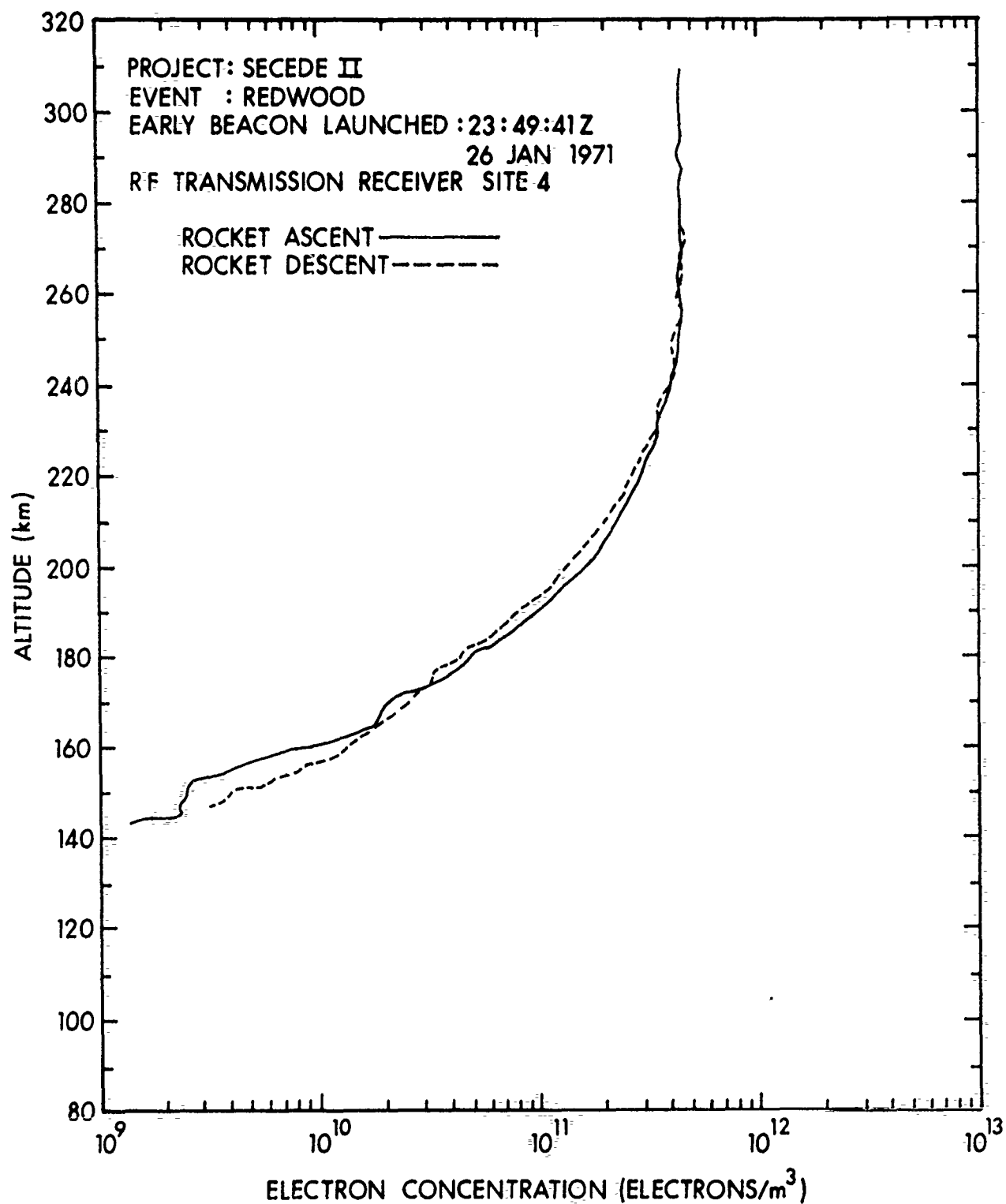


Figure 20. Site 4 electron density profile for Event REDWOOD early beacon.

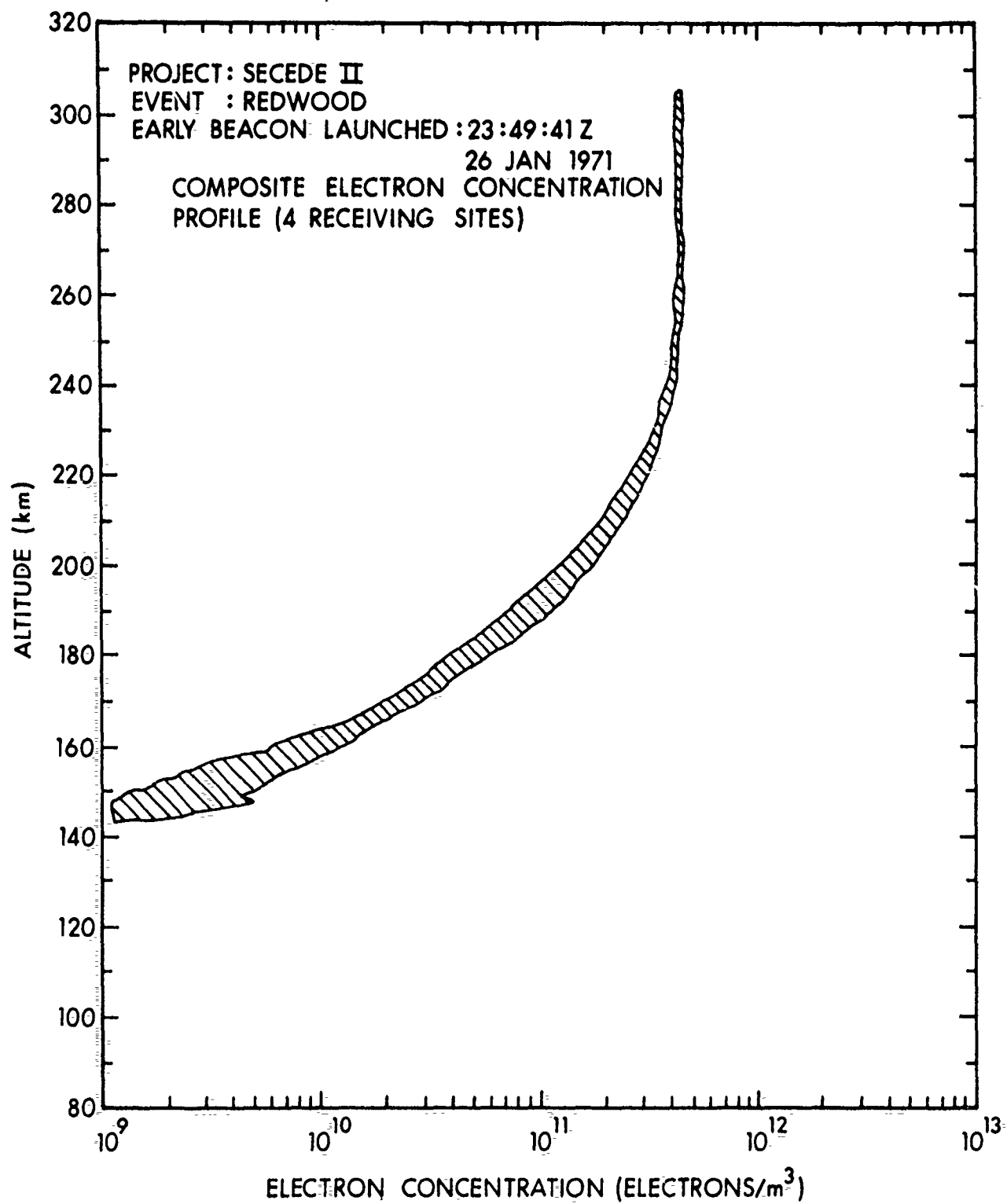


Figure 21. Four-site composite electron density profile for Event REDWOOD early beacon.

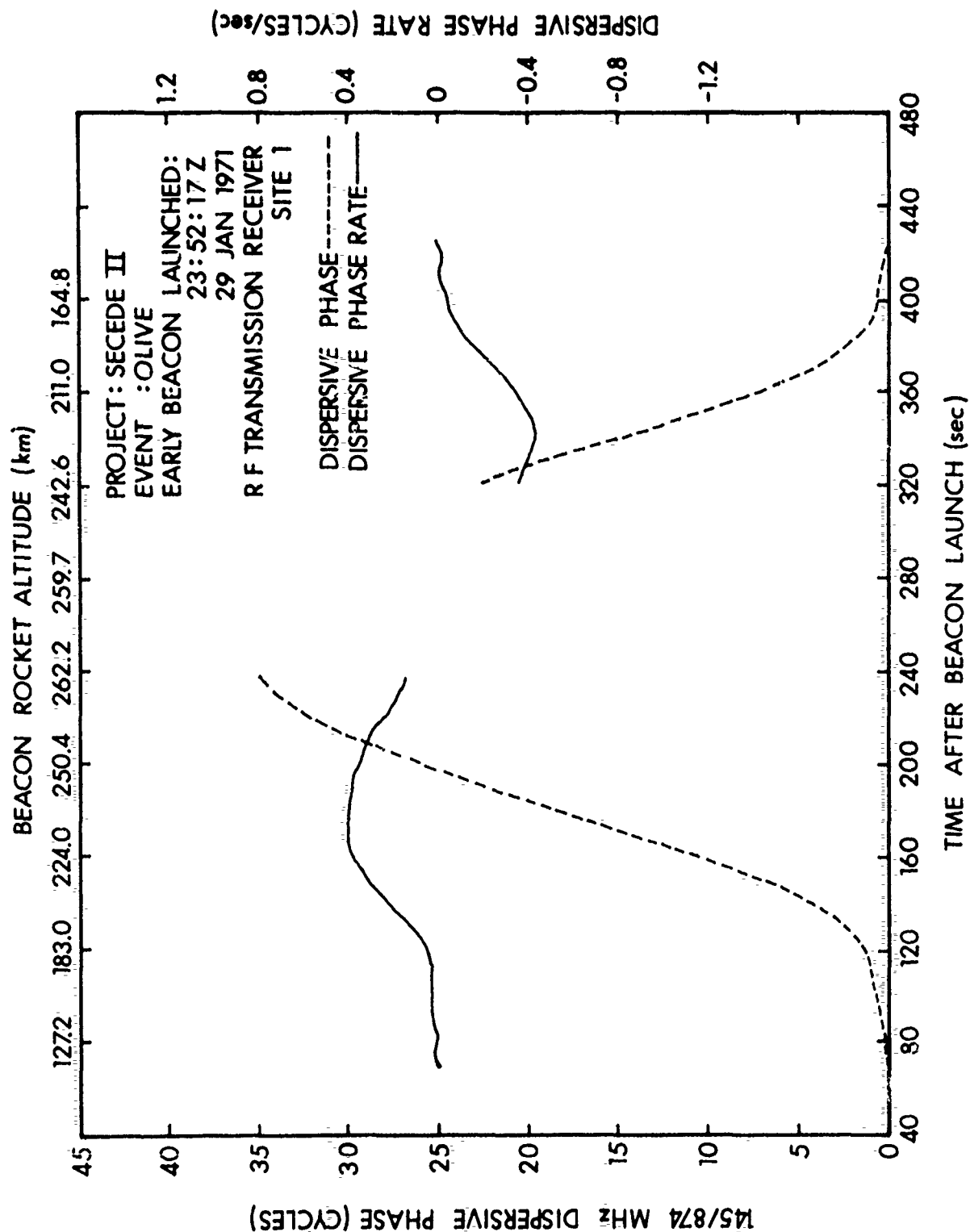


Figure 22. Site 1 dispersive phase for Event OLIVE early beacon.

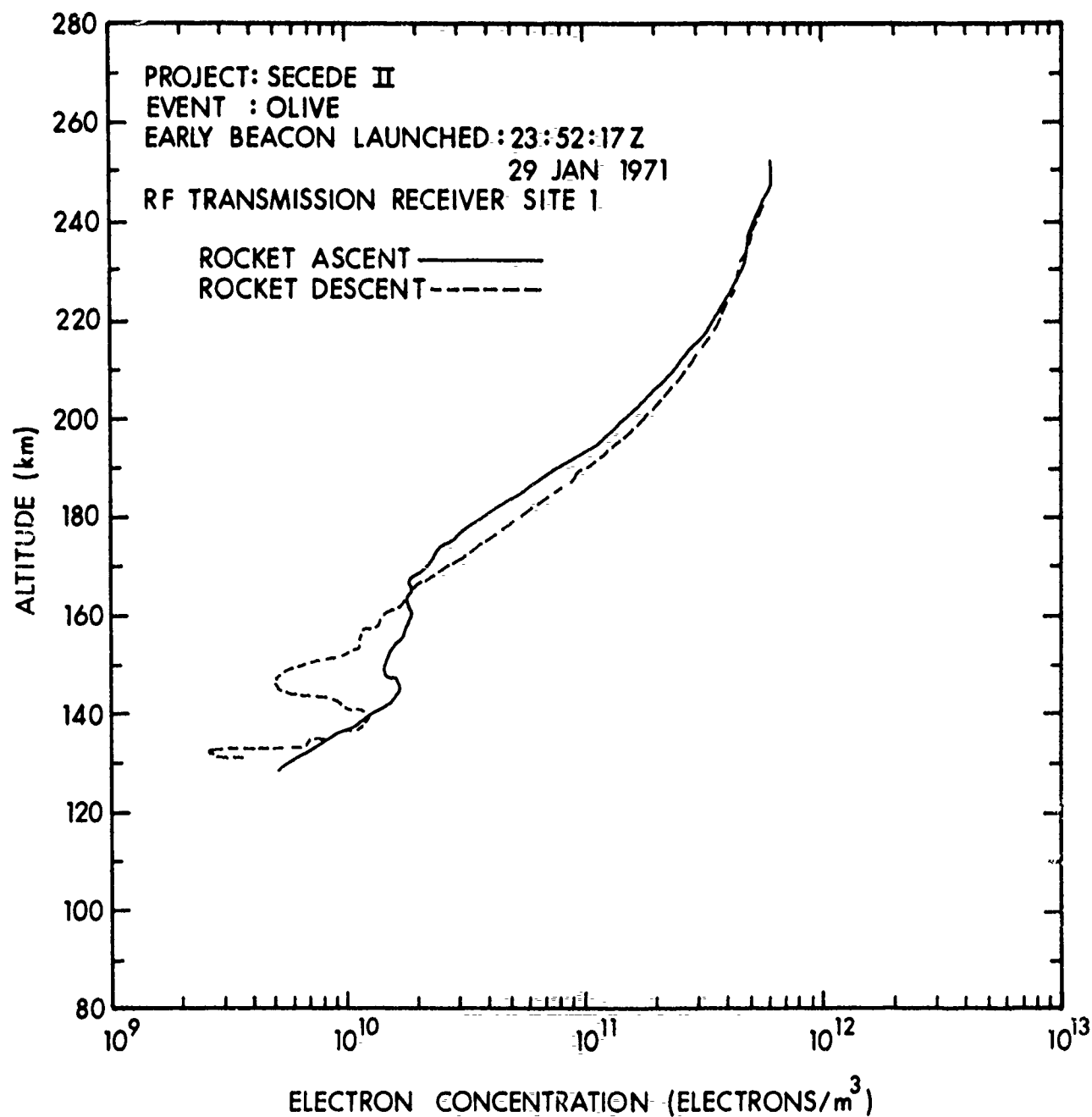


Figure 23. Site 1 electron density profile for Event OLIVE early beacon.

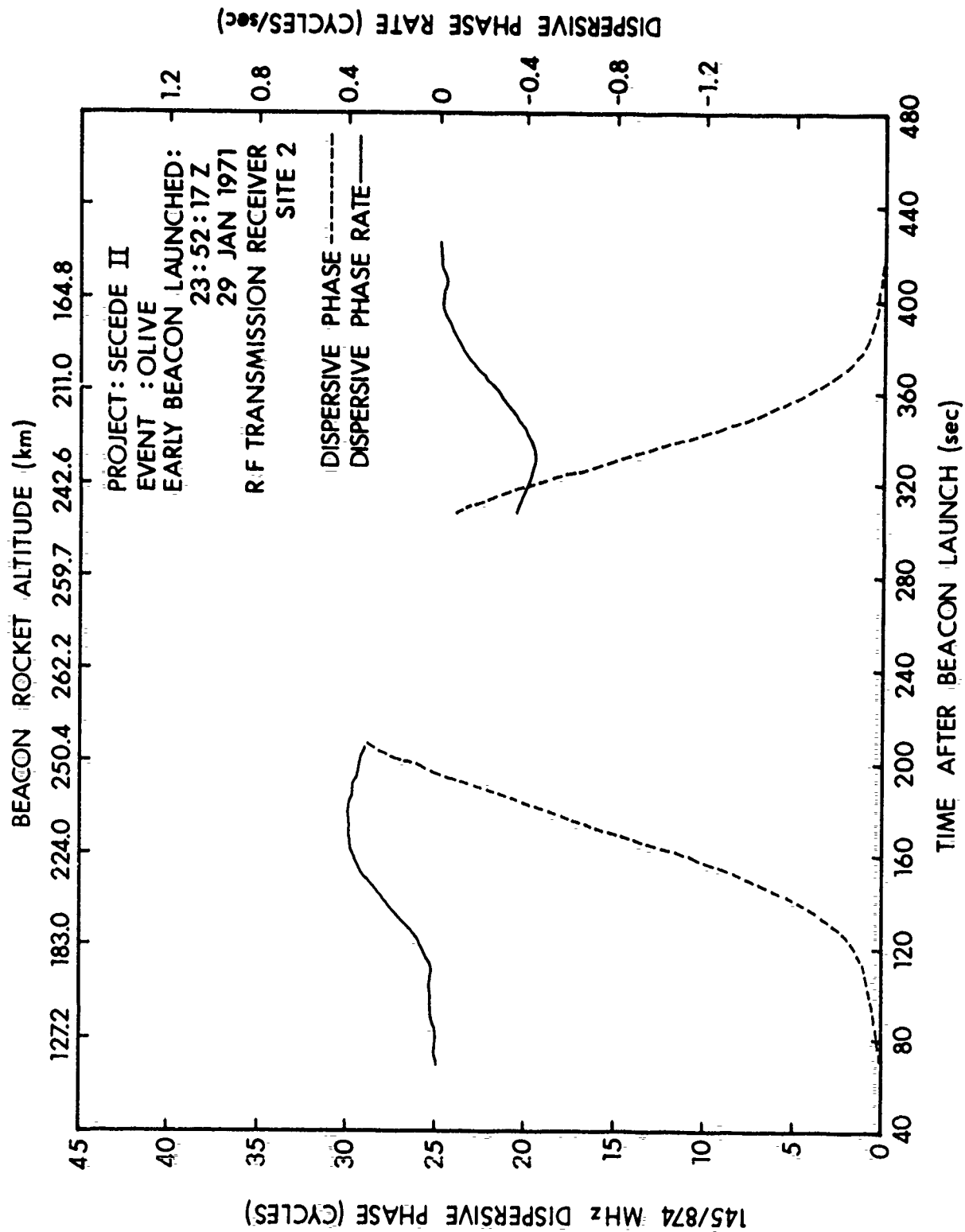


Figure 24. Site 2 dispersive phase for Event OLIVE early beacon.

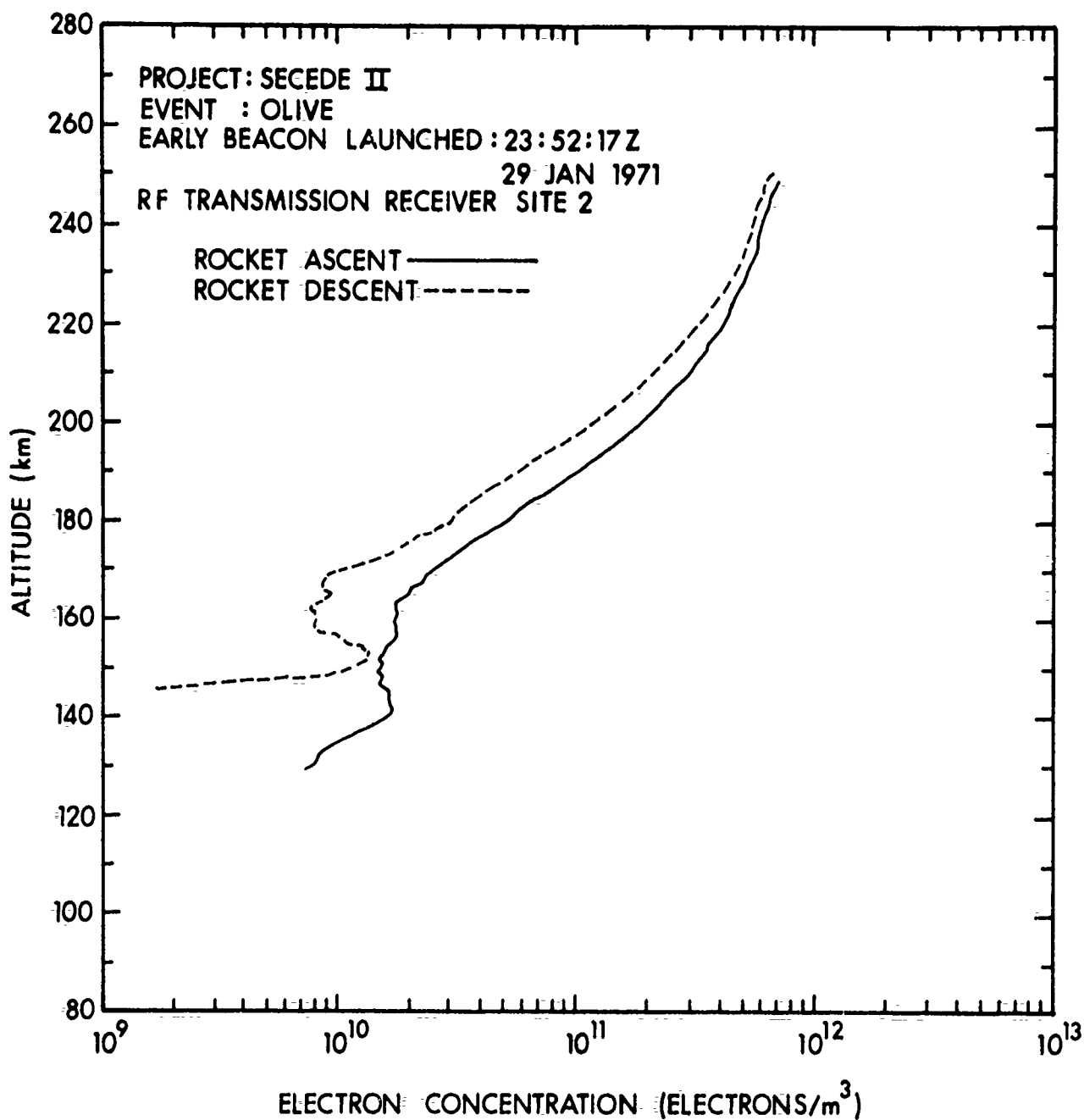


Figure 25. Site 2 electron density profile for Event OLIVE early beacon.

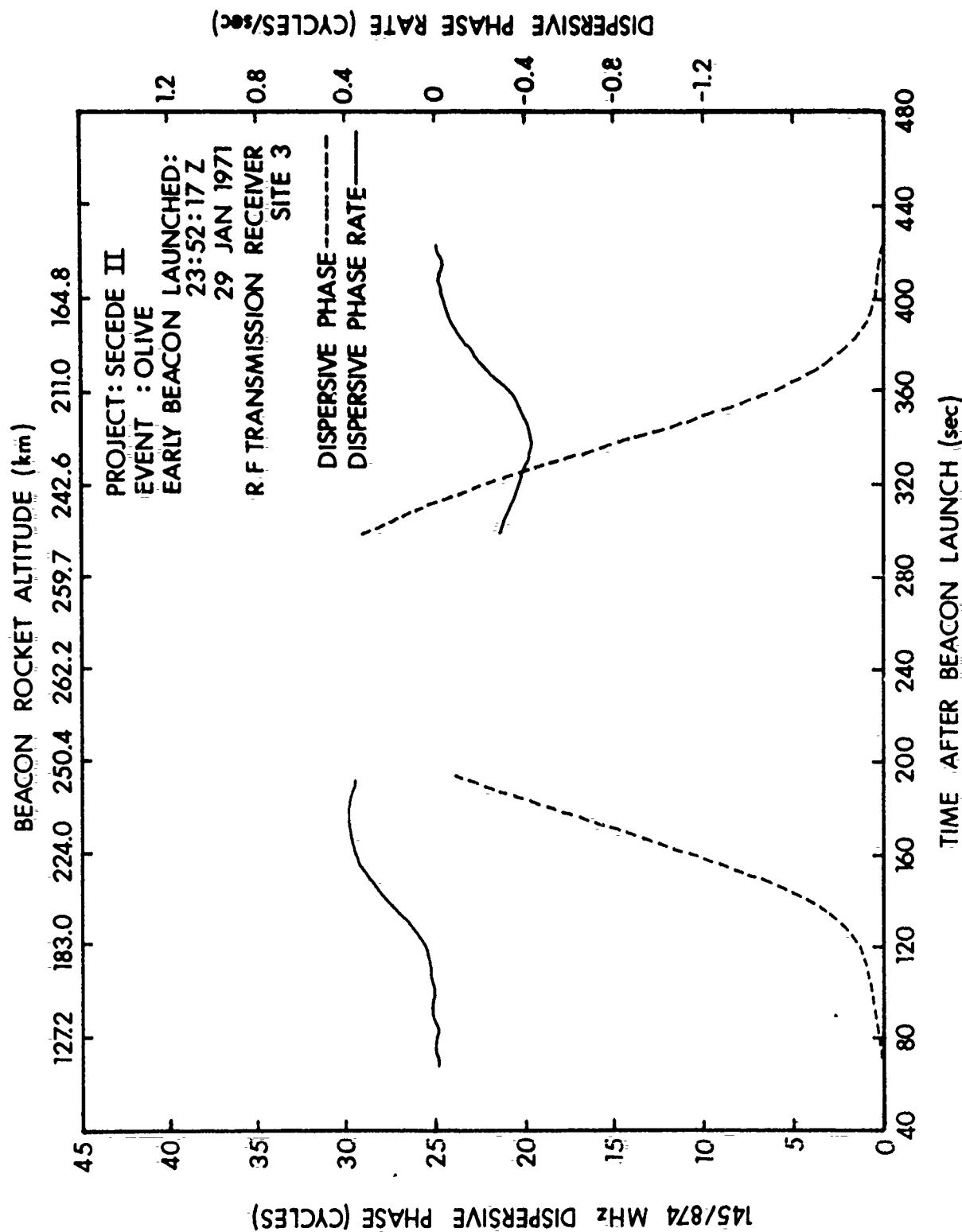


Figure 26. Site 3 dispersive phase for Event OLIVE early beacon.

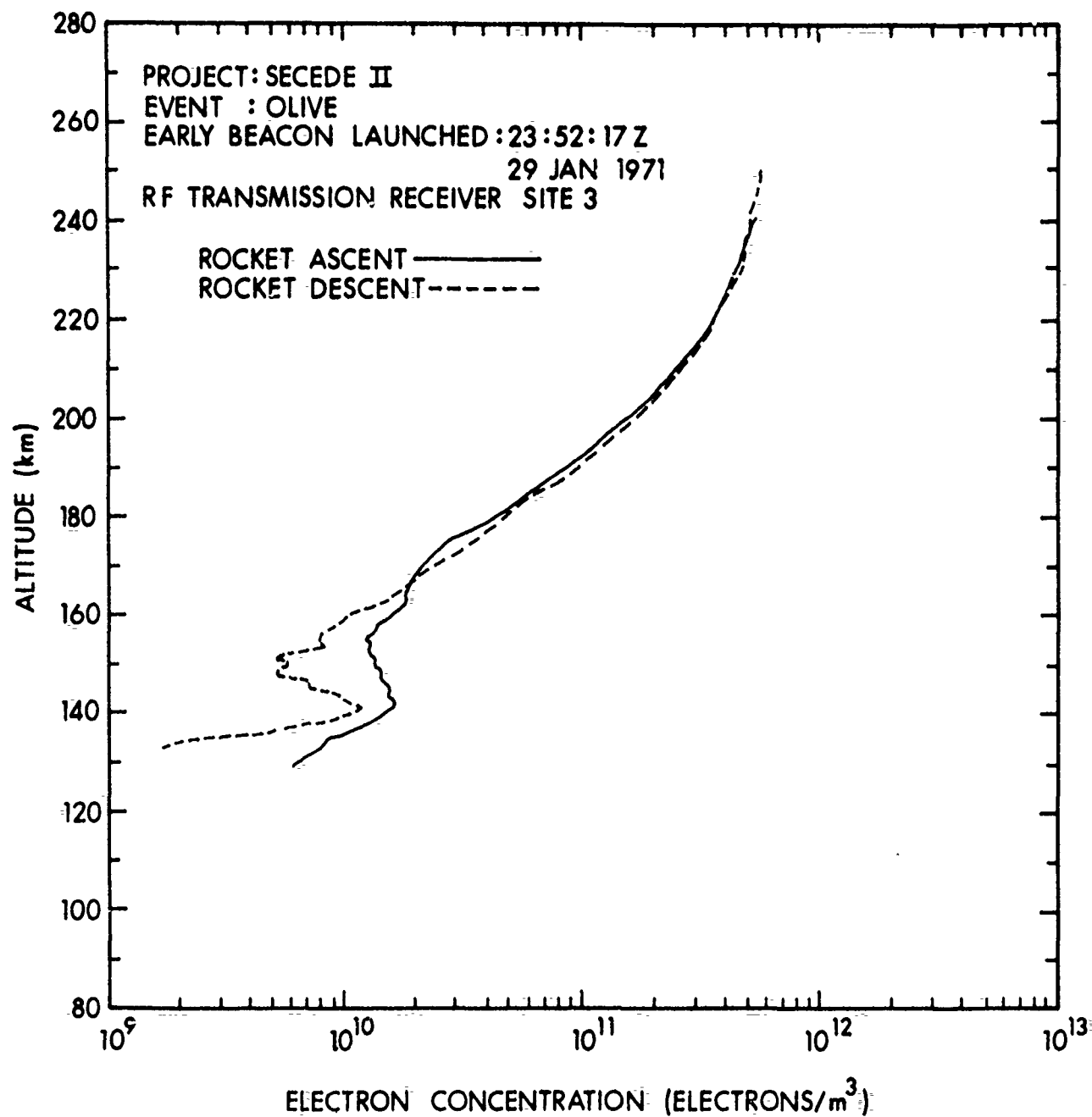


Figure 27. Site 3 electron density profile for Event OLIVE early beacon.

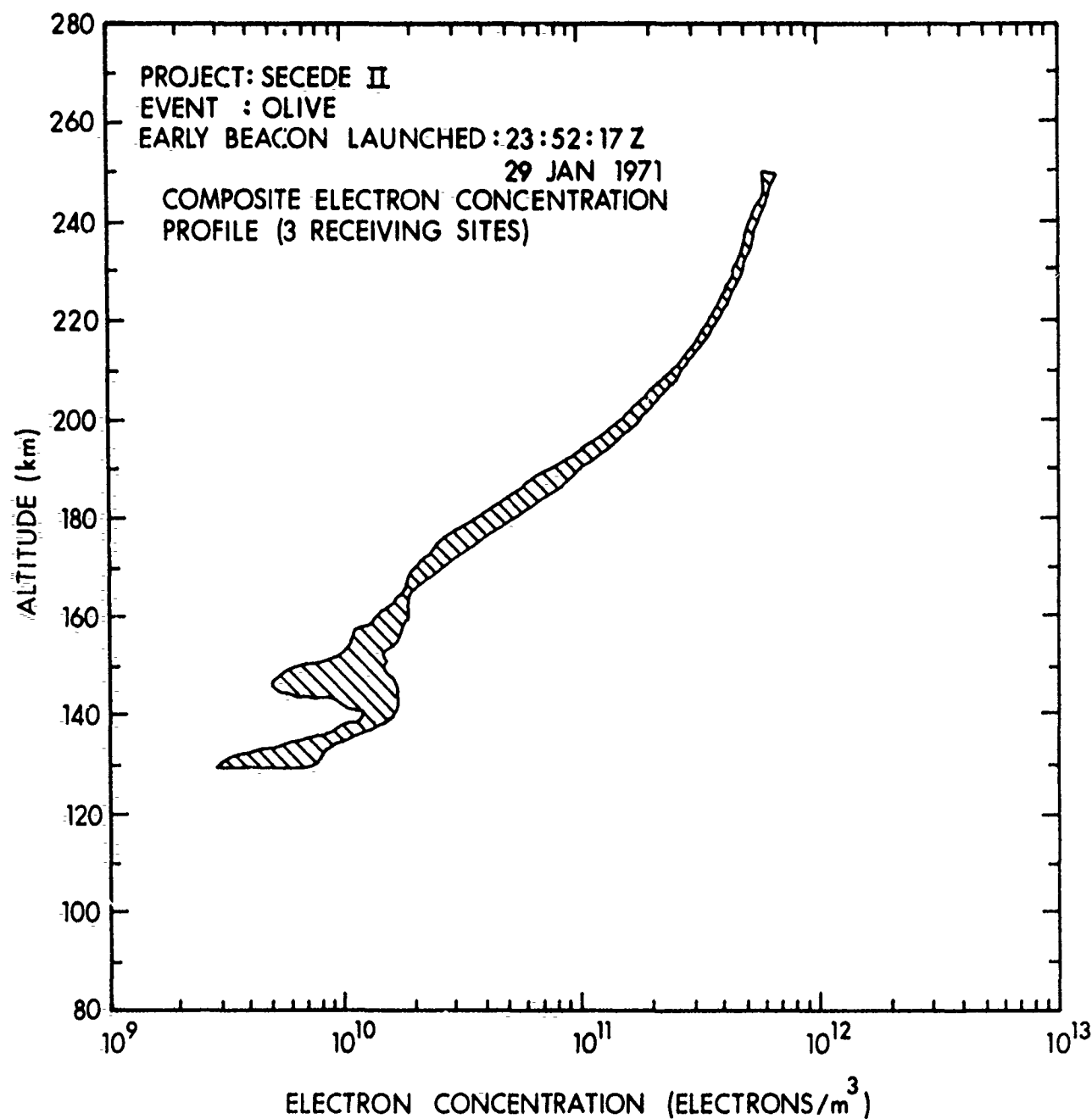


Figure 28. Three-site composite electron density profile for Event OLIVE early beacon.

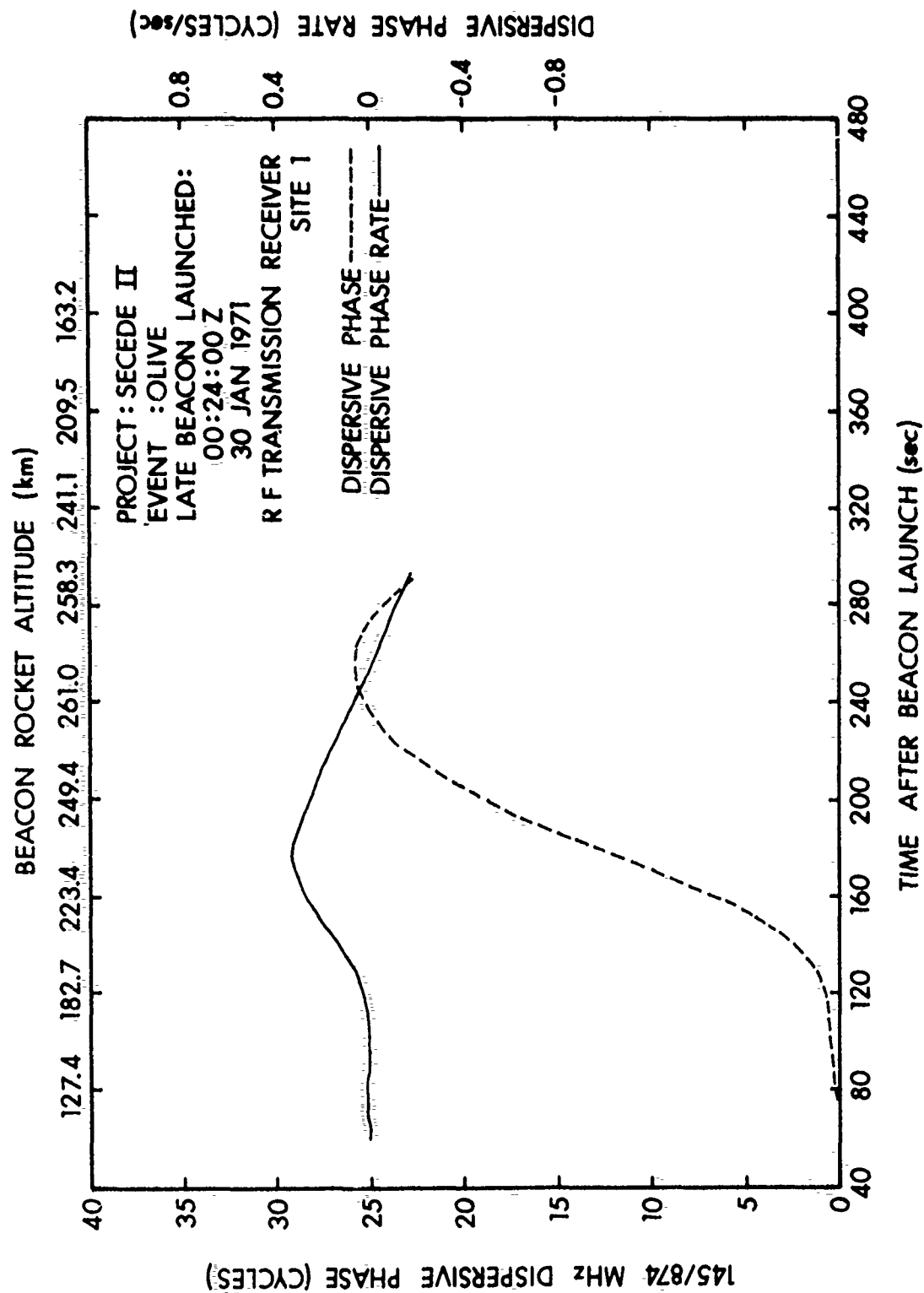


Figure 29. Site 1 dispersive phase for Event OLIVE late beacon.

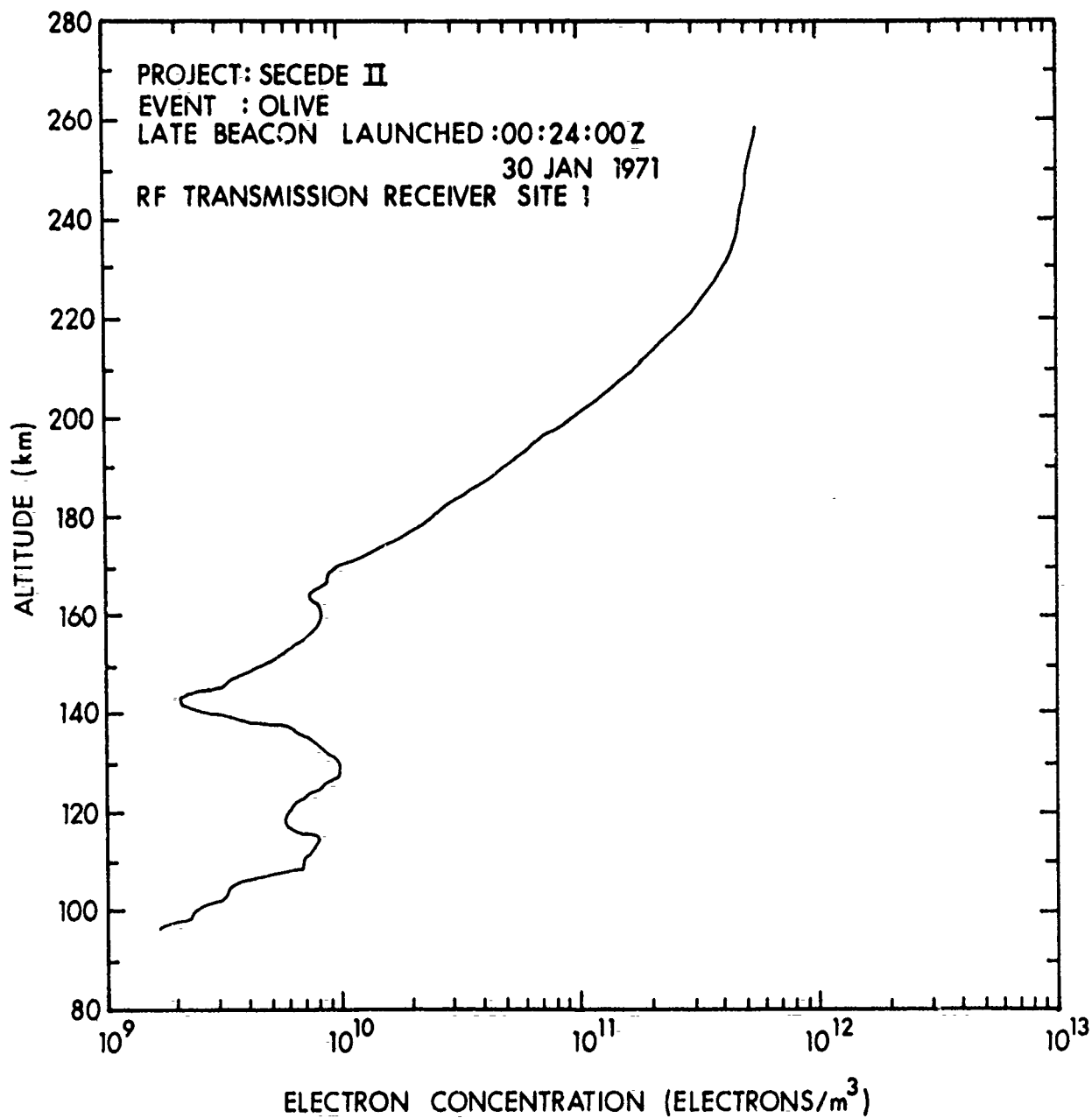


Figure 30. Site 1 electron density profile for Event OLIVE late beacon.

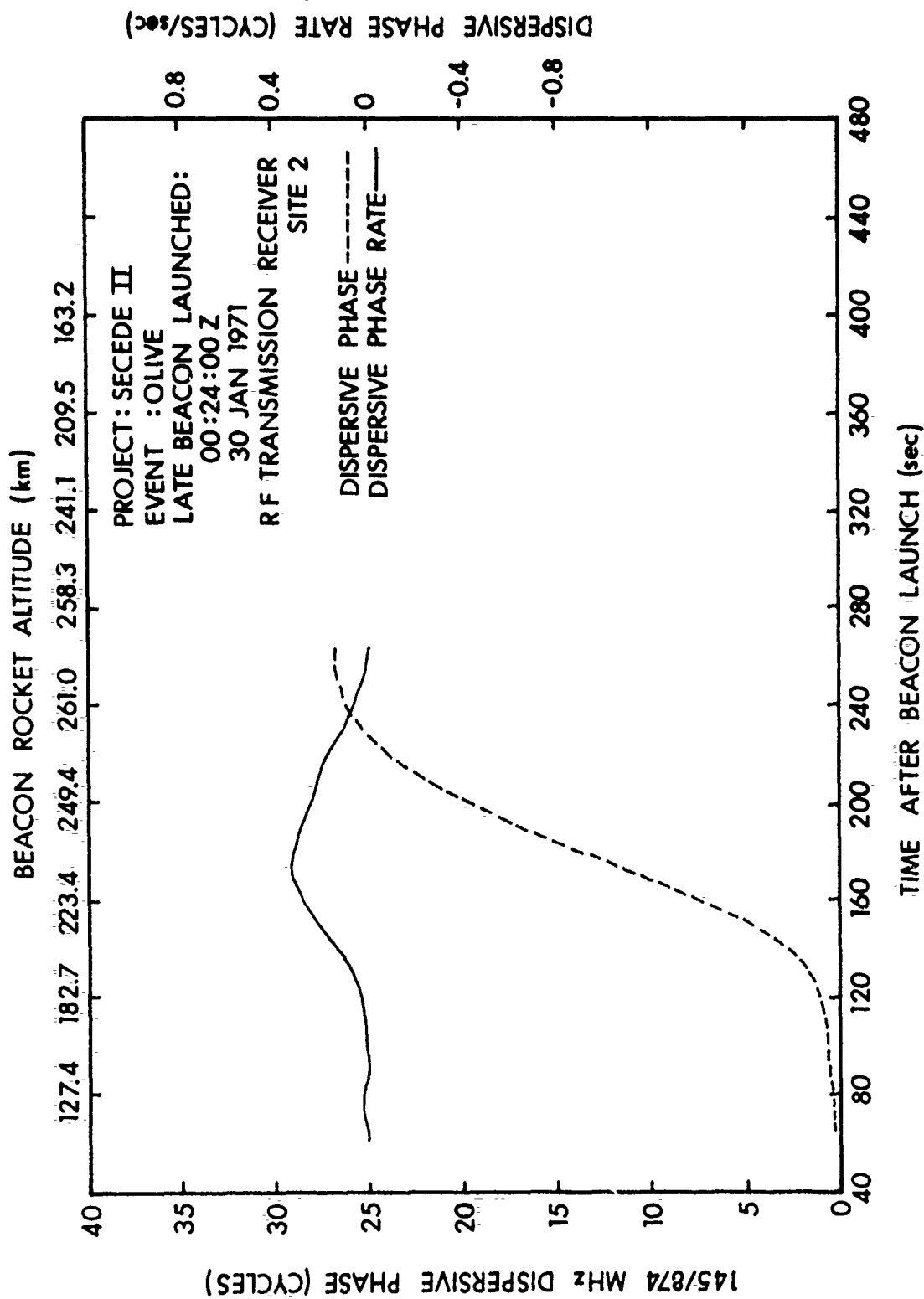


Figure 31. Site 2 dispersive phase for Event OLIVE late beacon.

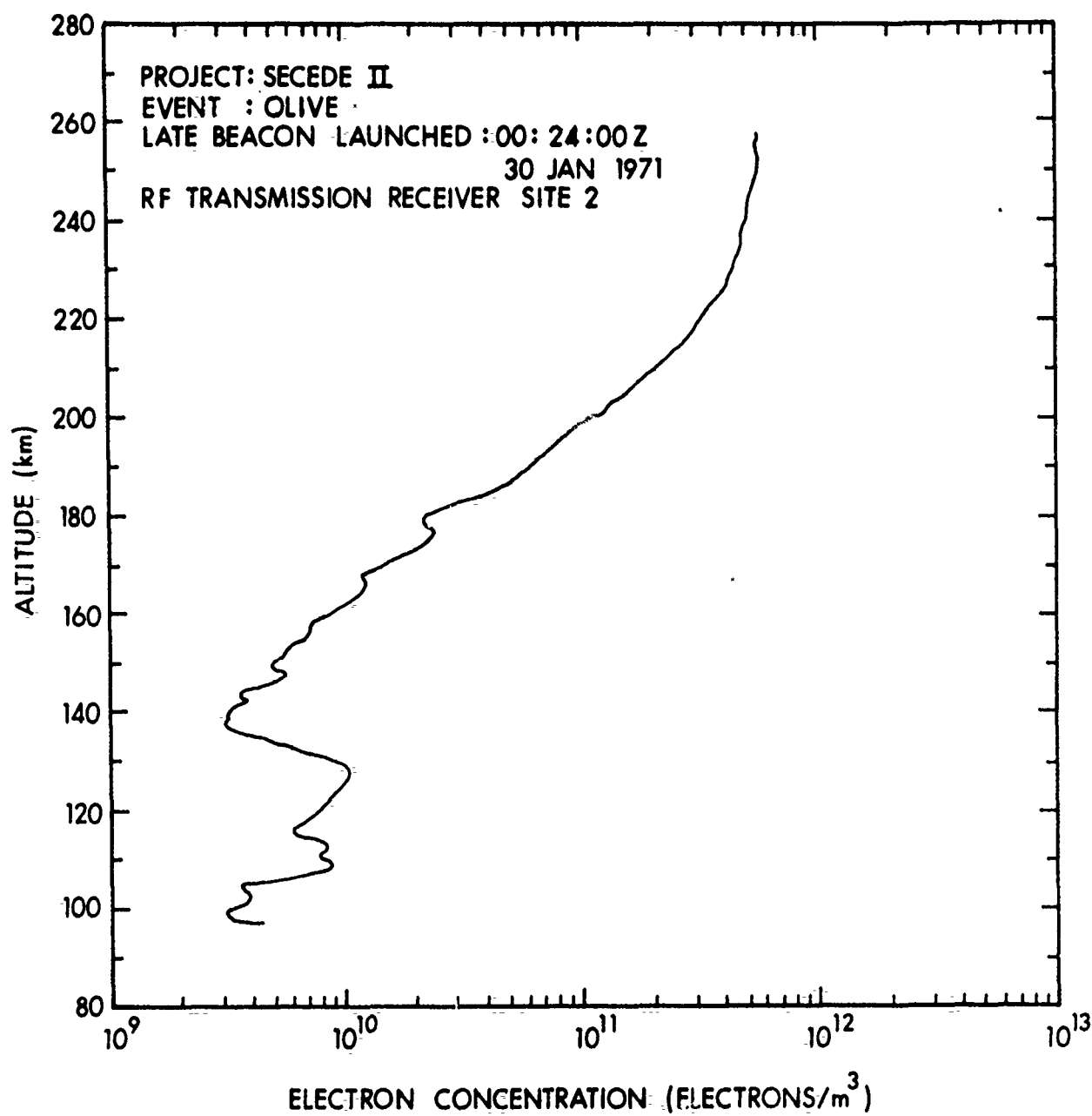


Figure 32. Site 2 electron density profile for Event OLIVE late beacon.

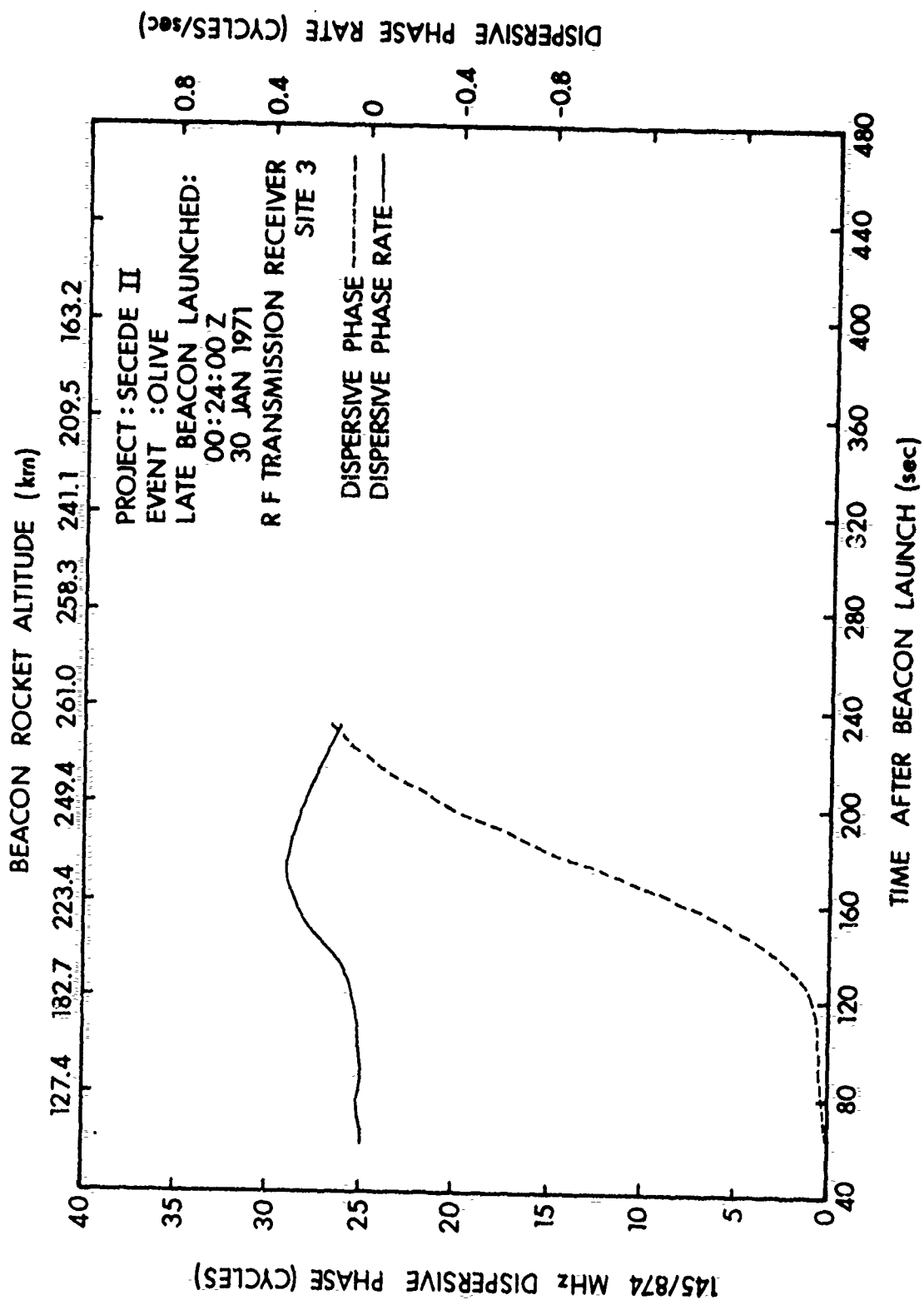


Figure 33. Site 3 dispersive phase for Event OLIVE late beacon.

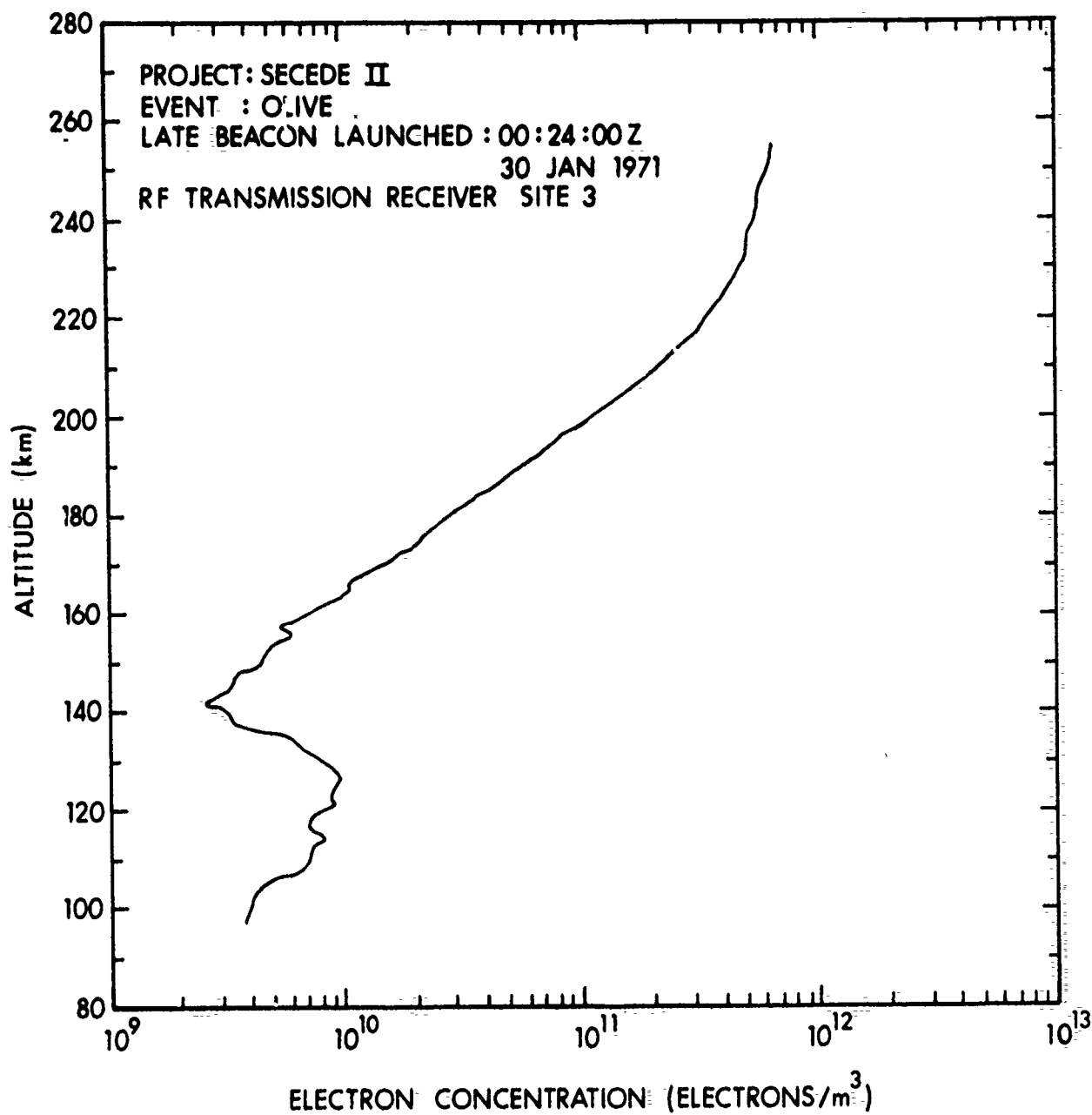


Figure 34. Site 3 electron density profile for Event OLIVE late beacon.

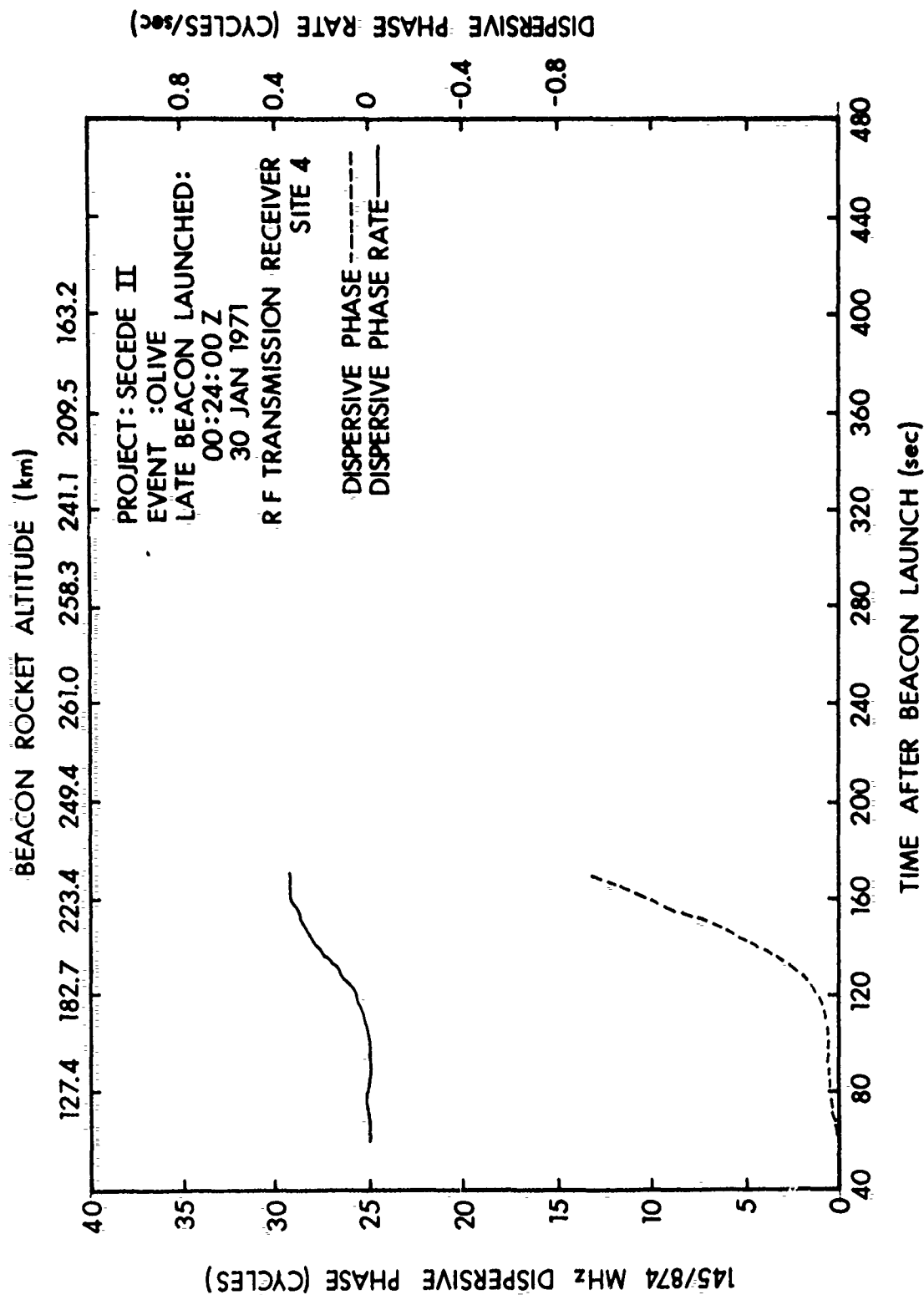


Figure 35. Site 4 dispersive phase for Event OLIVE late beacon.

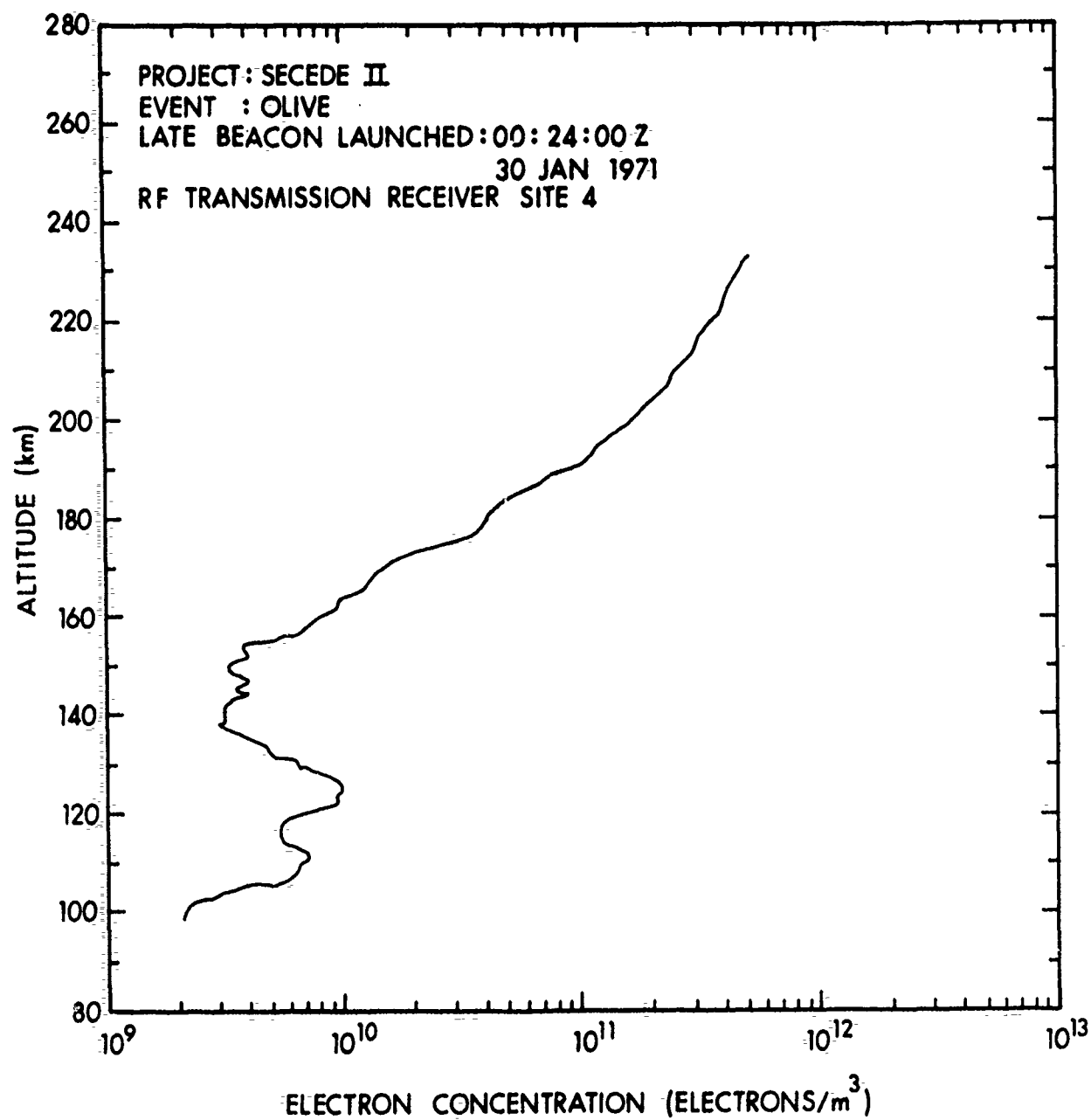


Figure 36. Site 4 electron density profile for Event OLIVE late beacon.

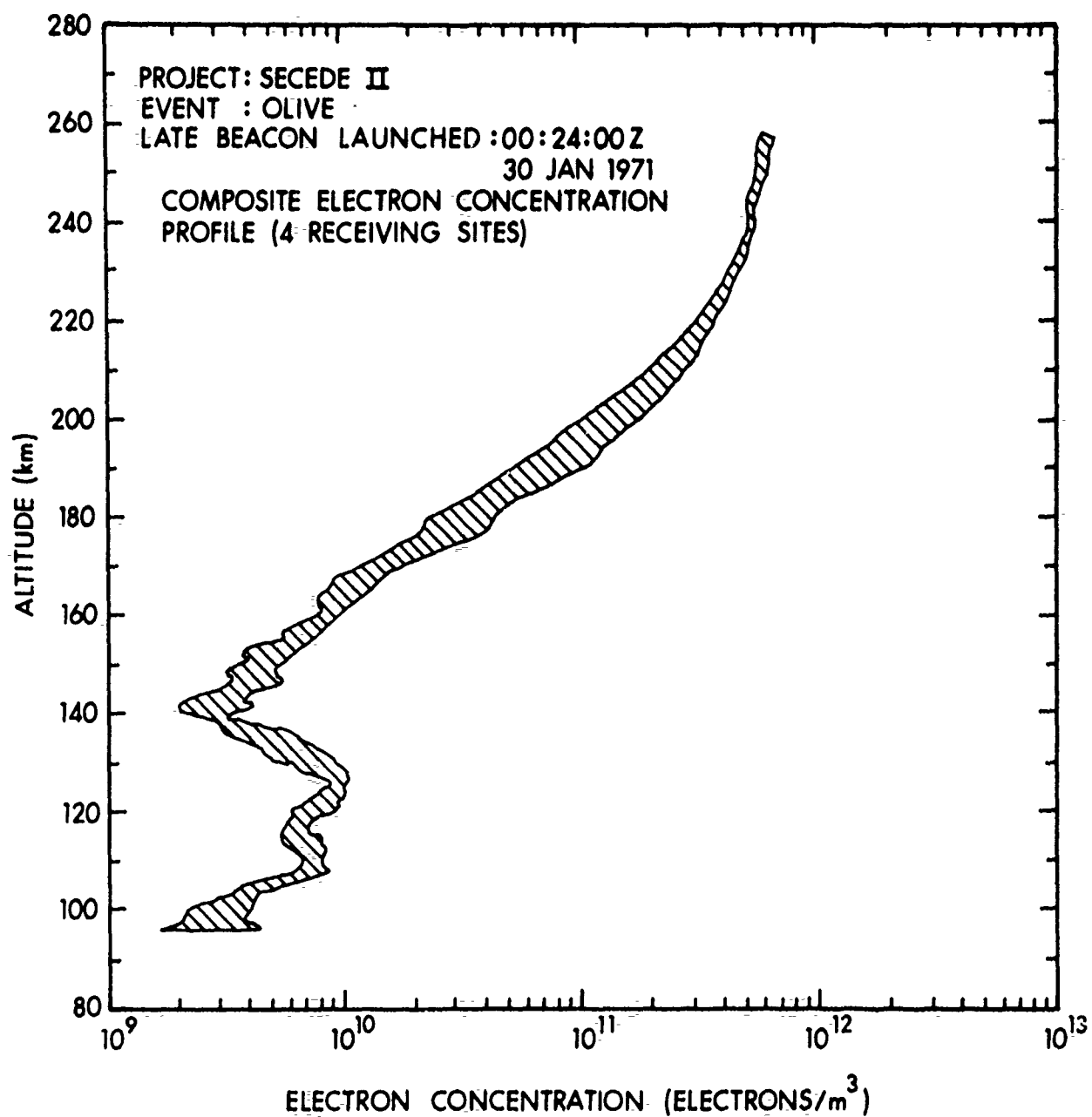


Figure 37. Four-site composite electron density profile for Event OLIVE late beacon.

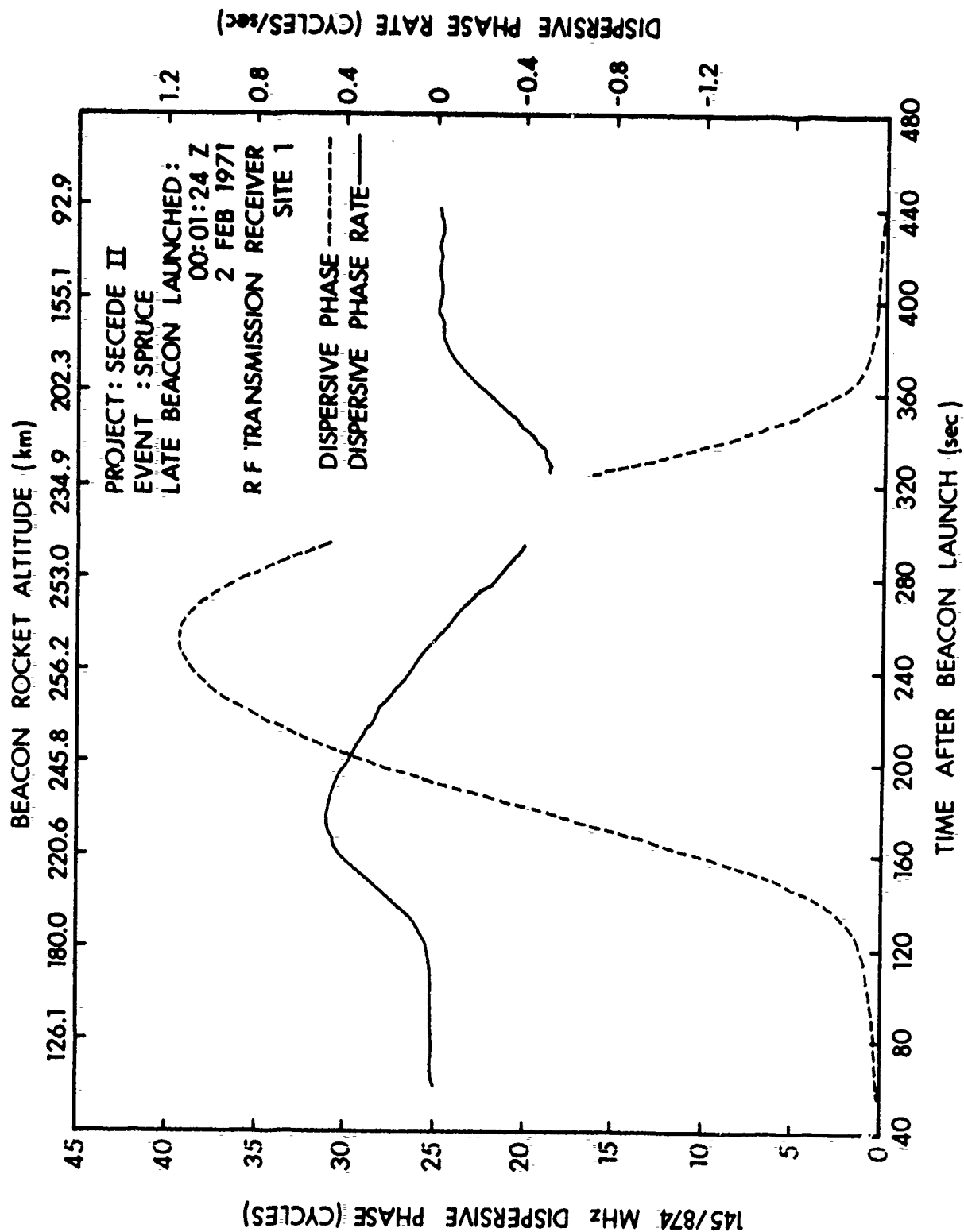


Figure 38. Site 1 dispersive phase for Event SPRUCE late beacon.

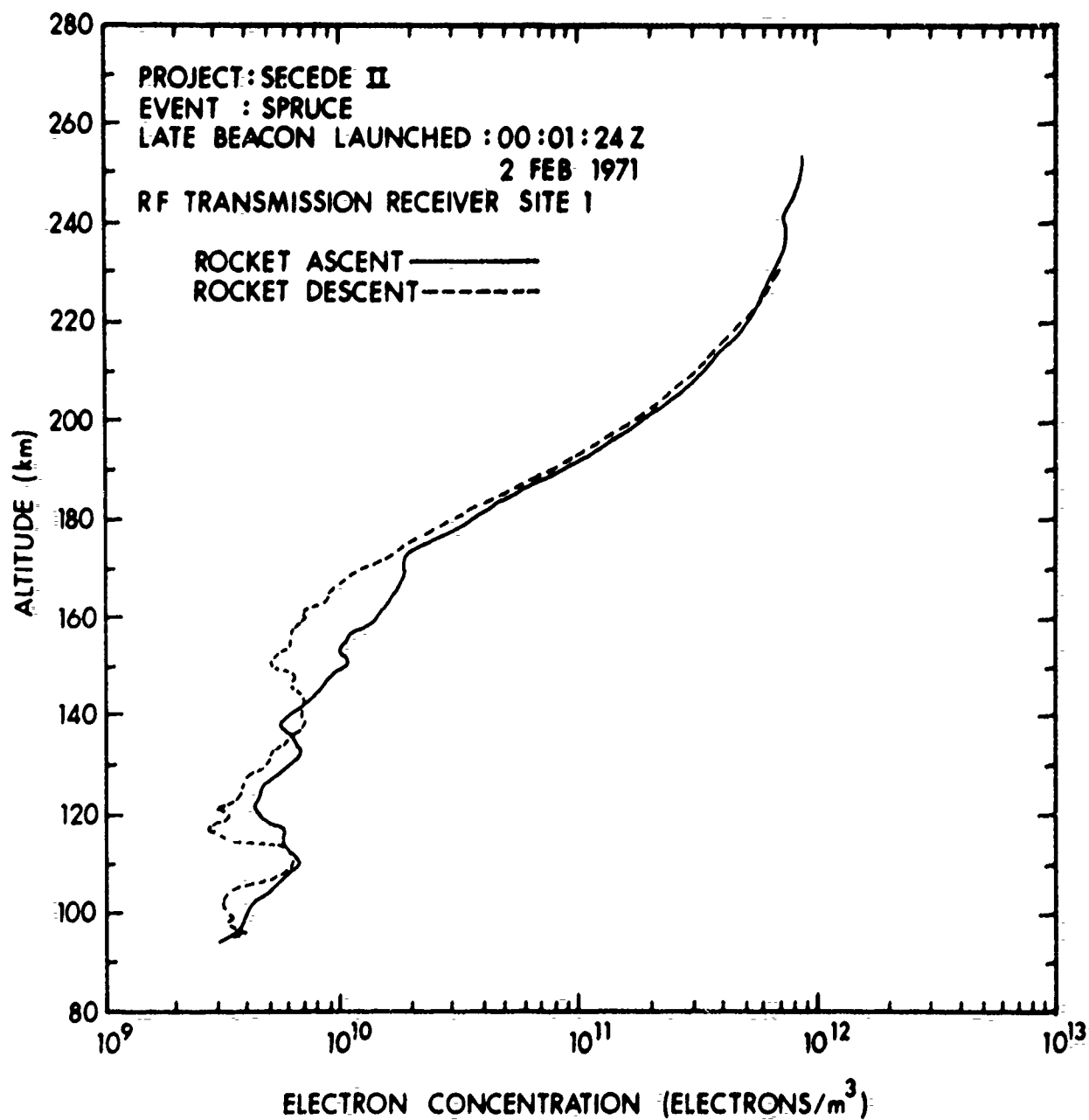


Figure 39. Site 1 electron density profile for Event SPRUCE late beacon.

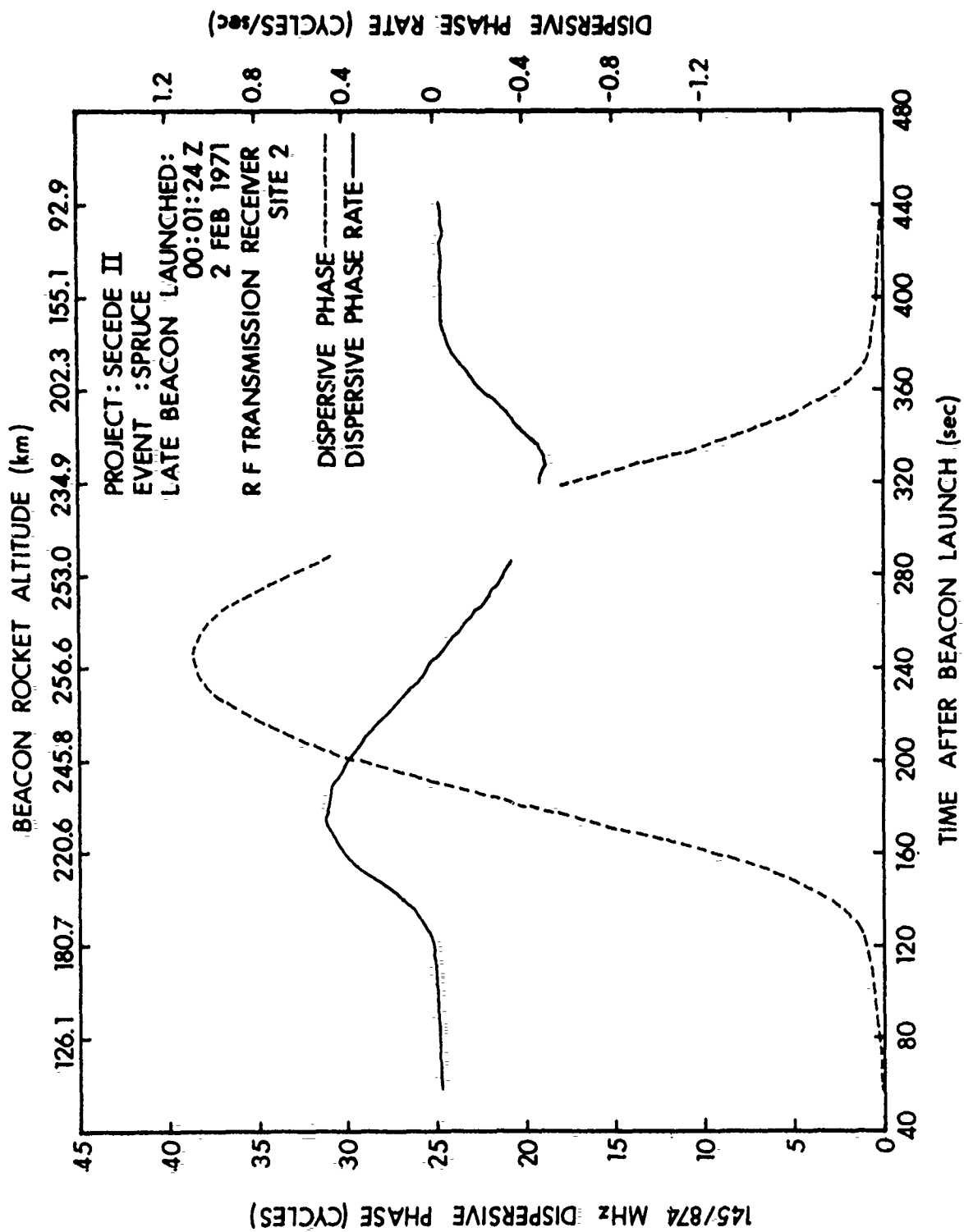


Figure 40. Site 2 dispersive phase for Event SPRUCE late beacon.

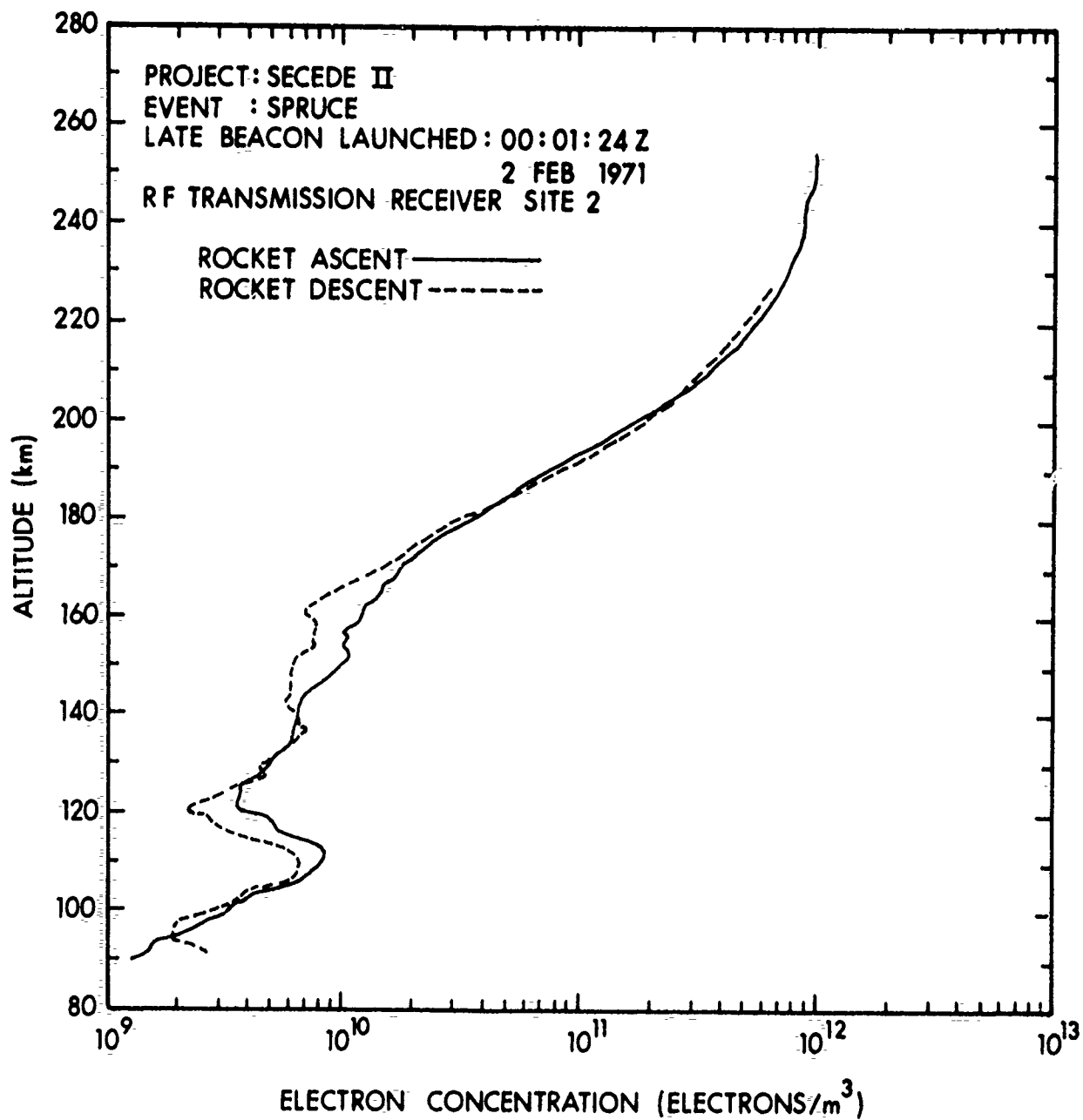


Figure 41. Site 2 electron density profile for Event SPRUCE late beacon.

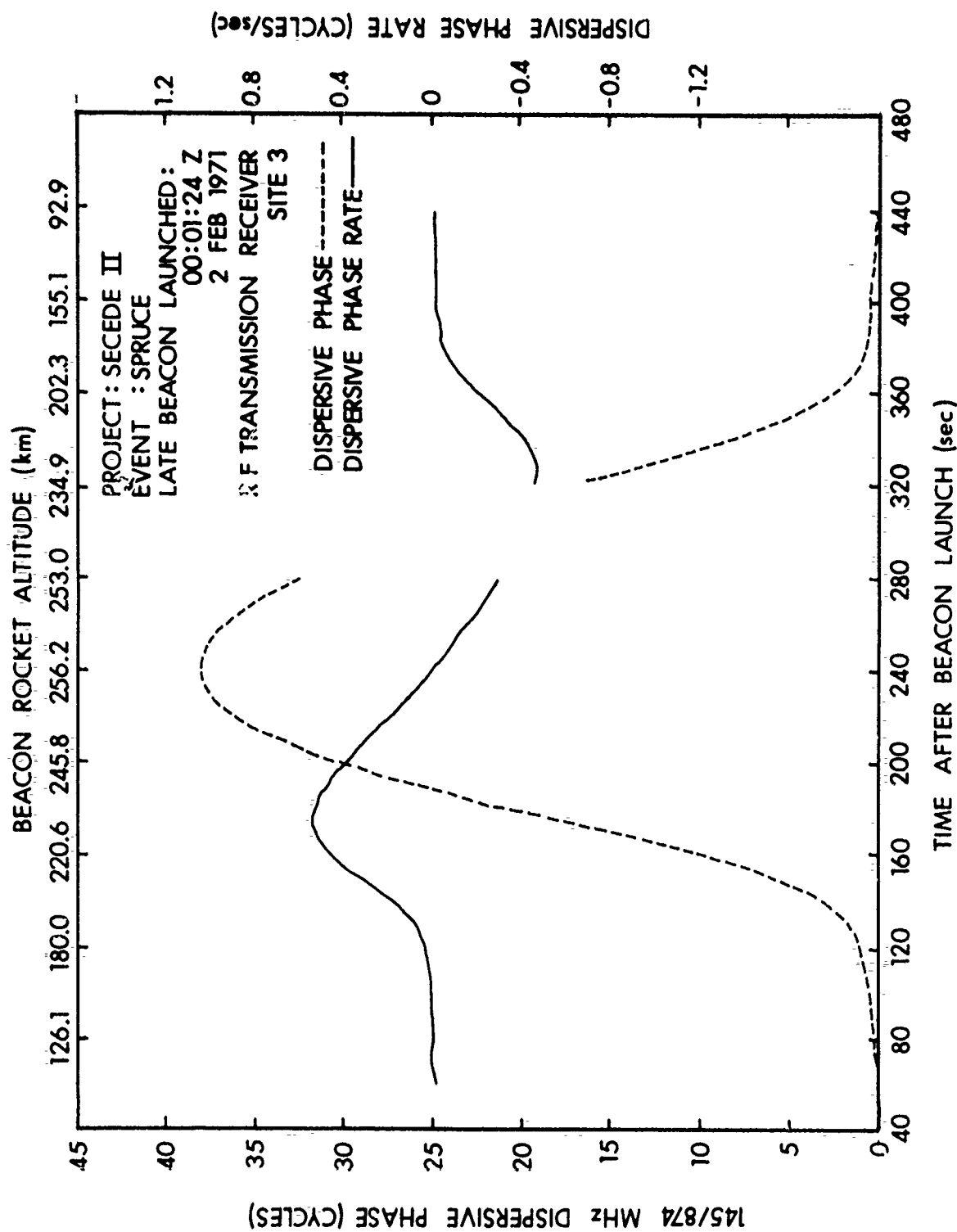


Figure 42. Site 3 dispersive phase for Event SPRUCE late beacon.

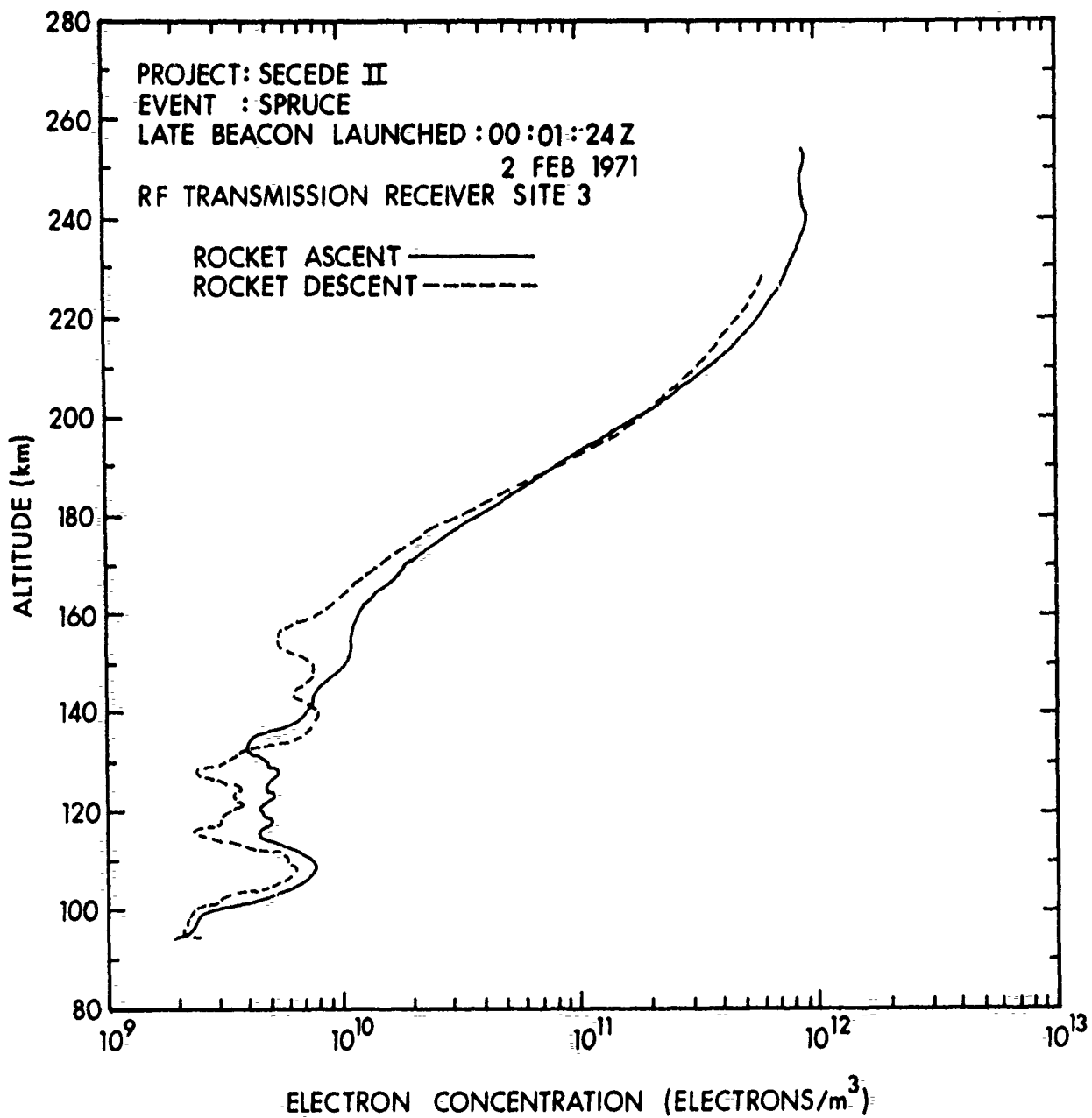


Figure 43. Site 3 electron density profile for Event SPRUCE late beacon.

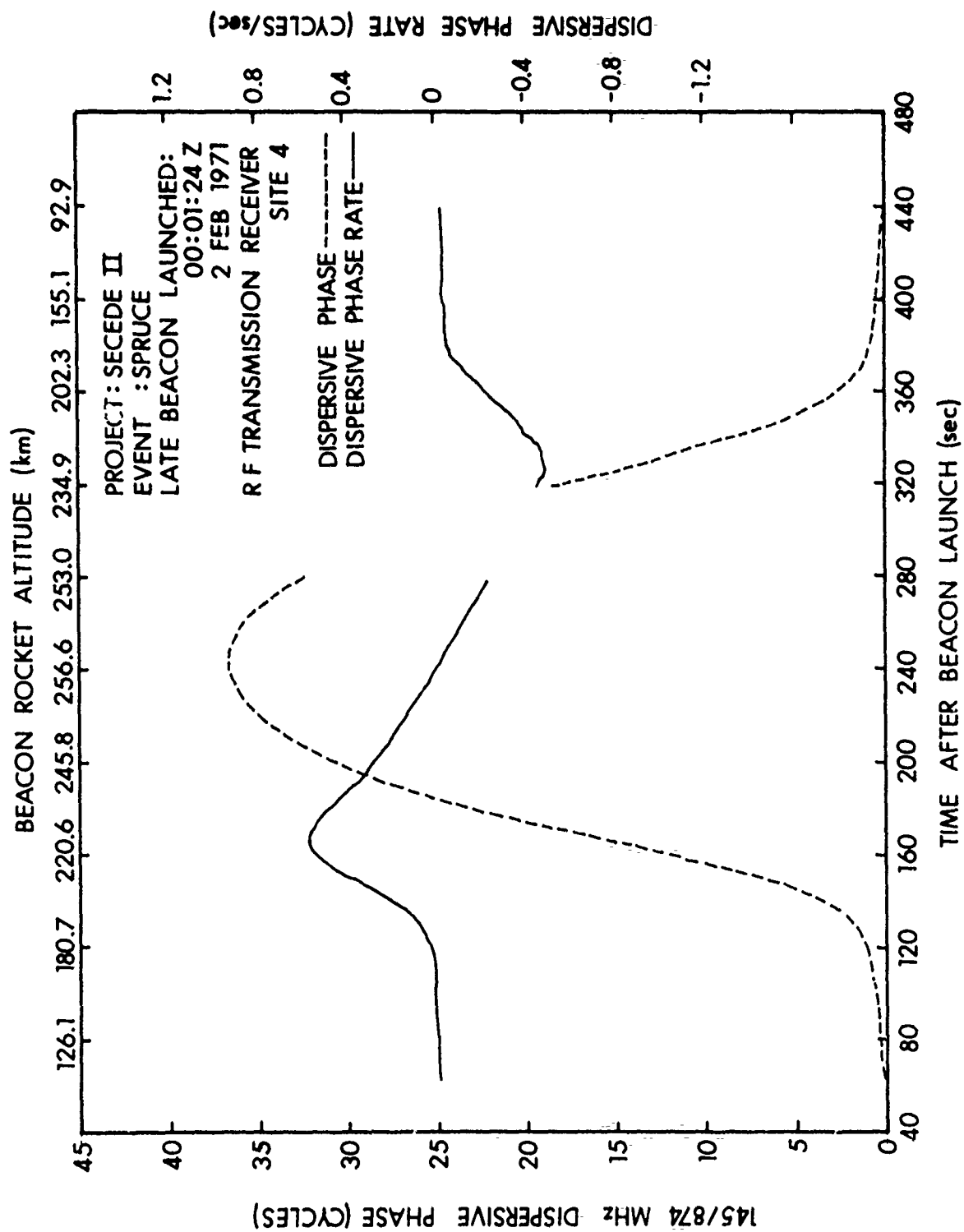


Figure 44. Site 4 dispersive phase for Event SPRUCE late beacon.

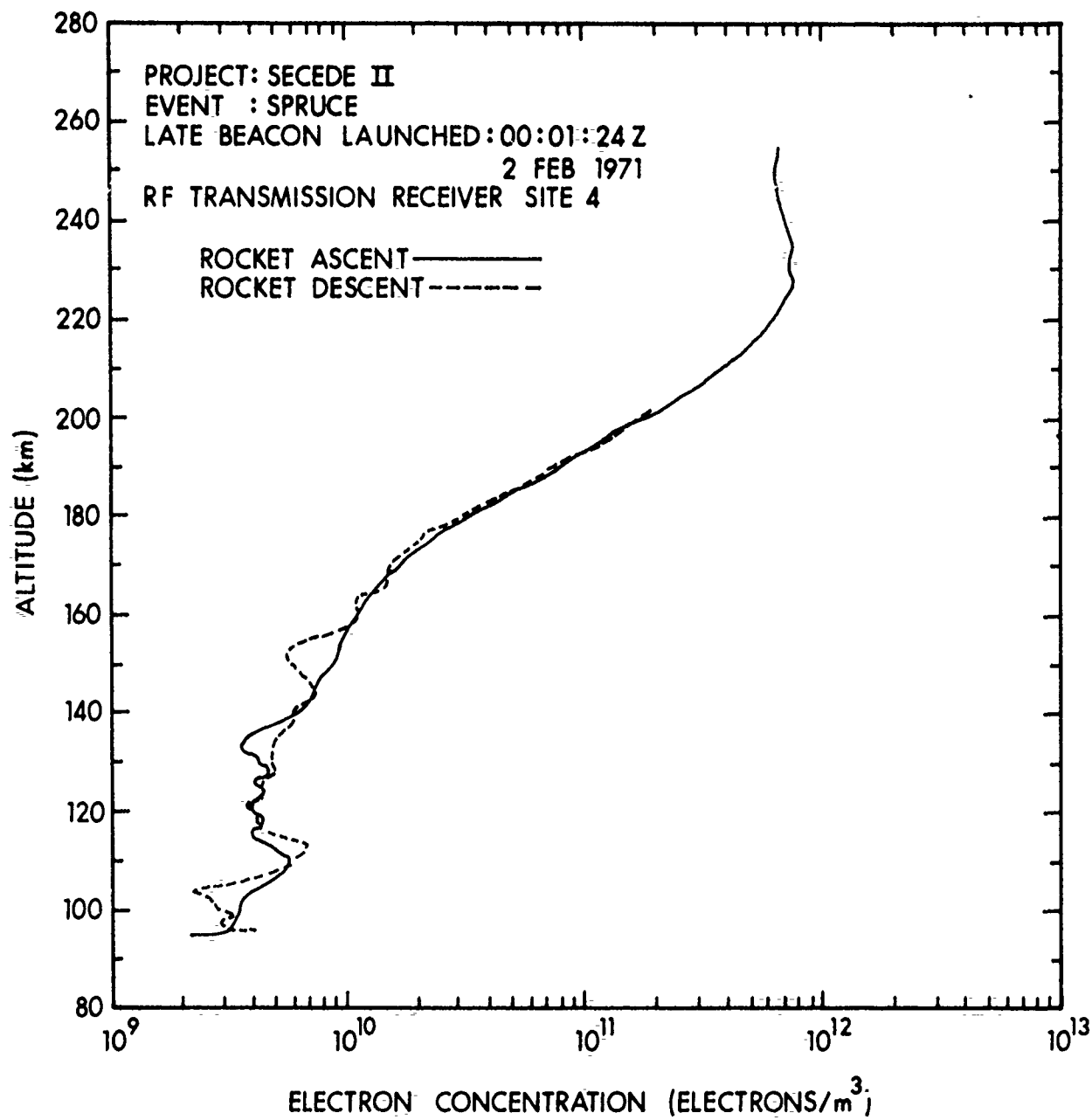


Figure 45. Site 4 electron density profile for Event SPRUCE late beacon.

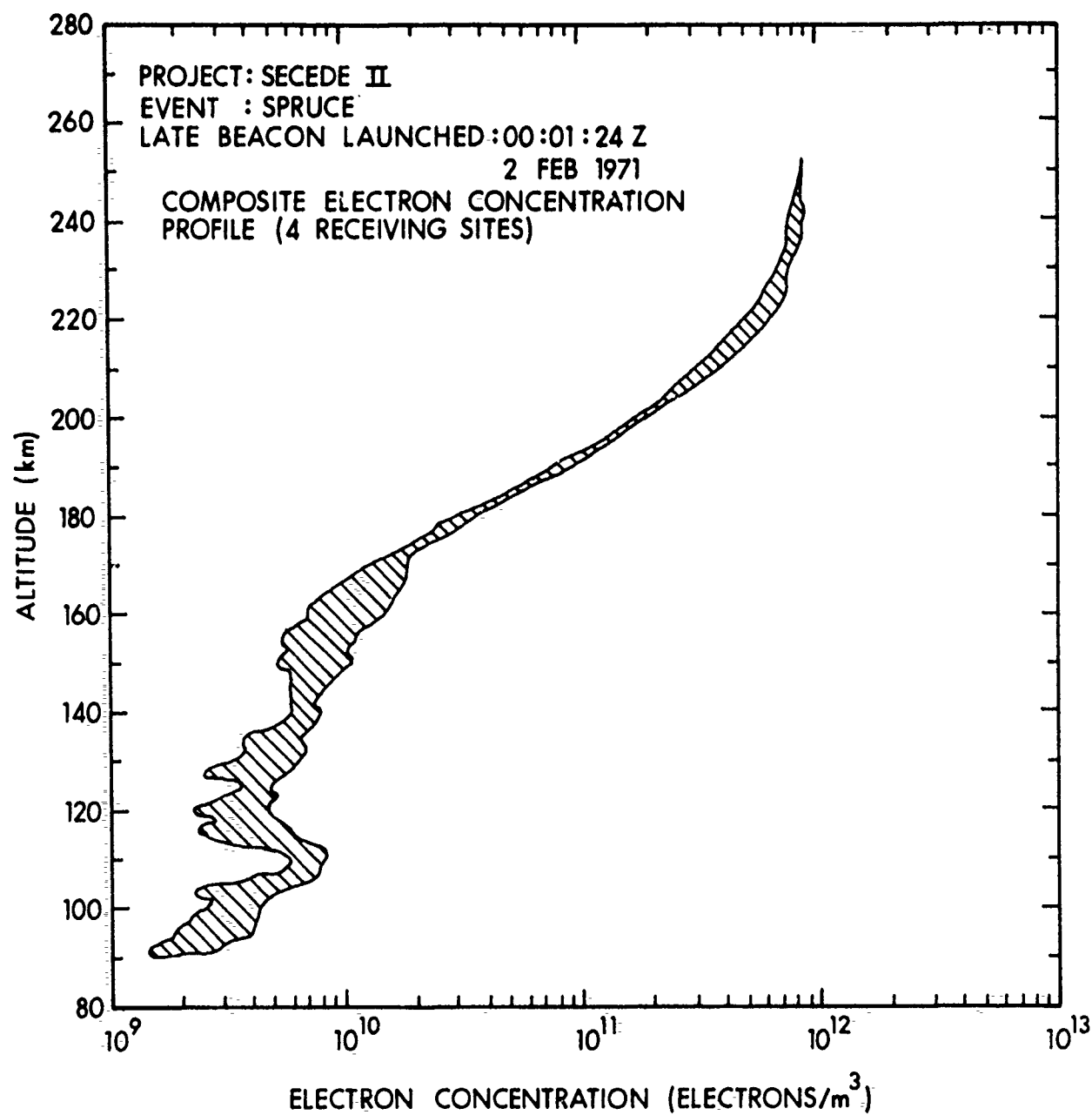


Figure 46. Four-site composite electron density profile for Event SPRUCE late beacon.

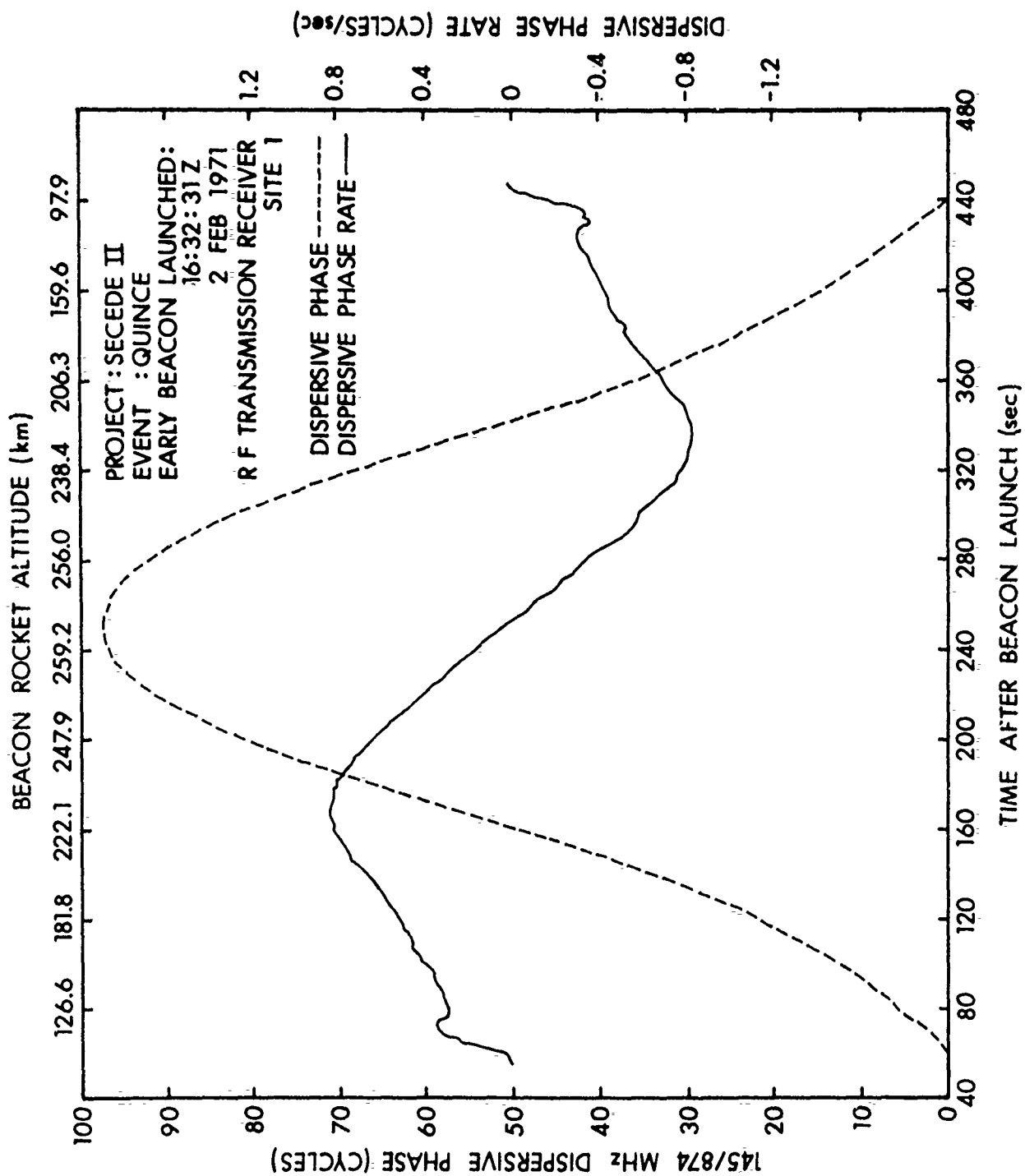


Figure 47. Site 1 dispersive phase for Event QUINCE early beacon.

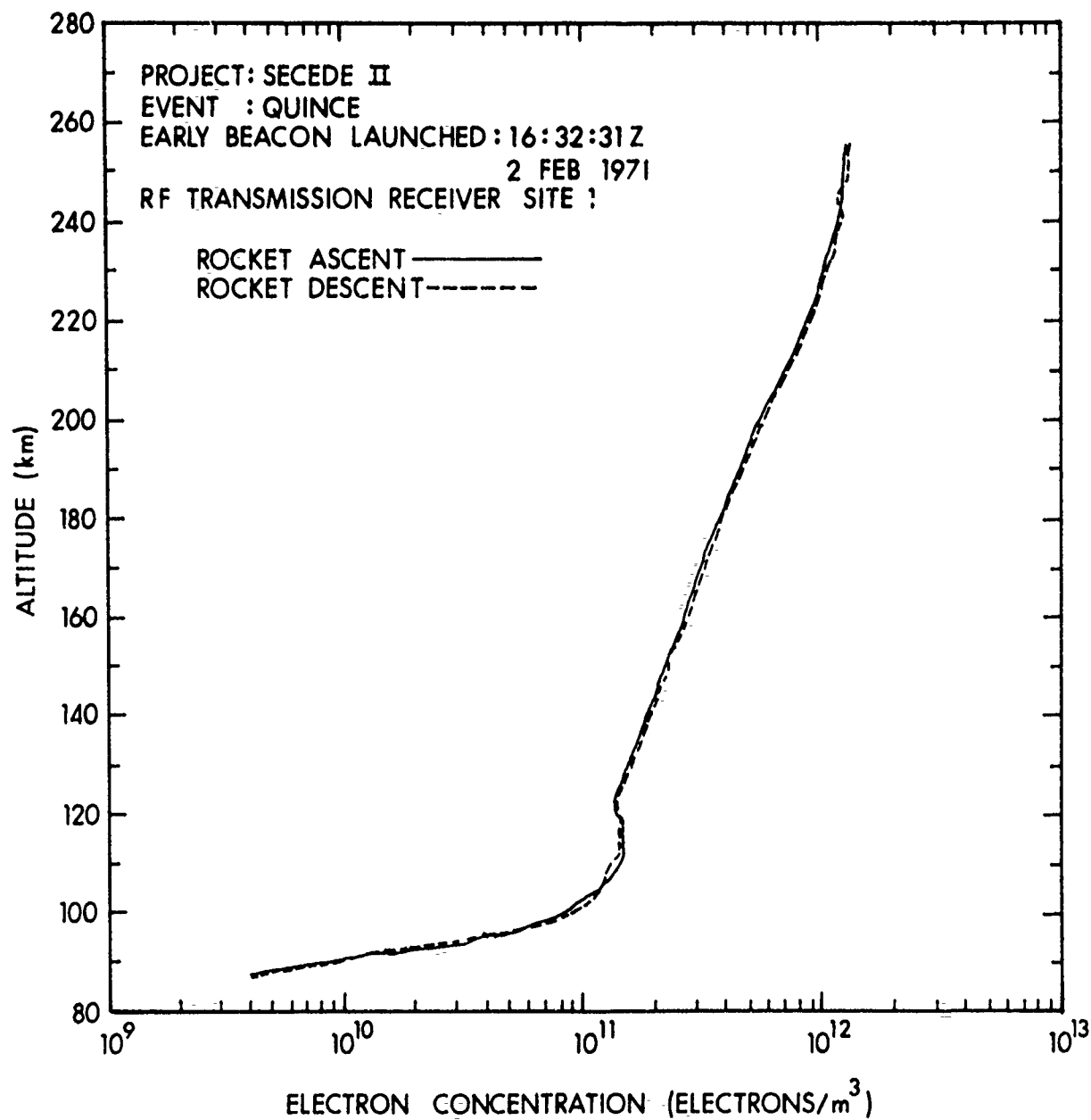


Figure 48. Site 1 electron density profile for Event QUINCE early beacon.

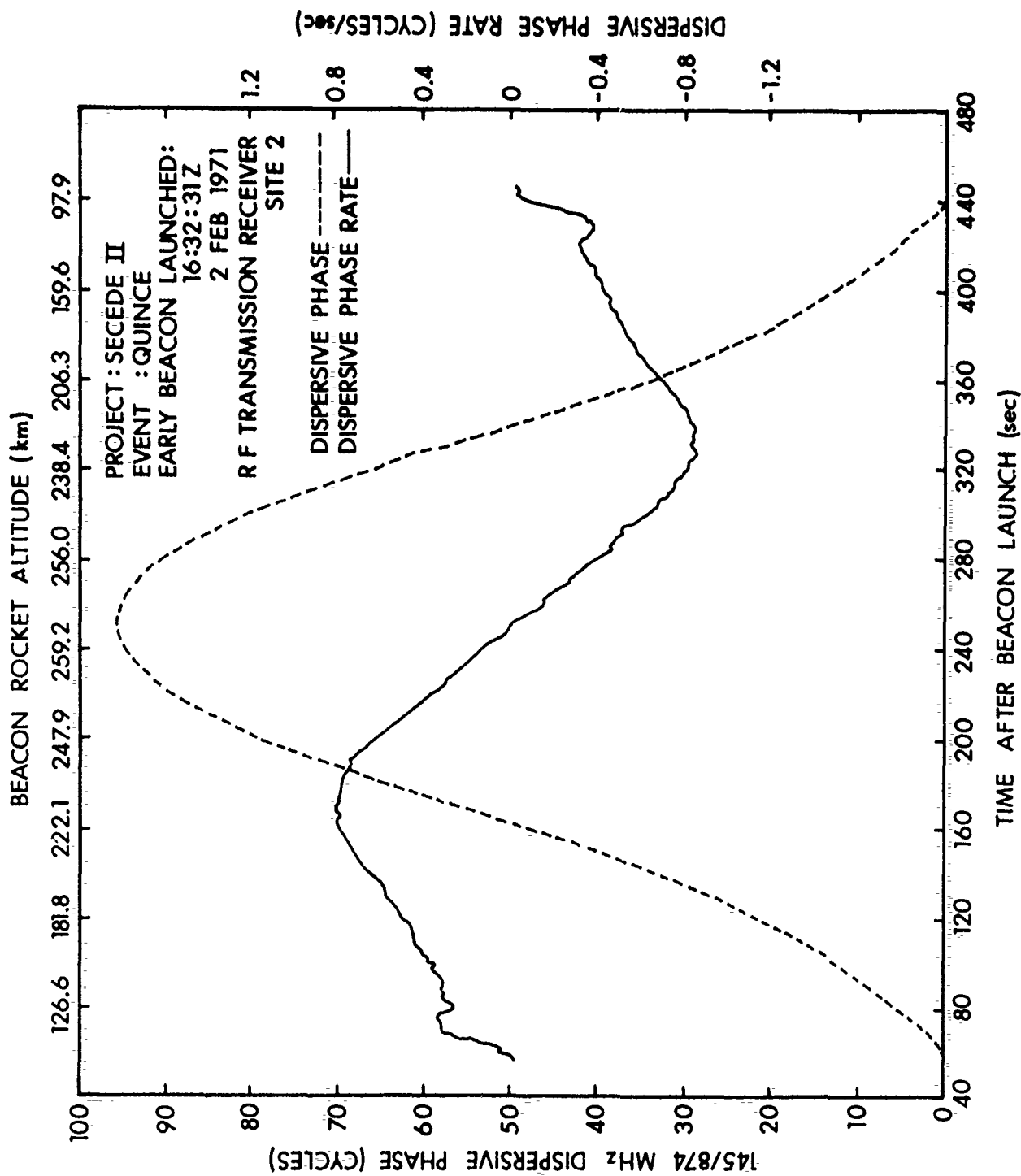


Figure 49. Site 2 dispersive phase for Event QUINCE early beacon.

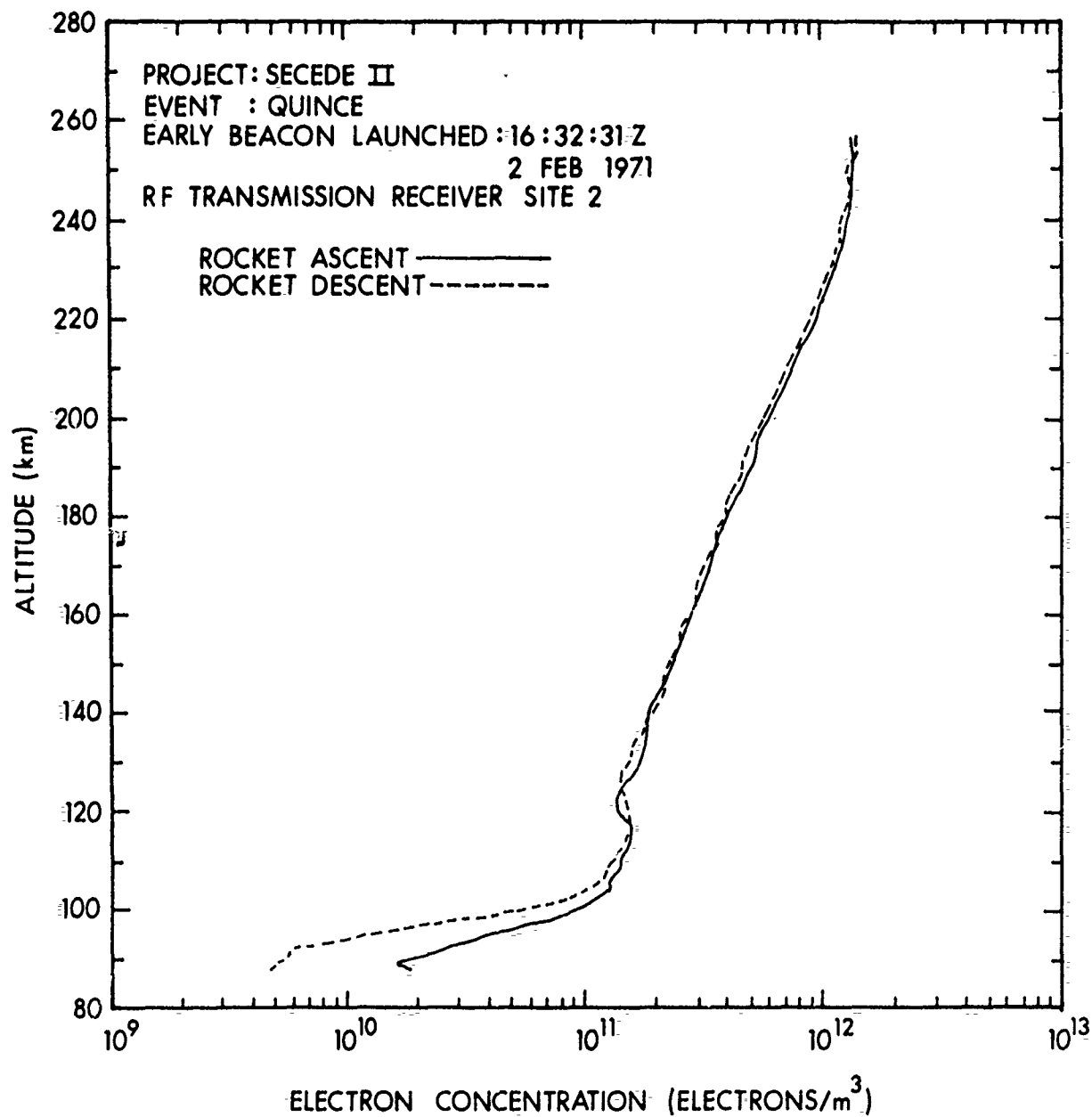


Figure 50. Site 2 electron density profile for Event QUINCE early beacon.

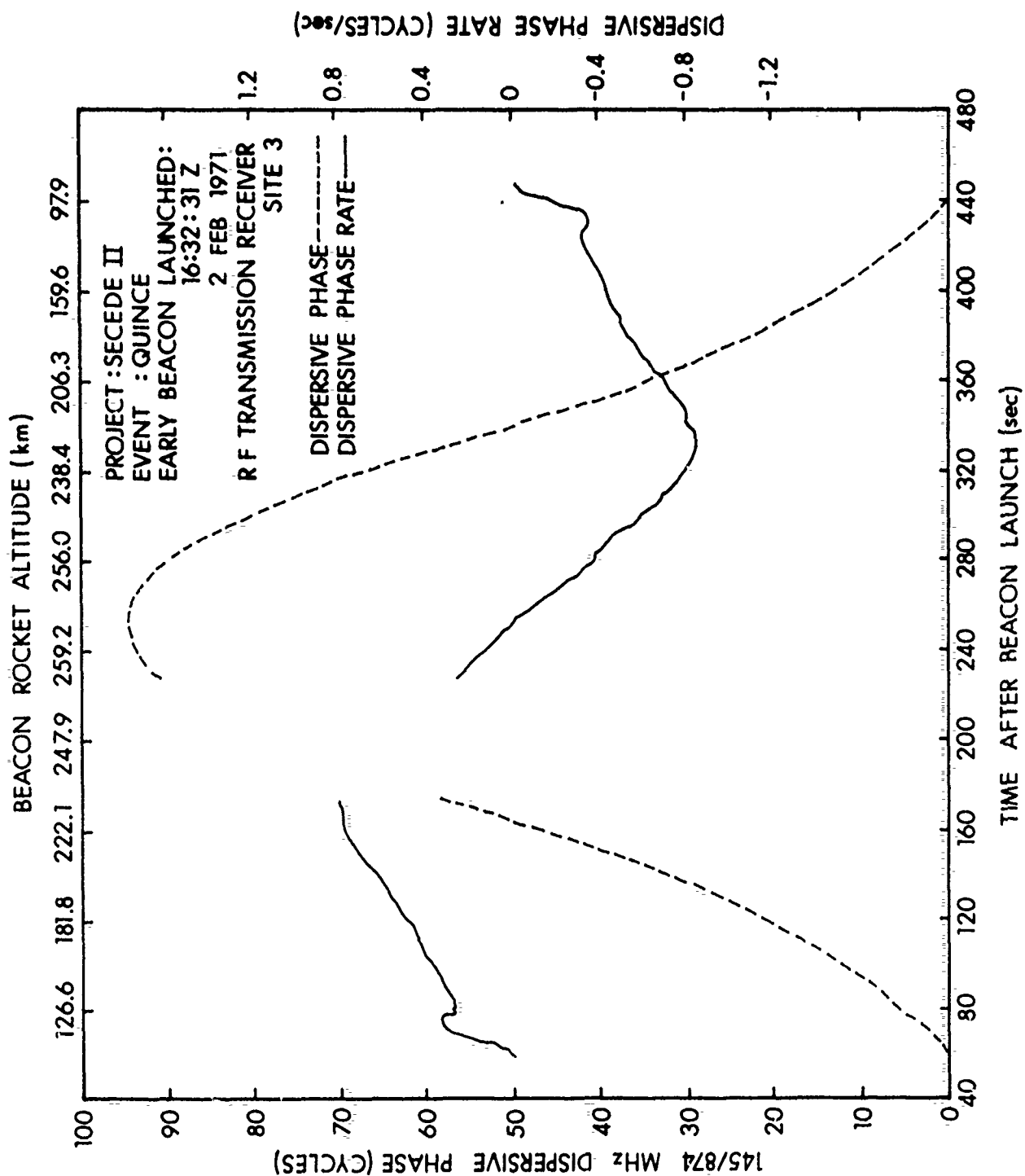


Figure 51. Site 3 dispersive phase for Event QUINCE early beacon.

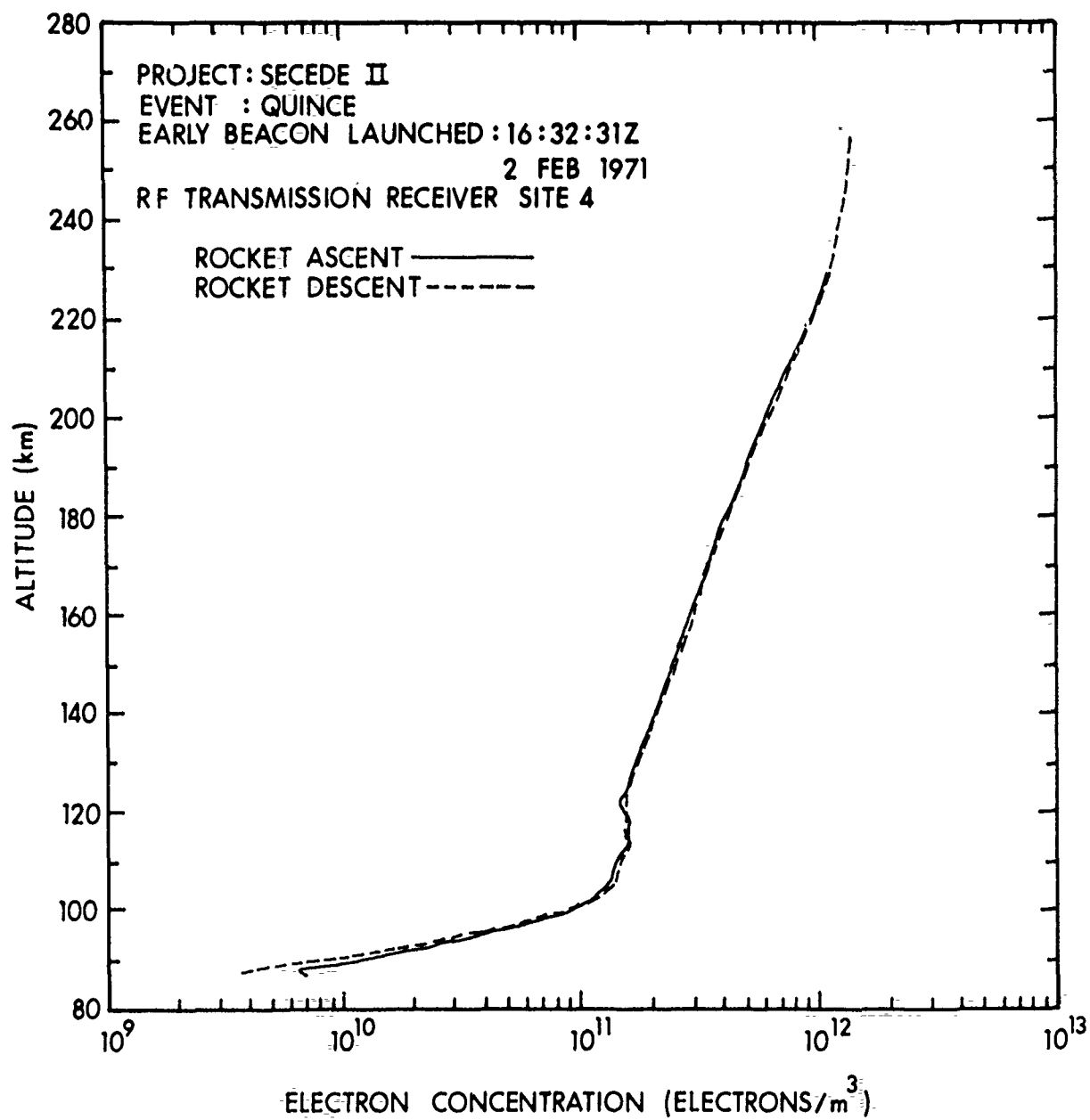


Figure 52. Site 3 electron density profile for Event QUINCE early beacon.

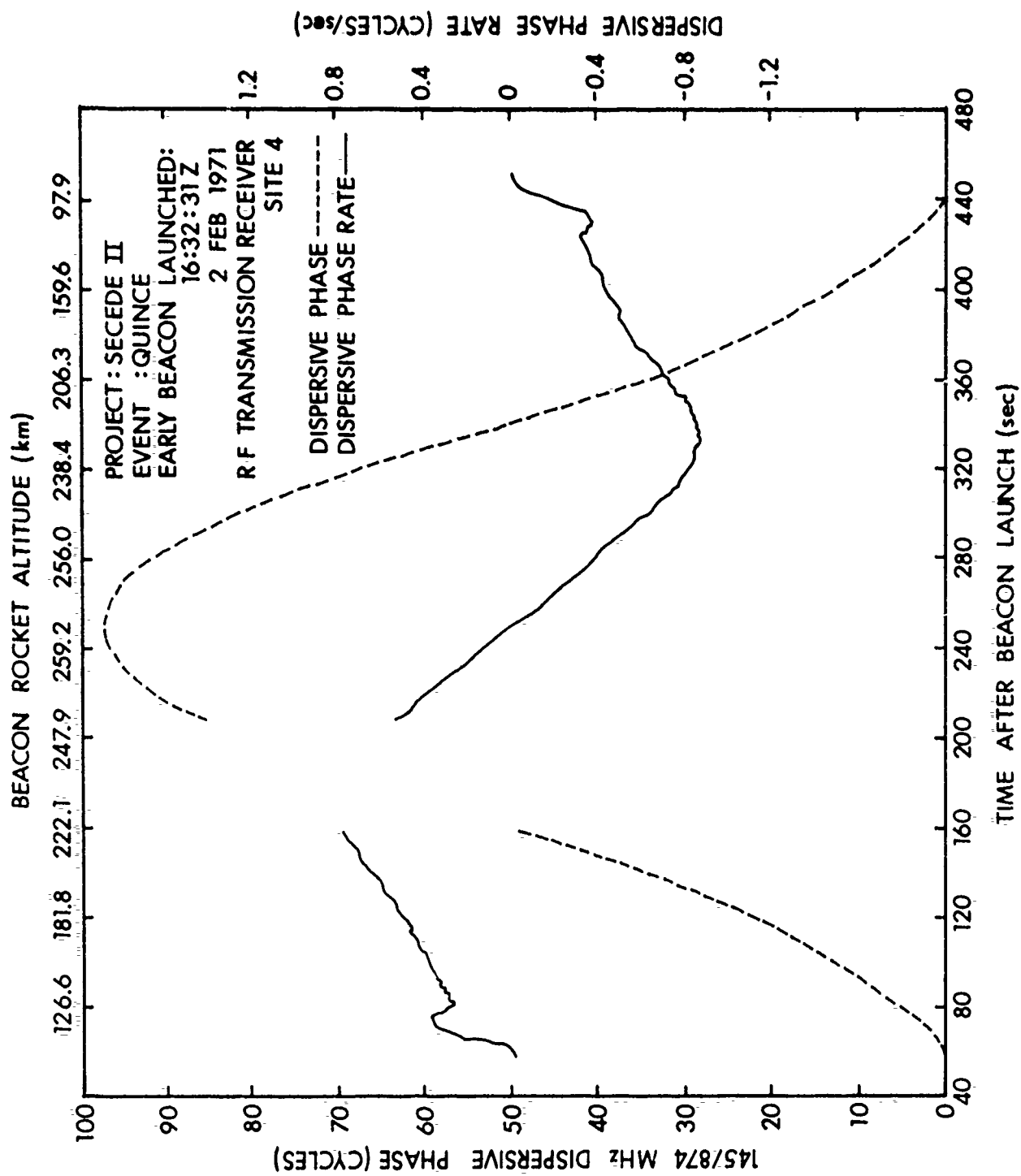


Figure 53. Site 4 dispersive phase for Event QUINCE early beacon.

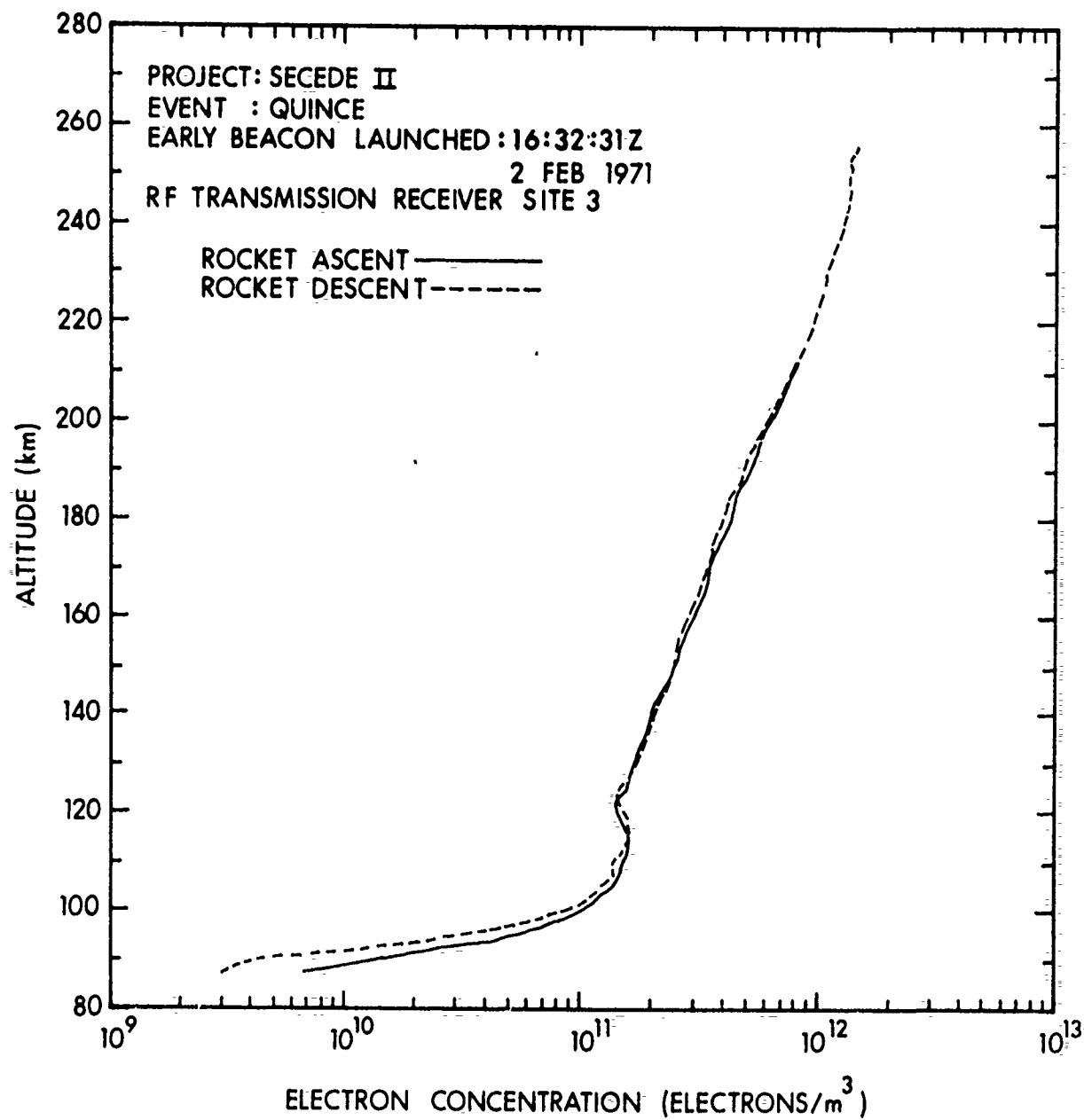


Figure 54. Site 4 electron density profile for Event QUINCE early beacon.

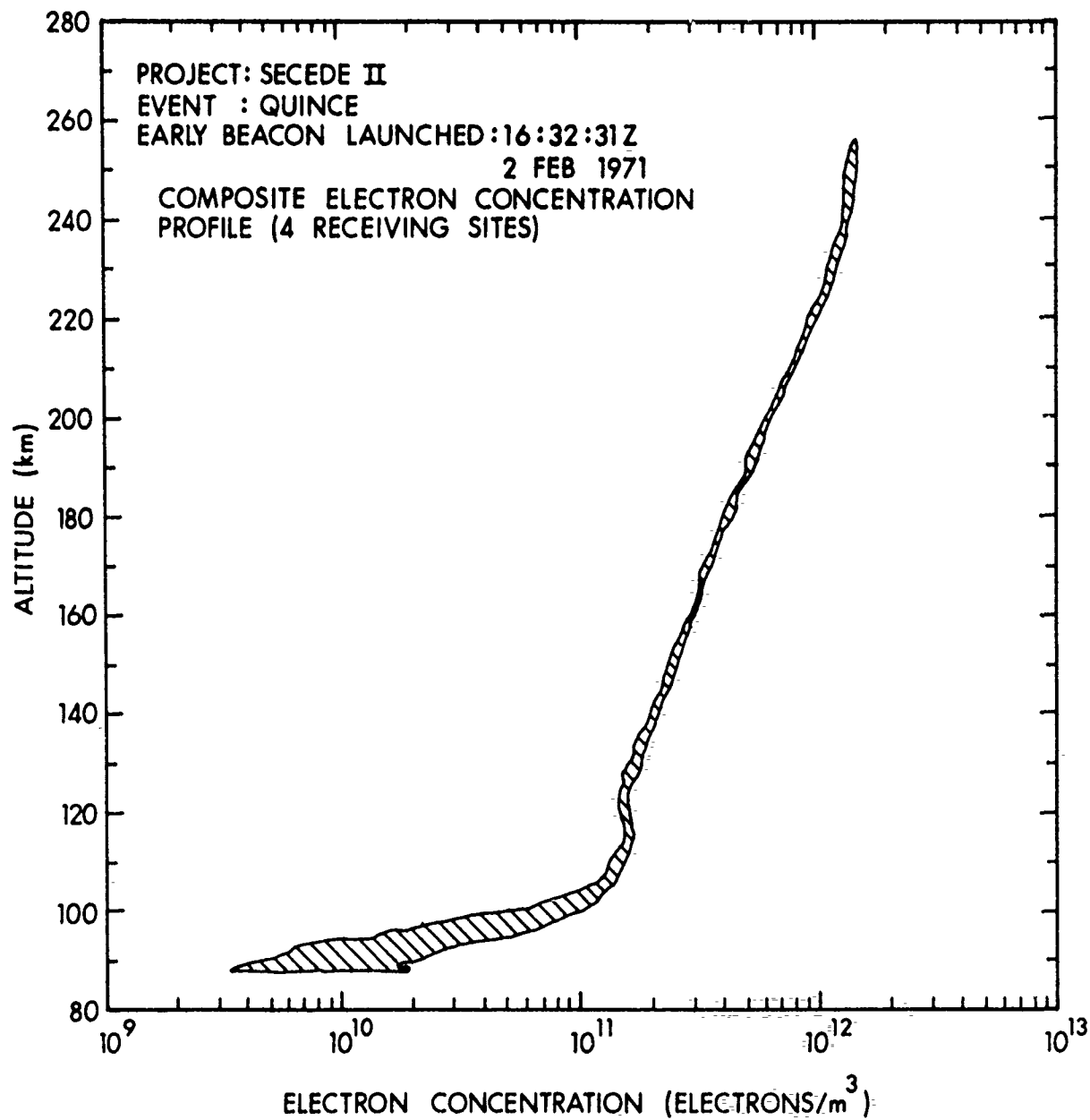


Figure 55. Four-site composite electron density profile for Event QUINCE early beacon.

REFERENCES

1. J. C. Seddon, "Propagation Measurements in the Ionosphere with the Aid of Rockets," J. Geophys. Res. Vol. 58, Sep 53, pp 323-335.
2. S. T. Markes, et al., "Summary Report on Strongarm Rocket Measurements of Electron Density to an Altitude of 1500 Kilometers," BRL Report 1187 (AD 404189), Jan 1963.
3. W. W. Berning, "Operation DOMINIC, FISH BOWL SERIES, Project Officer's Report 2018, Project 6.3, 'D-Region Physical Chemistry,'" Defense Nuclear Agency, Washington, DC, Nov 1964 (SECRET-RD).
4. W. A. Dean and H. T. Lootens, "Ionospheric Measurements with a Four-Frequency Phase Coherent Beacon," BRL Report 1396 (AD 835034), March 1968.
5. W. A. Dean and H. T. Lootens, "Certification Flight of MIGHTY SKY Project 603-C Rocket Payload," BRL Report 1418 (AD 843101), Oct 1968.
6. H. T. Lootens, "Rocket Measurements of Electron Density, Electron Temperature and Earth's Magnetic Field above Fort Churchill," BRL Report 1415, Aug 1968. (AD #676109)
7. R. E. Prenatt, W. A. Dean, and W. W. Berning, "Electron Content of Barium Plasmas in the High Atmosphere," BRL Report 1459 (AD 700960), Dec 1969.
8. W. A. Dean, "Auroral Zone Electron Density Profiles - Project SECEDE III Rockets," BRL Memo Report 2078 (AD 878631), Nov 1970.
9. R. E. Prenatt and G. A. Bowers, "The RF Transmission Experiment in SECEDE II and a Model for the Electron Concentration in the Ion Cloud from High Altitude Barium Release PLUM," BRL Report 1645, May 1973. (AD #911669L)
10. W. A. Dean and I. L. Chidsey, Jr., "Final Report on BRL Participation in Operation PCA 69," BRL Report 1669, Sep 1973. (AD #914672L)
11. W. A. Dean, "Electron Density Profiles for the 1969 PCA Event," Paper published in the Proceedings of COSPAR Symposium on Solar Particle Event of November 1969, AFCRL Report 72-0474, Special Report 144, 11 Aug 1972.
12. I. L. Chidsey, Jr., "Multifrequency Polar Cap Absorption Measurements," Paper published in the Proceedings of COSPAR Symposium on Solar Particle Event of November 1969, AFCRL Report 72-0474, Special Report 144, 11 Aug 1972.

REFERENCES (CONT.)

13. R. W. Honey, "RF Beacon Ground Stations Dispersive-Phase/
Differential Doppler Measurement System," RADC TR-72-151, Final
Technical Report, Electrac, Inc., Anaheim, CA, Mar 1972.
14. W. A. Dean, R. E. Prenatt, and G. A. Bowers, "The RF Transmission
Experiment for Operation BARBIZON," BRL Report in publication.

DISTRIBUTION LIST

<u>No. of Copies</u>	<u>Organization</u>	<u>No. of Copies</u>	<u>Organization</u>
12	Commander Defense Documentation Center ATTN: DDC-TCA Cameron Station Alexandria, VA 22314	1	Commander US Army Materiel Command ATTN: AMCDMA-ST 5001 Eisenhower Avenue Alexandria, VA 22333
1	Director Defense Advanced Research Projects Agency ATTN: Mr. R. Moore 1400 Wilson Boulevard Arlington, VA 22209	1	Commander US Army Materiel Command ATTN: AMCRD, BG H.A. Griffith 5001 Eisenhower Avenue Alexandria, VA 22333
3	Director Institute for Defense Analyses ATTN: Dr. E. Bauer Dr. C. Tchen Dr. H. Wolfhard 400 Army-Navy Drive Arlington, VA 22202	1	Commander US Army Materiel Command ATTN: AMCRD-T 5001 Eisenhower Avenue Alexandria, VA 22333
4	Director Defense Nuclear Agency ATTN: DDST, Mr. W. Berning RAAE, Dr. C. Blank Mr. D. Evelyn APTL Washington, DC 20305	1	Commander US Army Materiel Command ATTN: AMCRD-R 5001 Eisenhower Avenue Alexandria, VA 22333
2	General Electric Company TEMPO Center for Advanced Studies ATTN: Dr. W. Chan Dr. T. Barrett 816 State Street P. O. Drawer QQ Santa Barbara, CA 93102	1	Commander US Army Aviation Systems Command ATTN: AMSAV-E 12th and Spruce Streets St. Louis, MO 63166
3	Director National Security Agency ATTN: Mr. F. Bishop Mr. W. Gossard Mr. P. Waldo Fort George G. Meade, MD 20755	1	Director US Army Air Mobility Research and Development Laboratory Ames Research Center Moffett Field, CA 94035
		1	Commander US Army Electronics Command ATTN: AMSEL-RD Fort Monmouth, NJ 07703

DISTRIBUTION LIST

<u>No. of Copies</u>	<u>Organization</u>	<u>No. of Copies</u>	<u>Organization</u>
1	Commander US Army Missile Command ATTN: AMSMI-R Redstone Arsenal, AL 35809	1	Director US Army BMD Advanced Technology Center ATTN: Mr. M. Capps P.O. Box 1500 Huntsville, AL 35807
1	Commander US Army Tank-Automotive Command ATTN: AMSTA-RHFL Warren, MI 48090	1	HQDA (DAEN-RD-M/Dr. F. de Percin) WASH DC 20314
2	Commander US Army Mobility Equipment Research & Development Center ATTN: Tech Docu Cen, Bldg 315 AMSME-RZT Fort Belvoir, VA 22060	2	Director US Naval Research Laboratory ATTN: Code 5232D, Mr. J. Davis Code 7700, Mr. J. Brown Washington, DC 23090
1	Commander US Army Armament Command Rock Island, IL 61202	1	AFSC (DLCAW) Andrews AFB, DC 20334
2	Commander US Army Harry Diamond Laboratories ATTN: AMXDO-TI AMXDO-NP, Mr. Wimenitz 2800 Powder Mill Road Adelphi, MD 20783	2	RADC (OCSE/Mr. V. Coyne; TDR/Mr. O. Orcutt) Griffiss AFB, NY 13440
1	Commander US Army Research Office ATTN: Dr. A. Dodd P.O. Box 12211 Research Triangle Park, NC 27709	2	AFCRL (OPR/Mr. J. Ulwick; LKB/Dr. W. Swider) L.G. Hanscom Fld Bedford, MA 01730
4	HQDA (DACS-BMD-A/Dr. C. Johnson/ Mr. J. Shea/Mr. B. Sisco/ Mr. A. Gold) 1320 WILSON BLVD Arlington VA 22209	1	AFWL (DYT) Kirtland AFB, NM 87117
		1	AFAL (RSO/Mr. L. Meuser) Wright-Patterson AFB, OH 45433
		2	Director National Oceanic and Atmospheric Administration ATTN: Code R60, Dr. W. Utlaut Dr. A. Gallagher US Department of Commerce Boulder, CO 80302
		1	Director National Bureau of Standards ATTN: Dr. J. Cooper US Department of Commerce Washington, DC 20234

DISTRIBUTION LIST

<u>No. of Copies</u>	<u>Organization</u>	<u>No. of Copies</u>	<u>Organization</u>
1	Headquarters Energy Research & Development Administration Department of Military Applications ATTN: Mr. D. Gale Washington, DC 20545	1	Barry Research Corporation ATTN: Dr. G. Barry 1530 Page Mill Road Palo Alto, CA 94304
3	Director Lawrence Livermore Laboratory ATTN: Dr. K. Watson Dr. R. Donaldson Dr. C. Gilbert P.O. Box 808 Livermore, CA 94550	1	Battelle Memorial Institute Columbus Laboratories ATTN: STOLAC 505 King Avenue Columbus, OH 43201
3	Director Los Alamos Scientific Laboratory ATTN: Dr. E. Hones, Jr. Dr. D. Kerr Dr. M. Peek P.O. Box 1663 Los Alamos, NM 87544	2	Bell Telephone Laboratories ATTN: Mr. L. Fretwell, Jr. Dr. N. Zabusky Whippany, NJ 07981
2	Director Sandia Laboratories ATTN: Dr. J. Eckhart Dr. C. Mehl P.O. Box 5800 Albuquerque, NM 87115	1	Edgerton, Germeshausen, & Grier, Inc. ATTN: Mr. J. Walker P.O. Box 809 Los Alamos, NM 87544
1	Headquarters National Aeronautics & Space Administration ATTN: Dr. A. Opp Washington, DC 20546	1	General Electric Company ATTN: Dr. G. Millman Court Street Syracuse, NY 13201
1	Aeronomy Corporation ATTN: Dr. S. Bowhill P.O. Box 2209, Station A Champaign, IL 43201	2	GCA Corporation Technological Division ATTN: C, Space Sciences C, Engineering Burlington Road Bedford, MA 01730
3	AVCO Everett Research Laboratory ATTN: Dr. B. Kivel Dr. L. Linson Dr. J. Workman 2385 Revere Beach Parkway Everett, MA 02149	1	ITT Electro-Physics Laboratory, Inc. ATTN: Mr. W. Whelan 9140 Old Annapolis Road Columbia, MD 21043
		2	Lincoln Laboratory, MIT ATTN: Mr. J. Evens Mr. M. Stone 244 Wood Street Lexington, MA 02173

DISTRIBUTION LIST

<u>No. of Copies</u>	<u>Organization</u>	<u>No. of Copies</u>	<u>Organization</u>
2	Lockheed Palo Alto Research Laboratory ATTN: Dept 52-14, Dr. B. McCormac Mr. R. Sears 3251 Hanover Street Palo Alto, CA 94304	5	Stanford Research Institute ATTN: Dr. W. Chesnut Dr. D. Johnson Mr. R. Leadabrand Dr. R. Leonard Dr. A. Peterson 333 Ravenswood Avenue Menlo Park, CA 94025
1	Mission Research Corporation ATTN: Dr. D. Sowle 735 State Street P.O. Drawer 719 Santa Barbara, CA 93101	1	Sylvania Electronic Defense Laboratories ATTN: Mr. J. Reese P.O. Box 205 Mountain View, CA 94042
1	MITRE Corporation ATTN: Dr. G. Meltz P.O. Box 208 Bedford, MA 01730	1	Technology International Company ATTN: Dr. W. Boquist 75 Wiggins Avenue Bedford, MA 01730
1	NETL, Inc. ATTN: Mr. J. Lansinger Building 2, Suite 108 300-120th Avenue NE Bellevue, WA 88005	1	Thiokol Chemical Corporation Astro-Met Division ATTN: Mr. G. Alford P.O. Box 1497 Ogden, UT 84402
1	Physical Dynamics, Inc. ATTN: Dr. A Hochstim P.O. Box 604 College Park Station Detroit, MI 48221	2	TRW Systems ATTN: Dr. B. Fried Dr. C. Kennel One Space Park Redondo Beach, CA 90278
1	R&D Associates ATTN: Dr. F. Gilmore P.O. Box 3580 Santa Monica, CA 90405	1	North Carolina State University ATTN: Dr. W. Flood Raleigh, NC 27607
2	Raytheon Company Sudbury Engineering Facility ATTN: Mr. L. Edwards Dr. H. Thome Sudbury, MA 01776	1	Rice University Engineering and Sciences ATTN: Dr. W. Gordon P.O. Box 1892 Houston, TX 77001
1	Space Data Corporation ATTN: Mr. R. Walker 1331 South 26th Street Phoenix, AZ 85034		

DISTRIBUTION LIST

<u>No. of Copies</u>	<u>Organization</u>
1	University of Alaska Geophysical Institute ATTN: Dr. T. Davis College, AK 99701
3	University of Pittsburgh Department of Physics ATTN: Dr. M. Biondi Dr. F. Kaufman Dr. W. Fite 4200 Fifth Avenue Pittsburgh, PA 15213
1	University of Rochester River Campus ATTN: Dr. A. Simon Rochester, NY 14627

Aberdeen Proving Ground

Marine Corps LnO
Dir, USAMSAA